Is the presence of biomolecules evidence for molecular preservation in the fossil record?

Caitlin Colleary

Dissertation submitted to the faculty of the Virginia Polytechnic Institute and State University in partial fulfillment of the requirements for the degree of

Doctor of Philosophy
In
Geosciences

Sterling J. Nesbitt
Shuhai Xiao
Benjamin Gill
Iuliana Lazar
Jakob Vinther

November 27, 2018
Blacksburg, VA

Keywords: biomolecules, taphonomy, preservation, protein, lipids, mammoths, dinosaurs

Is the presence of biomolecules evidence for molecular preservation in the fossil record?

Caitlin Colleary

ABSTRACT

The molecular components of life (i.e., biomolecules such as DNA, proteins, lipids) have the potential to preserve in animals that have been extinct for millions of years, offering a scale of analysis previously inaccessible from the fossil record. As new technology (e.g., high resolution mass spectrometry) has been incorporated into fossil analyses, researchers have begun to detect biomolecules in terrestrial vertebrates dating back to the Triassic Period (~230 Ma). However, these biomolecules have not been demonstrated to be the biological remains of ancient animals and may instead be exogenous organic contaminants. Here, I developed a series of analytical techniques to detect and interpret the preservation of the degraded remains of the most common protein in bone, collagen, in terrestrial vertebrates from two time slices that represent the two ends of the preservation spectrum. The "shallow time" study of mammoth bones from different burial environments (i.e., permafrost, fluvial and hot springs) and <150,000 years old (well within the accepted window of potential protein preservation) and the deep time study of dinosaurs (~212 – 66 Ma) from the same burial environment (i.e., fluvial), represents the current limit of reported remains of protein preservation in the fossil record. Unlike previous studies that have focused on organic extractions to detect biomolecules, I studied intact fossil bones and the rocks they were found in, to understand more about the effect of burial conditions on preservation and potential alternative sources of organic compounds. I found original amino acids (the degradation products of proteins) and lipids in the mammoth bones, although they were already heavily degraded in fluvial environments, even on such short timescales. I also found that there were amino acids and lipids preserved in the dinosaur bones, however tests on the age of the amino acids and they types of lipids present, demonstrate that they are not original to the animals in this study. Therefore, fluvial environments, one of the most common depositional environments, are not conducive to the preservation of proteins on long timescales and researchers should be cautious when using the biomolecules detected to make interpretations about the biology of ancient animals.

Is the presence of biomolecules evidence for molecular preservation in the fossil record?

Caitlin Colleary

GENERAL AUDIENCE ABSTRACT

An outstanding challenge in the geosciences is understanding how living tissues are altered and preserved when an organism enters the fossil record. Studying the information encapsulated in fossils holds the key to an organism's journey from death to discovery. Over the last few decades, studies of the taphonomy (i.e, how an organism decays and fossilizes) of extinct organisms have shifted their focus from *how* animals are preserved to *what* of the original tissues remain. The preservation of organic molecules (e.g., nucleic acids) over long time scales has raised a number of interesting questions (e.g., the preservation potential of DNA) and has been met with equal shares of optimism and apprehension. But ultimately, the preservation of molecular information has the potential to expand what is currently known about the biology of ancient animals and lead to a better understanding of the processes of fossilization, goals that require an understanding of how organic molecules (biomolecules) are altered over short-term and long-term scales and what organic compounds have persisted over the organism's journey from death to discovery.

Considering burial context is critical in determining if the biomolecules (i.e., DNA, proteins and lipids) being detected in fossils are the biological remains of ancient animals or organic contaminants from other sources. Therefore, I studied terrestrial vertebrates from two different periods of time: the "shallow time" dataset consists of mammoth bones from different burial environments (i.e., permafrost, fluvial, hot springs) that are all less than 150,000 years old and the deep time dataset consists of dinosaur bones from the same burial environments (i.e., fluvial) and range from ~212 to 66 million years old. Focusing on the influence of fluvial environments, where the majority of terrestrial vertebrate fossils are found, is key to understanding the long term preservation potential of the most common organic biomolecule in bone, collagen. Researchers have detected biomolecules like amino acids (as far back as the Triassic Period, ~230 million years), that they have linked to collagen preservation, however, no definitive evidence has been found to determine that the biomolecules detected belong to the animal preserved.

I studied intact fossil bone to determine what biomolecules are present and if they can be definitively linked to the animal in which they were found. Mammoth bones are preserved on a timeline that is conducive to collagen preservation (<150,000 years) and preserve original amino acids (the degradation products of collagen) and lipids. However, degradation of these biomolecules is already apparent in the bones found in fluvial environments. The dinosaur bones have both amino acids and lipids (as well as other organics, like lignin, which is found in plants) present in the bones that are not present in the rocks where the bones were found. However, tests on the ages of the amino acids indicate that the amino acids are not old enough to be original. Therefore, I have found no evidence of original biomolecules in the dinosaur bones and suggest researchers proceed with caution when attempting to make biological interpretations about ancient animals from biomolecules discovered in fluvial environments, particularly on long (i.e., millions of years) timescales.

DEDICATION

To my cousin Hank, for always being my biggest fan, for convincing me that being a scientist was a good idea (and super cool) and for being the only person in our family who actually understands my research.

ACKNOWLEDGEMENTS

Sterling and Michelle, for teaching me how to be a scientist. My committee members Shuhai, Ben and Iuliana, for making me think and Jakob, I wouldn't be here without you. VT Paleobiology grad students past and present for giving and taking advice and support, for commiserating and always being willing to play darts. My granny, for giving me the drive to give her a reason to brag about me. My dad for coming to visit me wherever I end up. My mom for teaching me how to write and for always telling me why she thinks I'm amazing. My sisters for understanding better than anyone else ever could. Aunt Kate and Uncle Rand for always being so supportive and giving me a place to go home to. My cousins, nephew and niece, for giving me a reason to believe in and work to inspire the next generation. Laura and Lex, for being there no matter what. Sam, for always giving me something to look forward to. Selva, for being an exhausting combination of thoughtful and questioning and for making me see things differently. Carrie, for teaching me how to communicate my science and for believing in my ideas to show kids what a real scientist looks like. My extraordinary lady paleontologist network, you know who you are and I love that you're always growing. My old man street beagle, Sancho, for snuggling with me whenever I needed to work and Luna for always being excited to see me. All the guys at the pub, especially owner John, for giving me the experience of having a bar where everyone knows my name. And of course, the things that kept me going and gave me time to breathe: coffee, cheap beer, my plants, projects, decorating, bubble baths, baseball, reading a book for fun, laying on the floor and listening to a record, darts, In Balance yoga, Kroger sushi burritos, fantasy football and looking at photos of organized refrigerators on pinterest.

Chapter 1: We would like to thank Aisling Farrell (Page Museum), Olga Potapova and James Mead (The Mammoth Site), Grant Zazula and Elizabeth Hall (Yukon Paleontology Program) and Mike Fosha (South Dakota Archaeological Society) for access to specimens. Robert Bodnar (Virginia Tech) for the use of his lab, supplies and for his thoughts on the maturation experiments, Charles Farley (Virginia Tech) for assistance with the Raman, Michelle Stocker (Virginia Tech) for conversations that led to this project and Evan Saitta (University of Bristol) for really insightful comments on the manuscript.

Chapter 2: Ruth Elsey and colleagues at the Rockefeller Wildlife Refuge, Louisiana. The curators and collections staff at the Natural History Museum at Los Angeles County, The Mammoth Site of Hot Springs, South Dakota, Natural History Museum of Utah, Petrified National Forest for the specimens used in this study. Everyone excavating in the Hayden Quarry in 2017 who would call me whenever they found a rib. Robert Bodnar (Virginia Tech) for the use of his lab, supplies and for his thoughts on the maturation. Dr. Hochella for supporting the trip to Washington and the researchers at the Environmental Molecular Sciences Lab (EMSL) at the Pacific Northwest National Lab (PNNL) for running analyses on additional compounds. The Virginia Space Grant Graduate STEM Research Fellowship for funding TOF-SIMS and AAR analyses. Augusta MacCracken and Chris Griffin for really insightful comments on the manuscript. Figure color palette from Wes Anderson's Fantastic Mr. Fox.

Chapter 3: Mike Hochella for funds that supported writing this manuscript. Selva Marroquín and Dana Korneisel for really insightful comments on the manuscript.

ATTRIBUTIONS

Chapter 1: CC conceived of the study, designed the study, performed experimental maturation, analyzed the data and wrote the manuscript. SOR carried out lipid analysis, assisted with data analysis and helped with the manuscript. HL performed experimental maturation, carried out Raman analyses, assisted with data analysis and helped with manuscript. SOR carried out lipid analysis, assisted with data analysis and helped with the manuscript. AD carried out TOF-SIMS analysis, assisted with data analysis and helped with the manuscript. SJN conceived of the study, coordinated the study and helped with the manuscript. All authors gave final approval of the manuscript.

Chapter 2: CC conceived of the study, designed the study, performed TOF-SIMS analysis, analyzed the data and wrote the manuscript. SOR carried out lipid analysis, assisted with data analysis and helped with the manuscript. KEHP. carried out amino acid racemization analyses and helped with the manuscript. MD. created new method for amino acid racemization analysis that improved data. AD carried out TOF-SIMS analysis, assisted with data analysis and helped with the manuscript. JGT carried out sample preparation and organic extractions for FTICR-MS analyses and helped with data analysis. RKC performed FTICR-MS analyses, helped with data analysis and helped with the manuscript. MT helped with interpreting and analyzing the FTICR-MS data. MFH conceived of and facilitated FTICR-MS analyses and helped with manuscript. SJN conceived of the study, coordinated the study and helped with the manuscript. All authors gave final approval of the manuscript.

Chapter 3: CC conceived of the study, designed the study, researched previous studies and wrote the manuscript. AD consulted on and helped with the manuscript. JV consulted on and helped with the manuscript. SJN consulted on and helped with the manuscript.

TABLE OF CONTENTS

LIST OF FIGURES AND TABLES

GRANT INFORMATION

Chapter 1: Funding for this project was from a series of small graduate student grants awarded to CC: The Palaeontological Association Stan Wood Award (PA-SW201501), The Geological Society Graduate Student Research Grant, Virginia Tech Graduate School Graduate Research Development Fund, Dr. Larry Agenbroad Legacy Fund for Research and the Virginia Space Grant Consortium STEM Graduate Research Fellowship. SOR was funded by the Marie Skłodowska-Curie Actions Research Fellowship Programme and the Irish Research Council (ELEVATE Career-Development Fellowship ELEVATEPD/2014/47). Work at MIT was supported by an award (NNA13AA90A) from the NASA Astrobiology Institute. The National Science Foundation Major Research Instrumentation program (DME-0923096) funded the time-of-flight secondary ion mass spectrometer at UT Austin.

Chapter 2: Funding for excavation at Ghost Ranch from NSF EAR 1337291. TOF-SIMS analyses were paid for by a Virginia Space Grant Consortium STEM Graduate Research Fellowship awarded to CC. SOR was funded by the Marie Skłodowska-Curie Actions Research Fellowship Programme and the Irish Research Council (ELEVATE Career-Development Fellowship ELEVATEPD/2014/47). Work at MIT was supported by an award (NNA13AA90A) from the NASA Astrobiology Institute. The National Science Foundation Major Research Instrumentation program (DME-0923096) funded the time-of-flight secondary ion mass spectrometer at UT Austin. Nanoscience and Engineering, Institute for Critical Technology and Applied Science (ICTAS) at Virginia Tech for student support and the National Center for Earth and Environmental Nanotechnology Infrastructure (NanoEarth), NSF grant ECCS-1542100 for funding research trip to Environmental Molecular Sciences Laboratory (EMSL) User Facility at the Pacific Northwest National Lab (PNNL), Richland, WA.

Chapter 3: Funding from the Virginia Space Grant Consortium STEM Graduate Research Fellowship, ICTAS, NanoEarth and facilities provided by the Department of Geosciences.

INTRODUCTION

The structure and function of nucleic acids, proteins, carbohydrates and lipids (i.e., biological macromolecules, or biomolecules) are a cornerstone in the study of living organisms. Biomolecules contain information about changes that occur during the life of an animal (Cleland et al. 2015), evolutionary adaptations (Campbell et al. 2010) and phylogenetic relationships (Orlando et al. 2014). Molecular paleontologists, therefore, seek to detect biomolecules in the fossil record to make interpretations about ancient animals, paleoenvironments and to better understand the processes involved in fossilization. The molecular fossil record has only begun to be explored in the last few decades, with the increased use of new technology (e.g., high resolution mass spectrometry) and a few basic principles have been established: 1) biomolecules vary in their decay resistance (Table i.i), 2) there are many variables that influence preservation (i.e., molecular structure, depositional environment and diagenetic history) and 3) degradation follows a fixed number of pathways (Eglinton & Logan 1991, Briggs & Summons 2014, Collins et al. 2002). Whereas, studies on molecular preservation often focus on exceptionally preserved fossils (e.g., feathers, hair, organs, etc.), biomolecules have been recently detected in fragmentary dinosaur bones, in environments that were not considered conducive to high quality preservation, suggesting that preservation may be more common than previously thought (Bertazzo et al. 2015).

Terrestrial vertebrates are most commonly represented in the fossil record by the remains of their skeletons, especially on long timescales (~450 Ma). Since the earliest paleontological discoveries, anatomical features of the bones themselves have been analyzed and compared to understand how ancient animals evolved and are related to one another. As the use of mass spectrometers is becoming more common in fossil studies, the scale that fossils can be studied is

changing dramatically (Figure i.i). The promise of detecting the original biological remains of ancient animals has inspired studies on terrestrial vertebrates, specifically dinosaurs, to search for original proteins. Proteins have an extraordinary diversity of form and function in living organisms (e.g., antibodies, hormones, structural) but are comprised of only 20 amino acids that vary in their arrangement (Creighton 1993). The primary organic component of bone is the structural protein collagen (a triple helix composed of amino acids in the formula glycine (Gly)-X-X, where X is often represented by proline and hydroxyproline) (Szpak 2011) which is the focus of molecular investigations of fossil bone. The potential for nucleic acids to be preserved is on the scale of ~1 million years, but the potential for proteins to preserve is on the scale of ~10s to ~100s of millions of years (Briggs & Summons 2014) and the range of potential protein preservation is only starting to be explored (Wiemann et al. 2018).

The strongest support for the oldest intact protein preserved was found in a 3.8-million-year-old ostrich eggshell (Demarchi et al. 2016). Studies that attempted to find proteins preserved on longer timescales (e.g., the Mesozoic Era, ~251 – 66 Ma) focused on the degraded remains of collagen, including peptide sequences (Schroeter et al. 2017, Schweitzer et al. 2007), the amide bonds that link amino acids to form peptides (Lee et al. 2017) and amino acids prevalent in collagen (Surmik et al. 2016, Bertazzo et al. 2015). These studies successfully detected the presence of biomolecules on extremely long timescales (>60 Ma), however they have failed to address: 1) if the biomolecules detected are the biological remains of the animals being studied, 2) if there are additional sources of organic contaminants or 3) what fragmentary proteins can say about ancient animals. One of the main goals of finding original biomolecules in the fossil record is to make interpretations about ancient animals. Studies that have focused on the preservation of pigments (i.e., melanin) have made interpretations regarding the evolution of

feathers (Li et al. 2010) and the vertebrate eye (Gabbott et al. 2016), as well as predictions about the behavior of ancient animals (Brown et al. 2017) that could not otherwise be discerned from the fossil record. In studies of fossilized bone, the potential for proteins to preserve at all and over millions of years longer than nucleic acids (i.e., DNA) has led to attempts to discern detection limits for collagen and its degradation products (i.e., peptides and amino acids) (Surmik et al. 2016). However, proteins, particularly fragmentary proteins, do not contain as much information about animals as DNA (e.g., genomic data that can determine how animals are related to one another). It is unclear what short peptide sequences or individual amino acids can affirm about the physiology or evolutionary relationships of ancient animals is unclear, despite being often evoked as the ultimate justification of such studies (Schweitzer et al. 2007, Cleland et al. 2015, Bertazzo et al. 2015, Schroeter et al. 2017, Lee et al. 2017). To answer these critical questions, the preservation potential of proteins in deep time must be addressed. In particular, we must quantify the potential for these biomolecules to persist in certain types of depositional environments or lithologies and generally establish how stable proteins are over time, as well as scrutinize whether the evolution or affinities of animals can actually be addressed by partial protein sequences. Additionally, although the ability to detect biomolecules (e.g., amino acids) in deep time has been well established, most studies have failed to determine the source or age of these organic compounds, therefore limiting the utility of these discoveries. Determining if these key biomolecules are original to the buried organism is the main goal of this dissertation research, which will have implications for the validity of various claims across the field of paleontology.

Chapter Summaries

To examine the potential for ancient protein to preserve on long timescales, I tested two

datasets: 1) a "shallow time" dataset (up to ~150,000 years) (Chapter 1) and a deep time dataset (up to ~212 Ma) (Chapter 2). The goal of Chapter 1 was to develop analytical techniques to detect biomolecules (i.e., amino acids and lipids) and to make interpretations regarding the source of these biomolecules and the influence of the depositional environment (i.e., fluvial) on preservation. I found strong evidence of biomolecule preservation in all of the mammoth bones, however, even on short timescales, biomolecules degrade quickly in fluvial environments and more predictable, environments where heat is clearly added (spring) or contaminants are abundant (tar). The goal of Chapter 2 was to address the potential for biomolecules to preserve on long timescales by detecting the degraded remains of proteins (i.e., amino acids), evaluating additional organic preservation (i.e., lipids and lignin) and testing whether the organics were old enough to be original to the animals in question as opposed to more recent contamination. I found that amino acids can be detected on very long timescales (as old as ~212 Ma, during the Triassic Period); however, after a number of additional analytical tests, I found that the amino acids are not old enough to be considered original. Therefore, there is no evidence of original protein preservation on these timescales (tens of millions to hundreds of millions of years) in these specimens, likely due to the fluvial depositional environment. These findings suggest that future work on the preservation of proteins on these timescales in fluvial depositional environments should be cautious about making interpretations based on the presence of biomolecules.

One of the key methods I used, time-of-flight secondary ion mass spectrometry (TOF-SIMS) has become popular among molecular paleontologists in the last two decades. However, the use of this technology is not standardized across the field and misinterpretations about what data can be acquired and how to acquire the data, interpret results and report the data so that

studies can be replicated are common. These misinterpretations are impeding further expanding the use of this instrument that could be critical in further developing how we detect and interpret biomolecules in the fossil record. Therefore, Chapter 3 reviews previous fossil studies using TOF-SIMS and makes recommendations for standardizations in sample size, preparation, instrument parameters, data output and data analysis and makes suggestions for future work.

References

Bertazzo, S. et al. 2015. Fibres and cellular structures preserved in 75-million–year-old dinosaur specimens. *Nature Communications*, *6*, p.7352.

Briggs, D.E. and Summons, R.E., 2014. Ancient biomolecules: their origins, fossilization, and role in revealing the history of life. *BioEssays*, *36*(5), pp.482-490.

Brown, C.M. et al. 2017. An exceptionally preserved three-dimensional armored dinosaur reveals insights into coloration and Cretaceous predator-prey dynamics. *Current Biology*, *27*(16), pp.2514-2521.

Campbell, K.L. et al. 2010. Substitutions in woolly mammoth hemoglobin confer biochemical properties adaptive for cold tolerance. *Nature Genetics*, *42*(6), p.536.

Cleland, T.P., Schroeter, E.R. and Schweitzer, M.H., 2015. Biologically and diagenetically derived peptide modifications in moa collagens. *Proceedings of the Royal Society of London B*, *282*(1808), p.20150015.

Collins, M.J. et al. 2002. The survival of organic matter in bone: a review. *Archaeometry, 44*(3), pp.383-394.

Creighton, T.E., 1993. *Proteins: structures and molecular properties*. Macmillan.

Demarchi, B. et al. 2016. Protein sequences bound to mineral surfaces persist into deep time. *Elife*, *5*, p.e17092.

Eglinton, G. and Logan, G.A., 1991. Molecular preservation. *Philosophical Transactions of the Royal Society B*, *333*(1268), pp.315-328.

Gabbott, S.E. et al. 2016. Pigmented anatomy in Carboniferous cyclostomes and the evolution of the vertebrate eye. *Proceedings of the Royal Society of London B*, *283*(1836), p.20161151.

Lee, Y.C. et al. 2017. Evidence of preserved collagen in an Early Jurassic sauropodomorph dinosaur revealed by synchrotron FTIR microspectroscopy. *Nature Communications*, *8*, p.14220.

Li, Q. et al. 2010. Plumage color patterns of an extinct dinosaur. *Science*, *327*(5971), pp.1369-1372.

Orlando, L. et al. 2013. Recalibrating *Equus* evolution using the genome sequence of an early Middle Pleistocene horse. *Nature*, *499*(7456), p.74.

Schroeter, E.R. et al. 2017. Expansion for the *Brachylophosaurus canadensis* collagen I sequence and additional evidence of the preservation of Cretaceous protein. *Journal of Proteome Research*, *16*(2), pp.920-932.

Schweitzer, M.H. et al. 2007. Analyses of soft tissue from *Tyrannosaurus rex* may suggest presence of protein. *Science. 316*(5822). pp.227-280.

Surmik, D. et al. 2016. Spectroscopic studies on organic matter from Triassic reptile bones, Upper Silesia, Poland. *PLOS ONE*, *11*(3), p.e0151143.

Szpak, P., 2011. Fish bone chemistry and ultrastructure: implications for taphonomy and stable isotope analysis. *Journal of Archaeological Science*, *38*(12), pp.3358-3372.

Wiemann, J., Yang, T.R. and Norell, M.A., 2018. Dinosaur egg colour had a single evolutionary origin. *Nature*, p.1.

Table i.i. Preservation potential of biomolecules

Biomolecule	**Predicted decay resistance**	**Oldest occurrence in the fossil record**
Nucleic acids (DNA, RNA)	<1 million years	Horse bone (~570,000 years)
Proteins	10 – 100 million years	Ostrich eggshell (3.8 Ma)
Lipids	> 100 million years	Crustacean (~380 Ma)
Lignin	> 100 million years	Vascular plants (~310 Ma)

*Compiled from Eglinton & Logan 1991, Briggs & Summons 2014, Orlando et al. 2013, Demarchi et al. 2016, Melendez et al. 2013

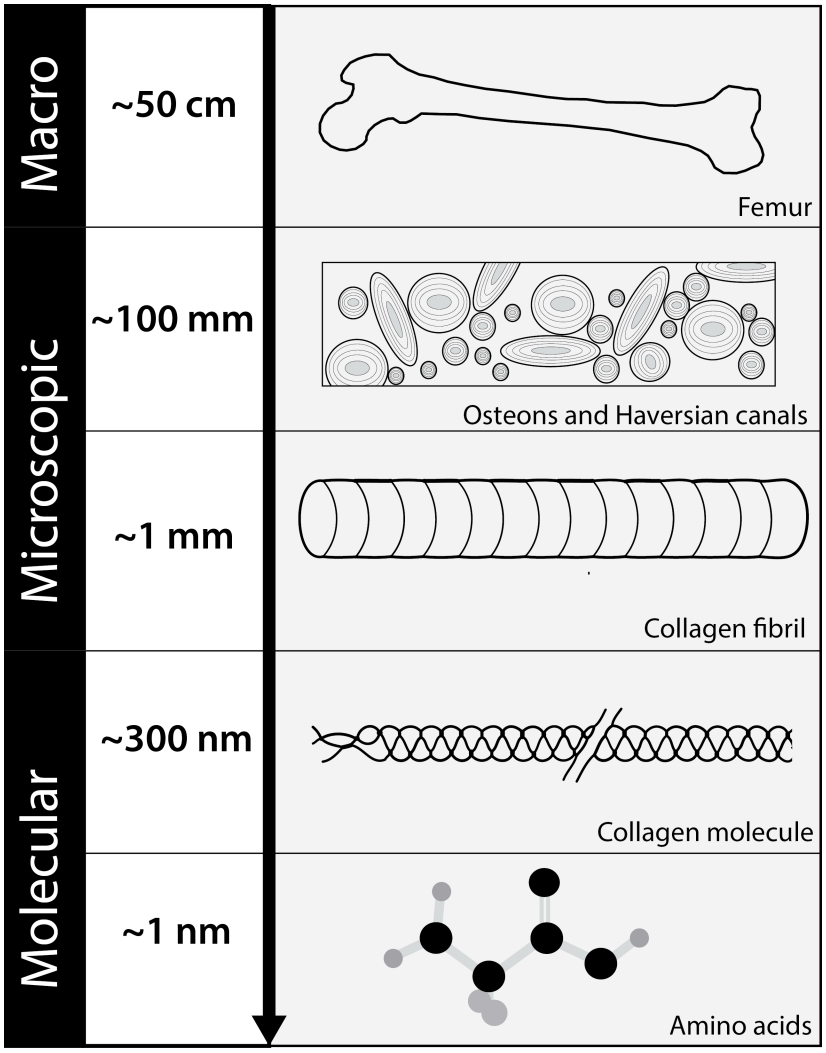

Figure i.i. The scales that fossil bones are analyzed. The macro-level is represented by anatomical features on the bone that can be used to study the evolution and relationships of animals. The microscopic level is represented by microstructures in the bones such as lines of growth (external fundamental systems). The molecular level (or micron level) is the newest scale at which to examine bones, including the presence of biomolecules.

CHAPTER ONE

CORRELATING ORGANIC PRESERVATION, BONE DEGRADATION AND BURIAL ENVIRONMENT IN MAMMOTH FOSSILS

Caitlin Colleary[1*], Hector M. Lamadrid[1,2], Shane S. O'Reilly[3,4], Andrei Dolocan[5], Sterling J. Nesbitt[1]

[1] Department of Geosciences, Virginia Polytechnic Institute and State University, Blacksburg, VA 24061
[2] Department of Earth Sciences, University of Toronto, Toronto, ON M5S 3B1, Canada
[3] Earth, Atmospheric and Planetary Sciences Department, Massachusetts Institute of Technology, Cambridge, MA 02139
[4] School of Earth Sciences, University College Dublin, Dublin 4, Ireland
[5] Texas Materials Institute, University of Texas at Austin, Austin, TX 78712

*Corresponding author: colleary@vt.edu

Formatted for *Scientific Reports*

Abstract

The detection of biomolecules and associated signatures (e.g., DNA, proteins, lipids, amino acids) in extinct organisms is becoming more frequent and these preserved biomolecules can inform the chemical and physical processes that occurred during the life of an organism. However, the focus has been on detecting biomolecules in fossil bone in isolation and studies have not considered bone degradation or the broader burial context to test for the original source of the organics being detected. Here, we use a multifaceted approach to detect the biomolecular signatures of proteins, determine potential contamination sources and analyze the degradation of the fossil bone. We compare the fossil data to experimentally matured bone to test for the degradation expectations of proteins using a proxy for degradation through time. By combining these analytical techniques, we are able to correlate the presence of proteins with the amount of bone degradation in different burial environments.

Introduction

The preservation of organic biomolecules (e.g., proteins, lipids, amino acids) in extinct organisms has become of increased interest to biologists as technology (e.g., high-resolution mass spectrometry, protein sequencing) has made it possible to detect and explore the preservation of biomolecules that preserve much longer than DNA (Briggs & Summons 2014). Proteins detected in extinct animals have been used to determine evolutionary relationships (Welker et al. 2015, Buckley 2015) environmental adaptations (Campbell et al. 2011) and attribute bone fragments to taxa (Buckley et al. 2010). Detecting and interpreting biomolecules preserved on long timescales (millions of years) becomes increasingly complicated by the degradation of bone tissue, fossilization and the addition of exogenous organic contaminants whether from the time of burial or after (Schweitzer 2011, Schroeter & Cleland 2016). Therefore, archaeological remains have been the focus of many studies related to these long lasting biomolecules (Demarchi et al. 2016) and it is still unclear how proteins degrade on these short time scales or how they are preserved in vertebrate fossils (Cappellini et al. 2014).

Despite a lack of understanding of how proteins break down and preserve on short time scales, studies have sought to detect proteins and the signatures of proteins (i.e., peptides and amino acids) as far back as the Mesozoic Era (251 Ma – 66 Ma) with peptides being reported from the Cretaceous Period (151 – 66 Ma) (Asara et al. 2007, Schroeter et al. 2017) and Jurassic Period (251 – 151 Ma) (Lee et al. 2017) and collagen-associated amino acids from the Triassic Period (~250 – 201 Ma) (Surmik et al. 2016). However, these findings have been contested as statistical artifacts (Pevzner et al. 2008), laboratory contamination (Bern et al. 2009), and bacterial biofilms (Kaye et al. 2008). The majority of these studies focus on methods that extract organics from demineralized bone (e.g., Cleland et al. 2015, Boatman et al. 2014, Schweitzer et

al. 2009, Asara et al. 2007, Schweitzer et al. 2005) and the effect these methods have on furthering the degradation of organics has not been examined. Additionally, the majority of studies have focused on a single bone that contains organic material (Schweitzer et al. 2007, Bertazzo et al. 2015) from a single locality. Despite a number of studies that have theorized preservational differences based on burial environment (Collins et al. 2002, Hedges 2002, Nielsen-Marsh & Hedges 2000) no study has yet compared biomolecule preservation across burial environments in the same taxon to test the potential long-term preservation patterns of proteins in the bone *in situ.*

Here, we analyzed mammoth rib bones (~<150 to 26 Ka) from permafrost, a channel deposit, a hot spring fed sinkhole and natural asphalt to test the relationships between organic preservation and bone degradation and how this is influenced by different burial environments. As a secondary analysis to compare the degradation of proteins in the mammoth bones, we did thermal maturation experiments on modern bones as a proxy for the thermal degradation of amino acids. Additionally, we used surface mass spectrometric techniques and lipid extractions to examine what areas within in the bone may have greater preservation potential.

Materials and Methods

a. *Elephant and mammoth bones*

Mammoth rib fragments from the Mammoth Site (07HS152), Shultz mammoth site (39MD900), Rancho La Brea (HC142067) and Canyon Creek, Yukon (YG546.52) were analyzed. A modern African elephant (*Loxodonta africana*) rib from a deceased zoo animal from the Mammoth Site collection that was never buried was analyzed at varying temperatures to test thermal degradation and make comparisons to the fossil specimens. The Mammoth Site of Hot Springs,

South Dakota is a sinkhole deposit (laminated fine-grained sediment from clay to coarse sand (Laury 1980)) that was heated by hot springs year round (~35° C) and is currently dated at ~26 Ka. The rib (07HS152) used in this study was buried at an estimated 7 m depth. The Schulz mammoth (39MD900) was excavated in a fine-grained stream channel deposit that was radiocarbon dated to ~ 37 - 39 Ka. Analyses of the site determined that the mammoth was buried in a low energy deposit (Fosha et al. 2013) and the rib used in this analysis was found in silt between two high-energy, gravel-filled gullies (Fosha et al. 2013). The Rancho La Brea mammoth rib fragment was excavated from Pit 9, which has a mean calibrated radiocarbon date of ~24.5 Ka (O'Keefe et al. 2008). The Yukon mammoth rib fragment was surface collected in Canyon Creek in 2014 and was originally preserved in permafrost. The age of this sample is not well-constrained because it was not collected *in situ*, however it can be estimated to be <150 Ka (pers comm. Grant Zazula).

b. Maturation experiments

A diamond saw (Dremel) was used to cut Modern African elephant rib bone into two sizes (2 mm and 1 cm) for the short (i.e., 24 hour) and long (i.e., up to 91 days) term experiments. For the 24 hour experiments, three 2mm^2 fragments were inserted into 3 x 15 mm platinum capsules and loaded by hand into cold-sealed pressure vessels at 100°C, 200°C, and 250°C at atmospheric pressure (following a similar loading procedure to Bodnar & Sterner 1987). The five long term experiments were cut into 1 cm fragments and placed in an oven at 100°C under vacuum at -25 in/Hg. The short term experiments were terminated at 24 hours, while the long term experiments were terminated at 7, 14, 30, 67, and 91 days.

c. Time-of-flight secondary ion mass spectrometry (TOF-SIMS)

Time-of-flight secondary ion mass spectrometry (TOF-SIMS) was performed using an ION-TOF TOF.SIMS 5 at The University of Texas at Austin, Texas Materials Institute. A pulsed (20 ns, 10 kHz) analysis ion beam of Bi_3^+ clusters at 30-kV ion energy was raster-scanned over 500 x 500 μm^2 areas. Bi_3^+ polyatomic sputtering was used to enhance the signal and reduce the fragmentation of large organic molecules. A constant flux, 21 eV electron beam was used during data acquisition to reduce sample charging. Secondary ions had positive polarity and an average mass resolution of 1-3000 (m/δm). The base pressure during acquisition was <1 x 10^{-8} mbar. Mass calibration was performed by identifying the peak positions of CH_2^+, CH_3^+, O^+, F^+, Na^+, K^+, Ca^+, and Cs^+ secondary ions. Regions of interest were chosen to reduce the effects of topography. Of the amino acids analyzed, aspartic acid (Asp) was not included because it could not be separated from the Cs which was used to sputter each sample (133 amu).

Amino acids were detected and mapped in the bone *in situ* using TOF-SIMS in modern elephant and fossil mammoth rib bones. Amino acid assignments (Table 1.1) were made based on the molecular weight of whole amino acid molecules, the assignments of fragmented amino acids established in previous fossil studies (Orlando et al. 2013) and additional amino acid fragments shared between samples that were identified in this study. In total, 67 amino acid fragments were selected for multivariate analysis, in particular principal component analysis (PCA), which was employed to understand both the similarities and differences between our samples. Two sediment matrix samples from two of the mammoth sites (i.e., the channel deposit and sink hole) were analyzed as controls.

d. Raman mass spectrometry

Raman analyses were conducted using a JY Horiba LabRam HR (800 mm) spectrometer with a 600 grooves/mm grating in the Department of Geosciences at Virginia Tech. The confocal aperture was 400 μm, with a slit width of 150 μm. Excitation was provided by two lasers to circumvent fluorescence of the sample, a 632.9 nm HeNe (power of 20 mW at the source and ~2mW at the sample) and a 785 nm (a solid state-diode laser operating at ~150 mW). The Raman uses an air-cooled (-70°C) CCD detector with a 1024 x 256 pixels front illuminated chip and a 600 grooves/mm gratings. The laser was focused through a 10 X objective with a working distance of ~15 mm from the sample surface. The best spectral data was achieved using no filter for 3 accumulations, with a collection time of 300 seconds. Areas of interest were also selected for fossil samples (400-1500 with the 632 nm laser and 2500-3300 with the 785 nm laser), which reduced background fluorescence.

e. Lipid Analyses

Outer surfaces of fossil and modern bones were cleaned using a solvent-washed scalpel and where possible, this material was retained and treated as a distinct sample. Where possible (Mammoth Site and Yukon), compact bone and spongy bone were separated using the scalpel and extracted separately. Fossil and sediment matrix samples were powdered using a SPEX 8500 shatterbox and stainless steel puck mill. Between 1 and 5 g of powdered sample was each accurately weighed into 60 mL glass centrifuge tubes. Samples were extracted with organic solvent as follows: 2:1 (v/v) methanol/dichloromethane (×3), followed by 9:1 (v/v) dichloromethane/methanol (×3). For each extraction, the tubes were sonicated for 10 min in an ultrasonic bath (room temperature). Extracts were separated from solid residues by

centrifugation, and supernatants from each step were combined to give a total lipid extract (TLE). TLEs were concentrated to minimal volume under a gentle stream of high purity N_2 gas. A portion each TLE was then subjected to acid methanolysis (0.5 N methanolic HCl, 60°C ~10 h), followed by silylation (99:1 N,O-Bis(trimethylsilyl)trifluoroacetamide /trimethylchlorosilane mixed with pyridine (1:1 v/v); 70°C, 2 h). Aliquote of the derivatized samples were analyzed by gas chromatography/mass spectrometry (Agilent 5890 GC hyphenated to an Agilent 5975C Mass Selective Detector). The GC was equipped with a Gertsel programmable temperature vaporizer (70°C ramped to 360°C at a rate of 720°C min^{-1}) and an J&W 60 m capillary column (0.25 mm inner diameter, 250 μm film thickness). The GC temperature program was: 70°C for 2 min, ramp at 10°C min^{-1} to 130°C, followed by a ramp to 300°C at 4°C min^{-1} and a final hold time of 20 min. The mass spectrometer was operated in electron impact ionization mode (70 eV), with a mass scan range from m/z 50 to 600. All solvents used were high-purity (OmniSolv) and all aqueous solutions were cleaned with dichloromethane prior to use, and procedural blanks were run to monitor background contamination.

Results and Discussion

a. Preservation

Amino Acids

Nineteen of the twenty amino acids were detected in their intact form in the modern elephant bone. Fragmentation is a byproduct of TOF-SIMS analysis (i.e., secondary ions) and previous studies (Orlando et al. 2013) using this technique to examine preservation of fossil bone have only reported amino acid fragments. However, the horse bone in that study was preserved extremely well in permafrost, so this is likely not indicative of degradation in the bone.

Our principal component analysis shows the variation between the fossil samples based on the 67 amino acid fragments selected (Figure 1). The PCA loadings (See Chapter 1 Supplement) show the influence of particular amino acids on the multivariate distribution of the fossils in the PCA space. Of two of the amino acids most commonly found in collagen, proline (Pro) is mainly responsible for the sample variation along the first principal component axis (that is, the greatest variation between fossils), whereas glycine (Gly) mainly influences the sample variation along the second principal component axis, which separates the fossils from the sediment matrix. Alanine (Ala), Gly and Pro are some of the most thermally stable amino acids and are commonly found in fossil samples (Wang et al. 2012). In this study, we find that Gly and Ala influence the variation between the fossils and the sediment matrix whereas Pro influences the variation between the mammoth fossils. The resulting variation in the PCA space based on the selected amino acid fragments shows that the mammoth fossils, the associated sediment matrix and modern elephant bone plot distinctly and can therefore be discerned from one another based on the variation in preservation of the amino acids. The fossil mammoth bones plot distinctly from one another along the first principal component axis. Particularly, the mammoth rib preserved in permafrost is distinct from the mammoth ribs preserved in the channel deposit and the sinkhole. This pattern, based on organic preservation, is reflected in additional analyses of the presence of lipids and the degradation of the fossil bones and therefore demonstrates a variation in preservation based on burial environment. Additionally, the low temperature and high temperature experiments may show different degradation processes because the modern bone is plotting between the two. We find that degradation of amino acids begins in shallow time and depends heavily on the type of environment the fossil is preserved in. These results can be

applied broadly to fossil studies in shallow time, but may also reflect the likelihood of preservation on long time scales in similar burial environments (e.g., fluvial deposits).

Lipids

The major detected lipids in this study were saturated and monounsaturated fatty acids, sterols, *n*-alkan-1-ols, *n*-alkanes, pentacyclic triterpenoids and 2-hydroxy acids. The channel deposit fossil and extracted outer surface material were dominated by hexadecanoic acid (16:0), oleic acid (18:1n-9), octadecanoic acid (18:0) and cholesterol (cholest-5-en-3β-ol; $27\Delta^5$) (Figure 2A). The fossil bone also contained appreciable 7-hexadecenoic acid (16:1n-7) and tetradecanoic acid (14:0). The sediment matrix contained a more diverse lipid profile with significant amounts of long chain (greater than 20 carbon chain length) 2-hydroxy acids, *n*-alkan-1-ols and *n*-alkanes (although 2-hydroxy-tetracosanoic acid was also detected in the fossils). The Schultz site sediment also contained the pentacyclic triterpenoids α-amyrin (urs-12-en-3β-ol) and β-amyrin (olean-12-en-3β-ol).

The sinkhole fossil contained most lipids in the spongy bone and only trace levels of lipids in the compact bone (Figure 2B) and comprised a mixture of fatty acids, *n*-alkan-1-ols and 2-hydroxy acids with 16 and 18 carbon chains lengths. Lower relative amounts of long chain *n*-alkan-1-ols, $27\Delta^5$ and β-sitosterol (24-ethylcholest-5-en-3β-ol; $29\Delta^5$) were also observed. Sterols and 2-hydroxy acids were not detected in the sediment matrix. The fossil surface and sediment also contained a number of unidentified compounds as major lipids. The permafrost fossil compact and spongy bones both contained $27\Delta^5$ as the major lipid, as well as a number of $27\Delta^5$ derivatives (Figure 2C). The spongy bone contained a significant amount of long chain *n*-alkanols, 2-hydroxy acids and *n*-alkanes, $29\Delta^5$, α-amyrin and β-amyrin.

Lipids in vertebrate bones are derived primarily from marrow adipose tissue and dominated by 16:0, 18:1n-9, 18:0, 14:0 and $27\Delta^5$ (Evershed et al. 1995; Colonese et al. 2015). This is confirmed here from the analyzed modern elephant bone (Figure 2D). We assess the preservation state of endogenous lipids and extent of exogenous contamination from the lipid data according to the following criteria: 1) fossils matching the occurrence and relative abundances of lipids from elephant and vertebrate bones are likely preserved endogenous signals; and 2) fossils with considerable amounts of lipid markers for soil plant matter and bacteria (Evershed et al. 1995, Kögel-Knabner, 2002) and/or similar lipids as sediment matrices are likely significantly contaminated with exogenous organic matter. If significant contamination from soil has occurred then vascular-plant lipids such as α/β-amyrin), $29\Delta^5$ and plant wax long chain fatty acids, *n*-alkanols, hydroxyl acids (with even carbon number predominance) or *n*-alkanes (odd carbon chain predominance) would be found (Kögel-Knabner, I. 2002; Napier & Graham 2010). Bacterial contamination of the fossils bones would be suspected if bacterial fatty acids such as methyl-branched C15 and C17 fatty acids and/or bacterial hopanoids (Evershed et al. 1995) were abundant.

Based on these criteria we conclude that the sediment matrix from the channel deposit was dominated by soil organic matter from plant litter. This conclusion is consistent with the freshwater stream depositional and environmental setting. Negligible amounts of plant lipids were detected on the surface of the fossil or from the fossil itself, indicating very little contamination and that the observed lipids in the fossil are endogenous. This conclusion is supported by fact that the lipid profile from the channel deposit fossil matches the expected profile for vertebrate bone lipids. In addition, the occurrence of lipids with labile unsaturated bonds (18:1n-9 and $27\Delta^5$) indicates exceptional preservation and little early diagenetic alteration.

In contrast to the channel deposit, the sediment matrix from the sinkhole did not contain a plant litter signal. The occurrence of hexadecane-1-ol, octadecan-1-ol as major lipids, together with *n*-alkanes between C18 and C20 indicates a microbial, likely microalgal, source of organic matter (Volkman 1986). While 16:0, 18:1n-9, 18:0, 14:0 and $27\Delta^5$ were present, the fossil also contains appreciable contamination with exogenous microalgal and vascular plant lipid signals. The permafrost fossil compact and spongy bones both contained $27\Delta^5$ as the major lipids, as well as 16:0, 18:1n-9, 18:0 as the major fatty acids. However, both the spongy and compact bone also contained vascular plant signals, particularly in the spongy bone. While a sediment control sample was not available for this fossil sample, it appears that significant contamination of the spongy bone has occurred and to a much lower degree for the compact bone. In general, there was no clear influence from bacterial lipids such as methyl-branched short chain fatty acids or hopanoids, indicating that extensive bacterial colonization and contamination did not occur.

While the preservation of endogenous lipids in archaeological and fossil remains of various vertebrates (Evershed et al. 1995; Thiel et al. 2013) has been reported, multiple samples with knowledge of context have rarely been analyzed. Based on our lipid data the sinkhole fossil is least preserved and most contaminated even though it is the youngest of the fossils we studied. The channel deposit fossil exhibits both exceptional preservation of endogenous lipids and little contamination, while the permafrost fossil contains well-preserved lipids but also significant exogenous contamination from plants. We attribute the poor preservation of the youngest fossil to the contrasting depositional environment, whereby the higher temperatures that the fossils in the hot-spring fed sinkhole were subjected to would result in a higher rate of decay in labile lipids like fatty acids. The microalgal signal that dominates the sediment matrix and that was also observed in the fossils could result from colonization by aquatic microalgae growing in the hot

spring. Since the preservation does not follow directly from the age of the fossils, the depositional and environmental conditions are the primary factor influencing preservation. In particular, as for DNA, temperature appears to be a major parameter influencing preservation of lipids in vertebrate bones since the youngest fossil was buried in a hot spring setting and the oldest fossil was deposited in permafrost.

b. Diagenesis

Proteins

Using the proxies for diagenesis in fossil bone developed using Raman spectroscopy by Thomas et al. (2007), the addition of accessory ions were identified in fossil mammoth bones as well as secondary mineralization of calcite. The presence of an Amide III band has been used to determine the presence of collagen and was detected in the African elephant and permafrost mammoth fossil, decreased in intensity in the channel deposit mammoth fossil, and is lost in the sinkhole mammoth fossil (Figure 3). The combination of these proxies for diagenesis indicates that the least amount of degradation has taken place in the permafrost mammoth, followed by the channel deposit mammoth, and the greatest amount of degradation is seen in the sinkhole mammoth. This data supports our findings regarding the preservation of amino acids and lipids, therefore demonstrating that the organics are being preserved and the bones are being degraded similarly, indicating that the organic preservation in the bone is original to the animal.

Maturation experiments

We use maturation experiments as a thermal proxy for the degradation of proteins in modern bones that have been used in comparative studies analyzing the molecular preservation of fossil

bone (Collins et al. 2002) and melanin (Colleary et al. 2015). The data on the 67 amino acid fragments in the experimental samples were included in the PCA plots with the fossil mammoth bones, associated rock matrix and unaltered modern elephant rib sample. The long term, lower temperature (100°C) experiments are most similar to the permafrost mammoth bone, which was subjected to the least degradation. The higher temperature experiment included, which was conducted for 24 hours at 200°C is most similar to the mammoth bones from the channel and sinkhole deposits. The sediment matrix samples from these two deposits are distinct and show the greatest variation from the rest of the samples, with the rib from the sinkhole displaying some similarities to the high temperature experiments and associated fossil material. The mammoth rib from natural asphalt is distinct from all fossil and sediment matrix samples, consistent with expectations of exogenous organic contaminants from the depositional environment (i.e., bitumen).

TOF-SIMS analysis of the matured elephant bone shows the loss of whole amino acids as the temperature increases. All 19 amino acids are detected in the 100°C experiments, with no apparent variation based on time intervals. In the 200°C experiments, however, ten whole amino acids are detected, whereas in the 250°C experiments, only 5 whole amino acids are detected. Gly and Pro, which are among the most thermally stable amino acids are found in all three experimentally matured bones, whereas Arg and Cys, which are the least thermally stable amino acids do not appear in any of the maturation samples.

The PCA analysis of 67 fragments includes 12 whole amino acids and associated amino acid fragments (Figure 1) and shows that the low temperature experiments (100°C) are more similar to the permafrost mammoth fossil that shows the highest organic preservation regardless of the time of the experiments. Additionally, the higher temperature experiment (200°C) is most

similar to the channel deposit and sinkhole mammoth fossils, which preserve less organic information. Twelve whole amino acid molecules are included in the PCA analysis because they are present in both the 100°C and 200°C experiments. These include: Gly, Ala, Ser, Pro, Val, Thr, Leu, Lys, Gln, Met, Phe, Tyr. The 250°C experiment only retains five whole amino acids (Gly, Ser, Pro, Asn, Phe) and is therefore not included in the PCA analysis, which cannot incorporate missing data. The preservation of Gly and Pro in the 250°C sample is consistent with thermal degradation expectations and have been used as indicators of collagen in deep time studies (Surmik et al. 2015). Cys and Arg are not present in any of the matured samples, which is consistent with these two amino acids being the least thermally stable (Wang et al. 2012).

Conclusions

By combining a series of analytical techniques we are able to demonstrate that the organic biomolecules detected are original to the animals in this study. We correlate both preservation and degradation, supporting a taphonomic point of view that the least degraded fossil preserves more organic information. Additionally, lipid biomarkers determine the source and extent of exogenous contamination in the fossils. The modern bone contains sterols and fatty acids, but n-alkanes, which are diagenetic products from labile lipids are not present. The degradation of proteins and amino acids in different burial environments on such short time scales should be considered when analyzing peptides and amino acids in fossils preserved on longer time scales. Examining the larger context of degradation and influence of temperature and burial environments in which biomolecules are detected is essential in deep time studies, particularly dinosaur fossils that are found in fluvial environments. Future studies will benefit from analyses

with sediment controls and surface mass spectroscopy that can compare preservation across the surface area of the fossil bone and can test the mechanisms for preservation.

References

Asara, J.M., Schweitzer, M.H., Freimark, L.M., Phillips, M. and Cantley, L.C., 2007. Protein sequences from mastodon and *Tyrannosaurus rex* revealed by mass spectrometry. *Science*, *316*(5822), pp.280-285.

Bern, M., Phinney, B.S. and Goldberg, D., 2009. Reanalysis of *Tyrannosaurus rex* mass spectra. *Journal of proteome research*, *8*(9), pp.4328-4332.

Bertazzo, S. et al. 2015. Fibres and cellular structures preserved in 75-million–year-old dinosaur specimens. *Nature Communications*, *6*, p.7352.

Boatman, E.M. et al. 2014. Synchrotron chemical and structural analysis of *Tyrannosaurus rex* blood vessels: the contribution of collagen hypercrosslinking to tissue longevity. *Microscopy and Microanalysis*, *20*(S3), pp.1430-1431.

Bodnar, R.J., and Sterner, S.M 1987. Synthetic fluid inclusions, in hydrothermal experimental techniques, G.C. Ulmer and H.L. Barnes, eds., Wiley-Interscience, New York. p.423-457.

Briggs, D.E. and Summons, R.E., 2014. Ancient biomolecules: their origins, fossilization, and role in revealing the history of life. *BioEssays*, *36*(5), pp.482-490.

Buckley, M., 2015. Ancient collagen reveals evolutionary history of the endemic South American ‘ungulates’. *Proc. R. Soc. B*, *282*(1806), p.20142671.

Cappellini, E., Collins, M.J. and Gilbert, M.T.P., 2014. Unlocking ancient protein palimpsests. *Science*, *343*(6177), pp.1320-1322.

Cleland, T.P. et al. 2015. Mass spectrometry and antibody-based characterization of blood vessels from *Brachylophosaurus canadensis*. *Journal of Proteome Research*, *14*(12), pp.5252-5262.

Colleary, C. et al. 2015. Chemical, experimental, and morphological evidence for diagenetically altered melanin in exceptionally preserved fossils. *Proceedings of the National Academy of Sciences*, *112*(41), pp.12592-12597.

Collins, M.J. et al. 2002. The survival of organic matter in bone: a review. *Archaeometry, 44*(3), pp.383-394.

Demarchi, B. et al. 2016. Protein sequences bound to mineral surfaces persist into deep time. *Elife*, *5*, p.e17092.

Evershed, R.P., Turner-Walker, G., Hedges, R.E., Tuross, N. and Leyden, A., 1995. Preliminary results for the analysis of lipids in ancient bone. *Journal of Archaeological Science, 22*(2), pp.277-290.

Kaye, T.G., Gaugler, G. and Sawlowicz, Z., 2008. Dinosaurian soft tissues interpreted as bacterial biofilms. *PLOS ONE*, *3*(7), p.e2808.

Kögel-Knabner, I., 2002. The macromolecular organic composition of plant and microbial residues as inputs to soil organic matter. *Soil Biology and Biochemistry*, *34*(2), pp.139-162.

Laury, R.L., 1980. Paleoenvironment of a late Quaternary mammoth-bearing sinkhole deposit, Hot Springs, South Dakota. *Geological Society of America Bulletin*, *91*(8), pp.465-475.

Lee, Y.C., et al. 2017. Evidence of preserved collagen in an Early Jurassic sauropodomorph dinosaur revealed by synchrotron FTIR microspectroscopy. *Nature Communications*, *8*. p. 14220.

Napier, J.A. and Graham, I.A., 2010. Tailoring plant lipid composition: designer oilseeds come of age. *Current Opinion in Plant Biology*, *13*(3), pp.329-336.

Nielsen-Marsh, C.M. and Hedges, R.E., 2000. Patterns of diagenesis in bone I: the effects of site environments. *Journal of Archaeological Science*, *27*(12), pp.1139-1150.

Orlando, L., et al. 2013. Recalibrating *Equus* evolution using the genome sequence of an early Middle Pleistocene horse. *Nature*, *499*(7456), pp.74-78.

Pevzner, P.A., Kim, S., Ng, J. 2008. Comment on "Protein sequences from mastodon and Tyrannosaurus rex revealed by mass spectrometry". *Science*, *321*(5892), p.1040.

San Antonio, J.D. et al. 2011. Dinosaur peptides suggest mechanisms of protein survival. *PLOS ONE*, *6*(6), p.e20381.

Schweitzer, M.H., 2011. Soft tissue preservation in terrestrial Mesozoic vertebrates. *Annual Review of Earth and Planetary Sciences, 39,* pp.187-216.

Schweitzer, M.H., et al. 2009. Biomolecular characterization and protein sequences of the Campanian hadrosaur *B. canadensis*. *Science*, *324*(5927), pp.626-631.

Schweitzer, M.H. et al. 2007. Analyses of soft tissue from *Tyrannosaurus rex* suggest the presence of protein. *Science*, *316*(5822), pp.277-280.

Schweitzer, M.H., Wittmeyer, J.L., Horner, J.R. and Toporski, J.K., 2005. Soft-tissue vessels and cellular preservation in *Tyrannosaurus rex*. *Science*, *307*(5717), pp.1952-1955.

Schroeter, E.R. et al. 2017. Expansion for the *Brachylophosaurus canadensis* collagen I sequence and additional evidence of the preservation of Cretaceous protein. *Journal of Proteome Research*, *16*(2), pp.920-932.

Schroeter, E.R. and Cleland, T.P., 2016. Glutamine deamidation: an indicator of antiquity, or preservational quality?. *Rapid Communications in Mass Spectrometry, 30*(2), pp.251-255.

Surmik, D. et al. 2016. Spectroscopic studies on organic matter from Triassic reptile bones, Upper Silesia, Poland. *PLOS ONE*, *11*(3), p.e0151143.

Thiel, V. et al. 2014. Occurrence and fate of fatty acyl biomarkers in an ancient whale bone (Oligocene, El Cien Formation, Mexico). *Organic Geochemistry*, *68*, pp.71-81.

Thomas, D.B., Fordyce, R.E., Frew, R.D. and Gordon, K.C., 2007. A rapid, non-destructive method of detecting diagenetic alteration in fossil bone using Raman spectroscopy. *Journal of Raman Spectroscopy*, *38*(12), pp.1533-1537.

Volkman, J.K., 1986. A review of sterol markers for marine and terrigenous organic matter. *Organic Geochemistry*, *9*(2), pp.83-99.

Welker, F., et al. 2015. Ancient proteins resolve the evolutionary history of Darwin's South American ungulates. *Nature*, *522*(7554), pp.81-84.

FIGURES

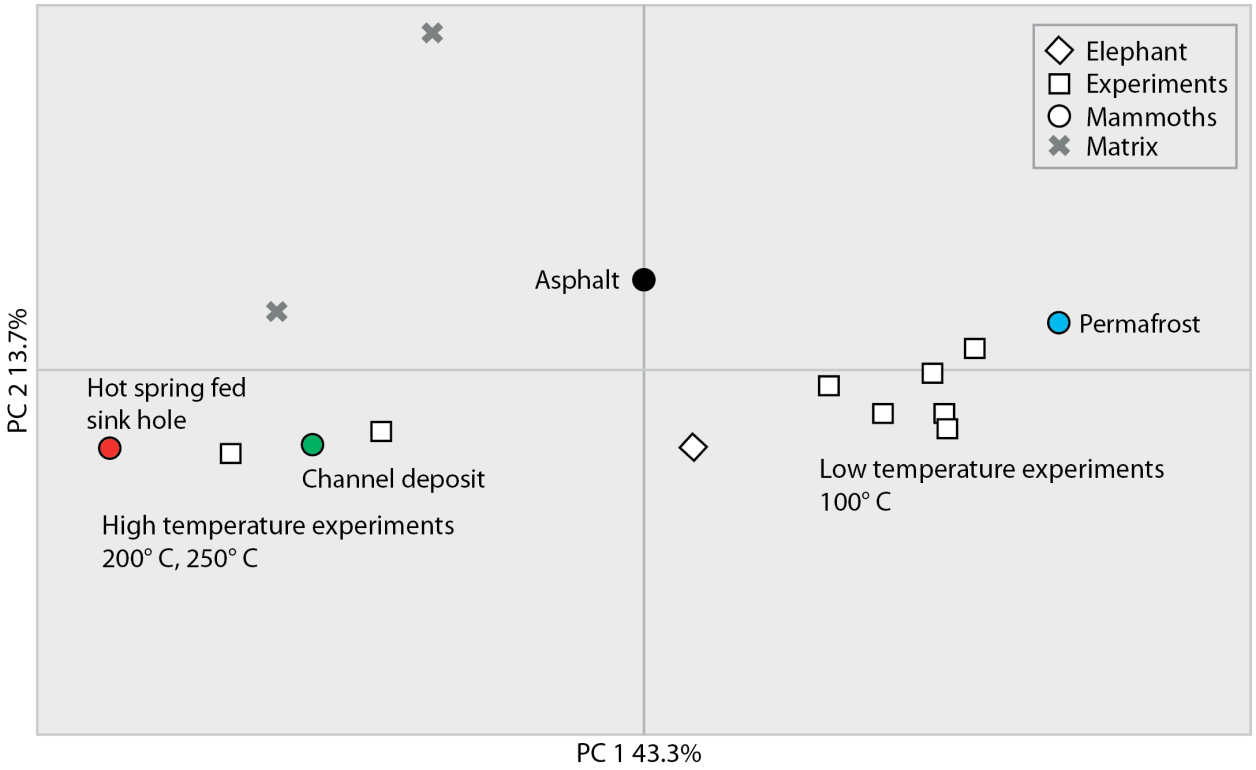

Figure 1.1 Principal component analysis (PCA) of 67 peaks associated with whole amino acid fragments detected using TOF-SIMS. The modern elephant bone (◊) plots near the Yukon mammoth fossil (○) and the low temperature maturation experiments (□). The Schultz site and Mammoth Site fossils (○) plot with the 200° C high temperature maturation experiment (□). The matrix (x) and the Rancho La Brea mammoth fossil (○) plot separately.

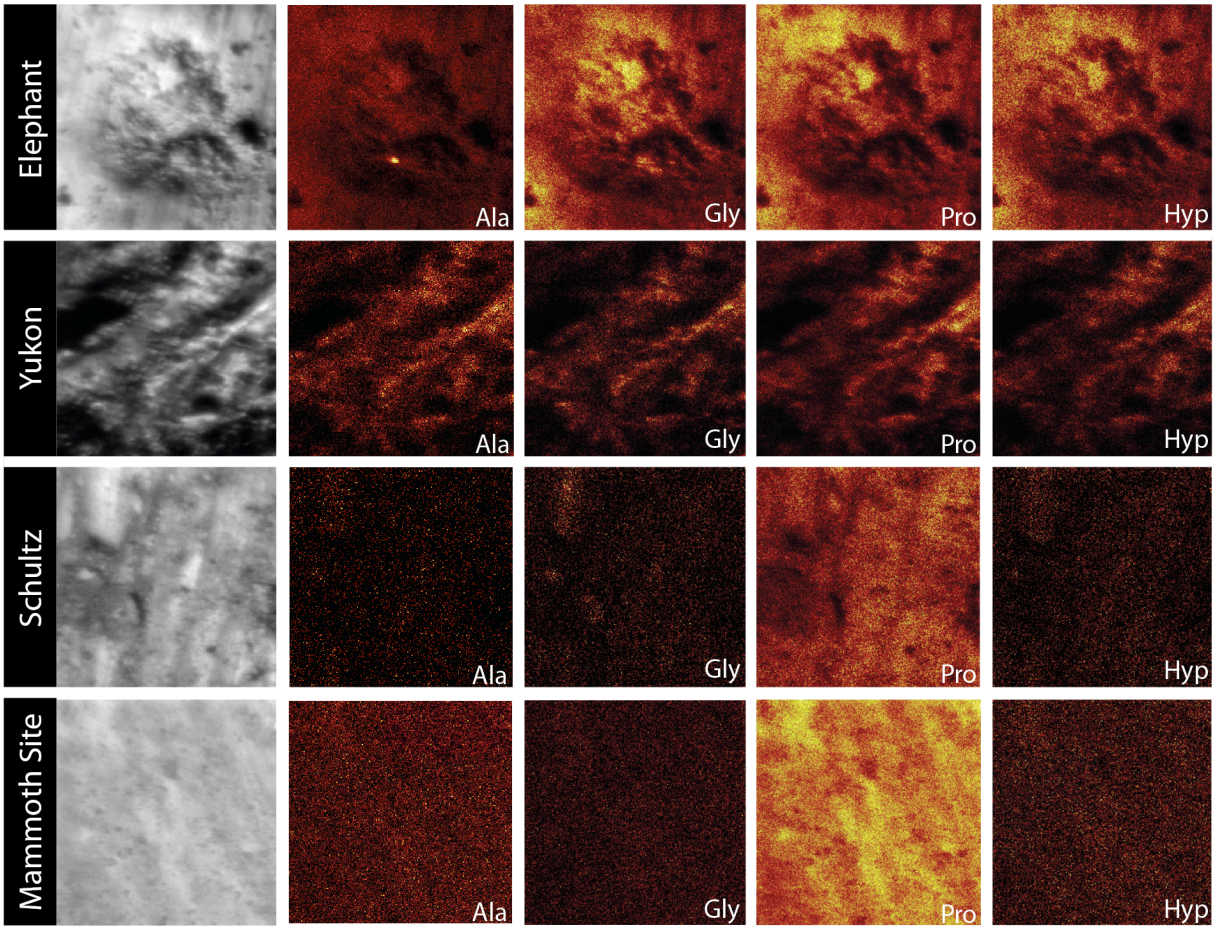

Figure 1.2 TOF-SIMS molecular maps showing the intensity of a given molecule in a 500 x 500 μm^2 area of the bone (lighter colors = higher intensity, darker colors = lower intensity). The top row is the unaltered elephant bone, the second row is the mammoth bone preserved in permafrost, the third row is the mammoth bone preserved in a channel deposit and the last row is the mammoth bone preserved in a hot spring-fed sink hole. The amino acids alanine (Ala), glycine (Gly), proline (Pro) and hydroxyproline (Hyp) are commonly found in the protein collagen. Gly, Pro and Hyp have high intensities in the elephant and Yukon bones, whereas the amino acids decrease in the Schultz and Mammoth Site bones, except for proline.

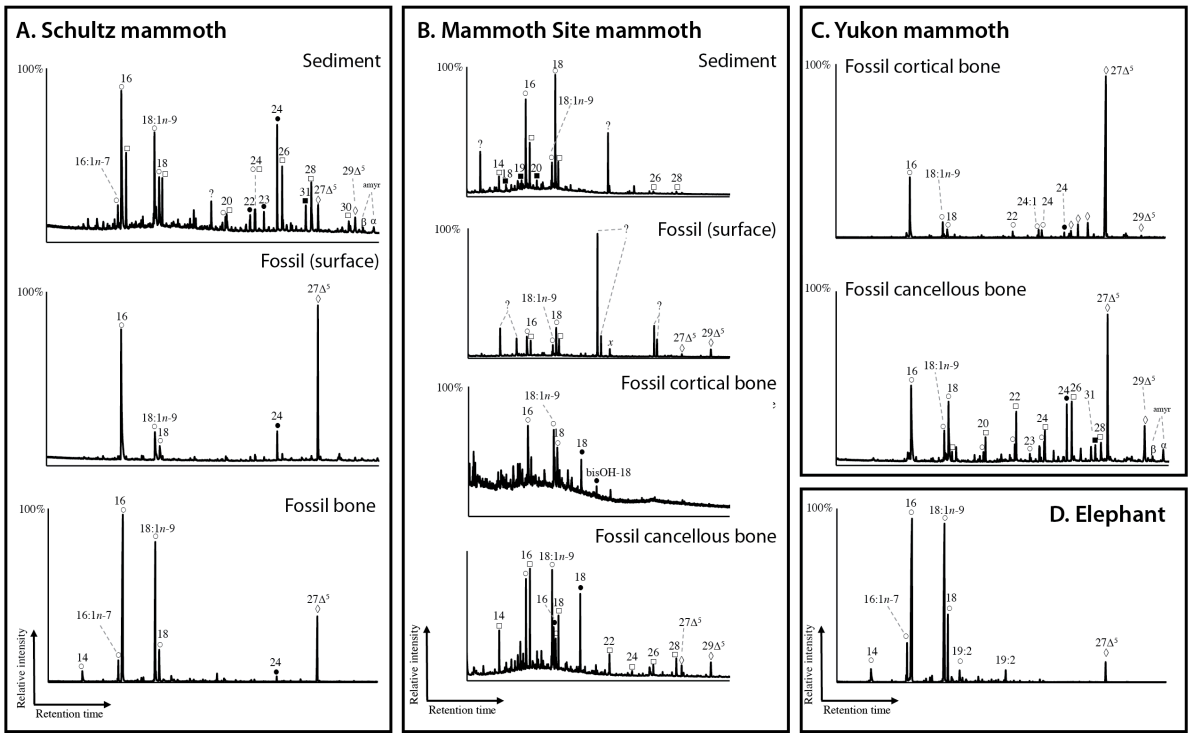

Figure 1.3 Partial total ion chromatograms showing the lipid distributions from the sediment matrices and fossil bones from Schultz mammoth, stream deposit (A), B. Mammoth Site, hot spring-fed sinkhole (B), Yukon mammoth, permafrost (C) and lipids from modern African elephant bone (D). '○' are fatty acids, '●' are 2-hydroxy fatty acids, '□' are n-alkan-1- ols, '■' are n-alkanes and '◊' are sterols. 'amyr' corresponds to alpha and beta amyrin.

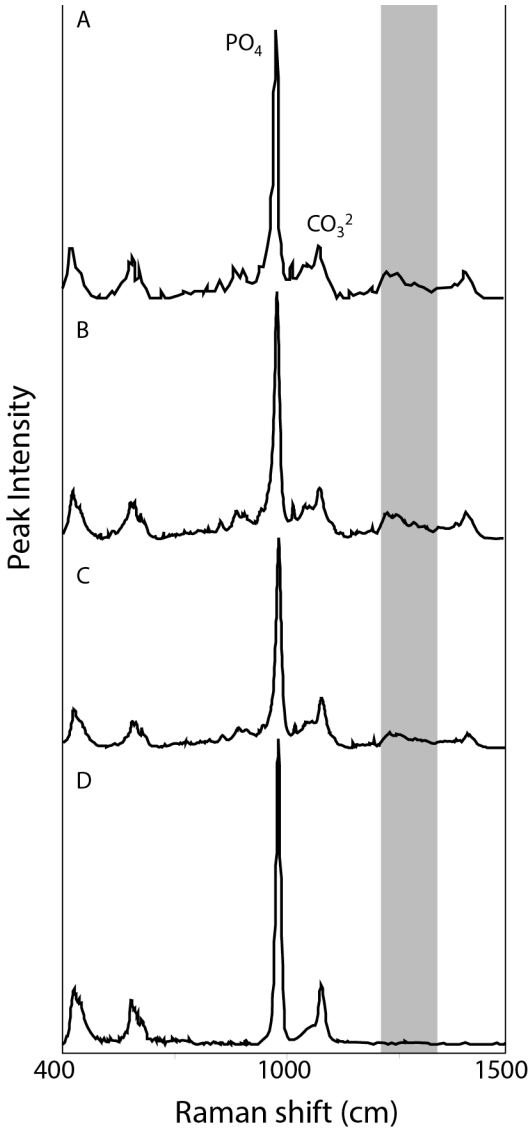

Figure 1.4 The accessory ion shift (PO_4 band) showing the degree of diagenetic alteration from the modern elephant to the Mammoth Site mammoth fossil (Thomas et al. 2007). The grey highlights the organic Amide III band that disappears as the degree of preservation declines from left to right.

Table 1.1 Amino acid assignments

Amino Acid	Mass	Chemical formula
Glycine	75	$C_2H_5NO_2$
Alanine	89	$C_3H_7NO_2$
Serine	105	$C_3H_7NO_3$
Proline	115	$C_5H_9NO_2$
Valine	117	$C_5H_{11}NO_2$
Threonine	119	$C_4H_9NO_3$
Cysteine	121	$C_3H_7SNO_2$
Leucine	131	$C_6H_{13}NO_2$
Asparagine	132	$C_4H_8N_2O_3$
Lysine	146	$C_6H_{14}N_2O_2$
Glutamic acid	147	$C_5H_9NO_4$
Methionine	149	$C_5H_{11}SNO_2$
Phenylalanine	165	$C_9H_{11}NO_2$
Arginine	174	$C_6H_{14}N_4O_2$
Tyrosine	181	$C_9H_{11}NO_3$

Amino acid fragments		
Mass	**Assignment**	**Source**
30	CH_4N	Orlando et al. 2013
39	C_2HN	Assigned
40	C_2H_2N	Assigned
41	C_3H_5	Assigned
43	C_3H_7	Orlando et al. 2013
44	C_2H_6N	Orlando et al. 2013
55	C_3H_5N	Assigned
56	C_3H_6N	Orlando et al. 2013
57	C_4H_9	Assigned
59	CN_3H_5 or C_3H_7O	Orlando et al. 2013
60	C_2H_6NO or C_3H_8O	Orlando et al. 2013
61	C_2H_5S	Orlando et al. 2013
67	C_4H_5N	Assigned
68	C_4H_6N	Orlando et al. 2013
69	C_4H_5O or $C_2H_3N_3$	Orlando et al. 2013
71	$C_3H_3O_2$	Orlando et al. 2013
72	$C_4H_{10}N$	Orlando et al. 2013
74	C_3H_8NO	Orlando et al. 2013
76	C_2H_6NS or C_5H_2N	Orlando et al. 2013
81	C_4H_5N2 or C_5H_7N	Orlando et al. 2013
82	$C_4H_6N_2$ or $C_3N_4N_4O$	Orlando et al. 2013
83	C_5H_9N	Orlando et al. 2013
85	$C_5H_{11}N$	Assigned
87	$C_3H_7N_2O$ or $C_3H_9N_3$	Orlando et al. 2013
88	$C_3H_6NO_2$ or C_6H_2N	Orlando et al. 2013

91	C_7H_7	Orlando et al. 2013
93	$C_3H_{11}NO_2$	Assigned
95	C_5H_5NO	Assigned
97	$C_4H_3NO_2$	Assigned
98	$C_4H_4NO_2$	Orlando et al. 2013
100	$C_4H_{10}N_3$	Orlando et al. 2013
102	$C_4H_8NO_2$	Orlando et al. 2013
103	$C_4H_9NO_2$	Assigned
104	$C_4H_{10}NS$ or C_8H_8	Orlando et al. 2013
107	C_7H_7O	Orlando et al. 2013
109	$C_7H_{11}N$	Assigned
110	$C_5H_8N_3$	Orlando et al. 2013
111	$C_5H_9N_3$	Assigned
112	$C_5H_{10}N_3$	Assigned
113	$C_6H_{11}NO$	Assigned
120	$C_8H_{10}N$	Orlando et al. 2013
122	C_7H_8NO	Assigned
127	$C_5H_{11}N_4$	Orlando et al. 2013
130	C_9H_8N	Orlando et al. 2013
138	$C_6H_6NO_2$	Assigned
141	$C_6H_9N_2O_2$	Assigned
152	$C_6H_8NO_2$	Assigned
159	$C_{10}H_{11}N_2$	Orlando et al. 2013
168	$C_8H_{10}NO_3$	Assigned
169	$C_8H_{11}NO_3$	Assigned
171	$C_6H_{11}N_4O_2$	Assigned
175	$C_9H_5NO_3$	Assigned
177	$C_9H_7NO_3$	Assigned

CHAPTER TWO

TAPHONOMY OF A WELL-PRESERVED TERRESTRIAL VERTEBRATE ASSEMBLAGE (LATE TRIASSIC PERIOD ~212 MA): DOES GOOD MORPHOLOGICAL PRESERVATION MEAN ORIGINAL BIOMOLECULES ARE PRESERVED?

Caitlin Colleary[1*], Shane O'Reilly[2], Kirsty E. H. Penkman[3], Marc Dickinson[3], Andrei Dolocan[4], Jason G. Toyoda[5], Rosalie K. Chu[5], Malak Tfaily[5], Michael F. Hochella[1,5] Sterling J. Nesbitt[1]

[1] Department of Geosciences, Virginia Tech, Blacksburg, VA 24061, United States
[2] School of Earth Sciences, University College Dublin, Dublin 4, Ireland
[3] BioArch, Departments of Biology, Archaeology and Chemistry, Biology S Block, University of York, York YO10 5YW, United Kingdom
[4]Texas Materials Institute, University of Texas at Austin, Austin, TX 78712, United States
[5]Environmental Molecular Sciences Laboratory, Pacific Northwest National Laboratory, Richland, WA, United States

*Corresponding author: colleary@vt.edu

Abstract

Exceptionally preserved fossils retain soft tissues and often the biomolecules that were present in an animal during its life. The majority of terrestrial vertebrates are not traditionally considered exceptionally preserved, with fossils falling on a spectrum ranging from very well-preserved to poorly preserved when considering completeness, morphology and the presence of microstructures. Within this variability of preservation, high quality macro-scale preservation (e.g., articulated skeletons) may not be reflected in molecular-scale preservation (i.e., biomolecules). Excavation of the Hayden Quarry (HQ; Chinle Formation, Ghost Ranch, New Mexico, USA) has recovered thousands of fossilized vertebrate specimens and has contributed greatly to our knowledge of early dinosaur evolution and paleoenvironmental conditions during the Late Triassic (~212 Ma). The number of specimens, completeness of skeletons and fidelity of osteohistological microstructures preserved in the bone all demonstrate the remarkable quality of the fossils preserved at this locality. As an excellent example of good preservation in a fluvial environment, we have tested different fossil types (i.e., bone, tooth, coprolite) to examine the molecular preservation and overall taphonomy of the HQ to determine if a site with high-fidelity preservation also lends itself to preserving original biomolecules. We find that despite good preservation throughout the HQ, original lipids and proteins are not present in the fossils as demonstrated through a series of analyses. By comparing the fossils to unaltered bone from extant vertebrates, experimentally matured bone, and Jurassic- and Cretaceous Period-age dinosaurian skeletal material from other fluvial environments, it is clear that fluvial environments are not conducive to the preservation of original proteins and other macromolecules on million-year time scales.

Introduction

If original biological compounds (biomolecules) preserve on long timescales (10 – 100 million-year scales), then more of the biological remains of extinct organisms can be uncovered from the fossil record than previously considered possible, expanding what is known about ancient biology and taphonomic processes. Studies on the preservation of biomolecules often focus on exceptionally preserved fossils that retain soft tissues (Briggs & Summons and the references therein); however, soft tissue preservation requires certain controls to occur (including sediment chemistry and microbial activity) and is extremely rare (Allison & Briggs 1993). Therefore, most fossils, particularly terrestrial vertebrates, are not considered exceptionally preserved, and the quality of preservation varies from well-preserved, articulated skeletons to weathered bone fragments (Bertazzo et al. 2015). The characterization of good preservation is dependent on scale: 1) good macro-level preservation is the presence of articulated skeletons or features on the bones (e.g., muscle scars); 2) good micro-level preservation is the retention of the microstructures in bone that are often examined in histological studies (e.g., external fundamental systems, three-dimensionally preserved canaliculi); and 3) good molecular-level preservation is the retention of original biomolecules (e.g., nucleic acids, proteins, lipids) (Orlando et al. 2014). With the advent of high-resolution mass spectrometry, recent studies have begun to question if biomolecules may actually be preserved in terrestrial vertebrates more readily than previously considered and in a greater range of depositional settings (Schweitzer et al. 2007, Bertazzo et al. 2015), which would open up much of the terrestrial record of vertebrates to recover more data for ancient animals.

The terrestrial fossil record is heavily biased toward fossils preserved in fluvial sedimentary settings, therefore the majority of studies that have investigated the preservation of

biomolecules in dinosaurs and other terrestrial vertebrates have done so in fossils that are preserved in stream channel, flood plain, delta, and coastal paleoenvironments (White et al. 1998, Schweitzer et al. 2007, Bertazzo et al. 2015, Lee et al. 2017, Schroeter et al. 2017). Course-grained sandstones and conglomerates are common lithologies in these paleoenvironments and are not normally considered to be conducive to exceptional or good preservation (Allison 1988), although some have suggested that the porosity of sandstones may actually improve molecular preservation (Schweitzer et al. 2007). Additionally, the influence of water on molecular-scale preservation in fluvial environments has not been experimentally tested, despite being hypothesized to not be conducive to the preservation of biomolecules (i.e., nucleic acids and proteins) (Eglinton & Logan 1991).

Therefore, to test how the quality of preservation in a fluvial terrestrial fossil assemblage affects molecular-scale preservation, we examined the Hayden Quarry (HQ) (Chinle Formation, Petrified Forest Member, Ghost Ranch, New Mexico), a locality that preserves an extraordinary Late Triassic (~212 Ma) record of dinosaur evolution and paleoenvironmental change (e.g., Irmis et al. 2007, Irmis et al. 2011, Whiteside et al. 2013). The HQ is made up of four quarries (H1–H4) that represent paleo-channels, with alternating mudstones and siltstones and poorly sorted sandstones and conglomerates (Irmis et al. 2007). The depositional environment is interpreted as episodes of transient flooding whereby plants and animals were washed in from land, punctuated with periods of standing water (Irmis et al. 2007: supplement). The HQ is a very well-preserved assemblage of terrestrial vertebrates, including both complete skeletons and very small vertebrates (with vertebrae discovered as small as ~1 mm) and histological analyses of the fossil bone show high fidelity micro-scale preservation (Werning 2013).

Here, we examine whether high quality macro and micro-level preservation are indicative of good molecular-level preservation. We analyzed three different types of fossilized tissues from one paleo-channel in the HQ (H4): the femur of the early theropod dinosaur *Tawa hallae* (GR1065) (Nesbitt et al., 2009), a phytosaur tooth (GR1064), and a coprolite with digested bone from an indeterminate vertebrate (GR1063). We also analyzed an additional bone from H4 (GR1066) and bone from an adjacent paleo-channel in the HQ (H2) (GR1067) to compare preservation across two closely associated fluvial environments and address variation in molecular preservation by fossil type. Additionally, we compared the Triassic fossil bone to Cretaceous and Jurassic Period dinosaur bones from similar depositional environments, bone from extant vertebrates, experimentally matured bone (i.e., bone from extant vertebrates that was subjected to a range of temperatures to accelerate the degradation process), and a matrix sample to control for how fluvial sedimentary environments influence the fidelity of molecular preservation over hundreds of millions of years.

Institutional Abbreviations: Ghost Ranch, Hayden Quarry (GR), Los Angeles Museum of Natural History (LACM), Mammoth Site of Hot Springs, South Dakota (MS)

Methods

Specimens

Thin sections from the Hayden Quarry (HQ) were analyzed to compare different types of fossils and to test the differences in analyzing thin sections and whole bone fragments using surface mass spectrometric techniques (e.g., time of flight secondary ion mass spectrometry). The HQ specimens thin sectioned and analyzed are: a tooth (phytosaur; GR1064), a bone (femur from the early theropod *Tawa hallae*; GR1065) and a coprolite from an unknown vertebrate (GR1063).

Additionally, dinosaur rib fragments used in analysis include a Cretaceous Period-aged theropod (LACM 23844), a Jurassic Period-aged sauropod (LACM 154089), and two Triassic Period-aged rib fragments from the H2 (GR1067) and H4 (GR1066). All of these fossils were weathered out of or excavated from fluvial depositional environments with sandstone or mudstone lithologies (Dodson et al. 1980, White et al. 1998, Irmis et al. 2007). A matrix sample collected in conjunction with the rib fragment (GR1066) from the HQ was included to compare to the organics found in the fossils. Recently deceased alligator (*Alligator mississippiensis* TMM M-12613) and elephant (African elephant MS-E01) bone samples were used to compare unaltered bone chemistry using the same techniques.

Maturation Experiments

Experimentally matured bone samples were analyzed from a previous study (Chapter 1). A diamond saw (Dremel®) was used to cut a fresh African elephant rib bone (deceased zoo animal, ME-E-01) into three 2 mm^2 fragments. The fragments were sealed in 3 x 15 mm platinum capsules, however this does not prevent water from evaporating. They were loaded into cold-sealed pressure vessels in the Hydrothermal Laboratory at Virginia Tech. These short-term experiments accelerate the degradation of the bone and were conducted for 24 hours at 100°C, 200°C and 250°C at atmospheric pressure (based on the protocol in Colleary et al. 2015). Long term experiments (up to one month) were conducted at the same temperatures, but the chemical compositions did not differ from the short-term experiments and the data are not included here.

Time-of-Flight secondary ion mass spectrometry (TOF-SIMS)

TOF-SIMS analysis was performed using an ION-TOF TOF.SIMS 5 at The University of Texas at Austin, Texas Materials Institute. A pulsed (20 ns, 10 kHz) analysis ion beam of Bi_3^+ clusters at 30-kV ion energy was raster-scanned over 500 x 500 μm^2 areas. Bi_3^+ polyatomic sputtering was used to reduce the fragmentation of large organic molecules. A constant flux, 21 eV electron beam was used during data acquisition to reduce sample charging. Secondary ions had positive polarity and an average mass resolution of 1-3000 (m/δm). The base pressure during acquisition was <1 x 10^{-8} mbar. Mass calibration was performed by identifying the peak positions of CH_2^+, CH_3^+, $C_2H_3^+$, and $C_3H_3^+$ secondary ions. Regions of interest were chosen to reduce the effects of topographyPositive and negative spectra used? (which even at micron-scales, can influence the time it takes certain molecules to reach the analyzer, therefore impeding correct molecular assignment).

We developed a chemical fingerprint of 87 secondary ion peaks and mapped the distribution of positive spectra of ionized molecules on the bone surface using TOF-SIMS in fresh bone and dinosaur fossils. Amino acids, amino acid fragments and mineral elements were chosen to characterize the preservation of each sample. The fingerprint was developed by combining relevant peaks from previous analyses (e.g., Orlando et al. 2014) and choosing additional peaks that are present in the samples (Table 2.1). Matrix (rock samples not containing fossils) from the same horizon as the fossils with in the HQ and fresh bone were used to compare the degradation of bone that occurs during fossilization.

Lipid Analyses

Two Triassic Period rib fossils (GR1065, GR1066) were separated from matrix sediment manually and the fossil surfaces were cleaned using a dental drill and solvent-cleaned steel drill-bits. Powders were drilled from cleaned fossils. The powder from the cleaning procedure for H2 was also retained. Sediment matrix was powdered using a solvent-cleaned mortar and pestle. Between 250 and 600 mg of powdered sample was each weighed into 12 mL glass tubes. Samples were extracted for 30 minutes (x 3) with 9:1 (v/v) dichloromethane/methanol using sonication for 30 minutes in an ultrasonic bath at room temperature (~21° C). Extracts were separated from solid residues by centrifugation, and supernatants from each step were combined to give a total lipid extract (TLE). TLEs were concentrated to minimal volume under a gentle stream of high purity N_2 gas. A portion each TLE was silylated with N,O-Bis(trimethylsilyl)trifluoroacetamide /trimethylchlorosilane mixed with pyridine (9:1 v/v) at 70°C for 2 hours. Aliquots of the derivatized samples were analyzed by gas chromatography/mass spectrometry (Agilent 5890 GC hyphenated to an Agilent 5975C Mass Selective Detector). The GC was equipped an Agilent J&W HP-5MS non-polar capillary column (30 m length, 0.25 mm inner diameter, 250 μm film thickness). The GC temperature program was: 70°C for 2 minutes, ramp at 10°C min^{-1} to 130°C, followed by a ramp to 300°C at 4°C min^{-1} and a final hold time of 20 minutes. The mass spectrometer was operated in electron impact ionization mode (70 eV), with a mass scan range from m/z 50 to 600. All glassware was fired (550°C overnight) and all solvents used were high-purity (OmniSolv). Procedural blanks were run to monitor background contamination.

FTICR-MS and Environmental Compounds

Fossil samples were prepared by powdering in individual mortar and pestles that were wrapped in aluminum foil, rinsed in nano pure water, rinsed in ethanol and then combusted at 400° C for 8 hours. Blanks were created by rinsing and collecting 2 mL of nano pure water, 2 mL of MeOH and ~2 mL of $CHCl_3$ from each mortar and pestle. We analyzed bone and sediment from HQ, two dinosaur bones (LACM 154089 and LACM 154089) and a modern elephant bone (MS-E-01). We combined two rib fragments from Ghost Ranch (GR1065, GR1066) as one sample. Each sample was powdered using the mortar and pestle until we had ~1.5 grams for each sample. The elephant sample was prepared in liquid nitrogen prior to powdering.

Three sets of extractions were conducted on each bone sample: water, methanol (MeOH,) and chloroform ($CHCl_3$) because each type of extraction removes different compounds for analysis. Water extractions were done first to extract water-soluble proteins and peptides. 5 mL of nano pure water was added to the powdered samples in leach-free falcon tubes and vortexed at 1000 rpm for 2 hours. Samples were then centrifuged for 5 minutes at 4500 rpm to pellet the samples. These steps were repeated using methanol (MeOH) to extract other organics and chloroform ($CHCl_{3)}$ to extract lipids. The samples were then stored overnight at 4° C.

The mass spectrometry analysis was performed using a 12T Fourier transform ion cyclotron resonance mass spectrometer (FTICR-MS) (Bruker solariX, Billerica, MA) outfitted with a standard electrospray ionization (ESI) interface. The mass spectrometer was set to acquire data in negative mode. Samples were directly infused using a 250uL Hamilton syringe at a flow rate of 3uL/min. Samples were diluted with Methanol, LC-MS Grade. The coated glass capillary temperature was set to 180ºC and the capillary set to + 4.2kV negative mode. The data were collected, 200 scans co-added from 100-900 m/z, at 4M with a resolution of 240K at 400m/z.

Chloride peaks were masking other peaks, so we then performed a solid phase extraction (SPE) on each of the samples before running them on the mass spectrometer again. Then the SPE fractions were analyzed on the mass spectrometer. Both negative and positive spectra were obtained to see the variation between the two.

Amino Acid Racemization

HQ bone and matrix samples, the two dinosaurian samples and the bone of an extant vertebrate were treated to release the peptide-bound amino acids, thus yielding the 'total' amino acid concentration, referred to as the ‘total hydrolysable amino acid fraction (THAA, H*) (see Penkman et al. 2008). Beyond the procedure outlined in Penkman et al. (2008) additional amino acids are also extracted from the samples. After demineralization of the bone, inorganic species are precipitated out of solution via neutralization with KOH. The samples were then centrifuged and the resulting supernatant extracted and dried via centrifugal evaporation (unpublished method). The HQ bone and matrix, sauropod bone, theropod bone, and bone from an extant vertebrate were analyzed by RP-HPLC, with standards and blanks run alongside samples. During preparative hydrolysis, both asparagine and glutamine undergo rapid, irreversible deamination to aspartic acid and glutamic acid respectively (Hill 1965). It is therefore not possible to distinguish between the acidic amino acids and their derivatives and they are reported together as ‘Asx’ and ‘Glx’ respectively. The amino acid content in all of the Mesozoic samples was extremely low, therefore an additional bleaching step was added to the analysis to extract more amino acids (Dickinson et al. 2018, unpublished data).

Results

To test if different types of contemporaneous organic fossils (i.e., bone, tooth, coprolite) can be distinguished from one another based on a chemical fingerprint in the same burial environment (HQ), we used surface mass spectrometry (TOF-SIMS) and compared the samples using multivariate statistics. Using TOF-SIMS, we analyzed a chemical fingerprint (87 organic and inorganic compounds and fragments, Table 2.1) for protein degradation products (amino acids and amino acid fragments) and the inorganic components of bone. The principle component analysis (PCA) compared the three different fossil types (i.e., bone, tooth, coprolite), the additional dinosaurian fossils, the unaltered bones of extant vertebrates and the experimentally matured bone to determine the variance between each of the samples (Figure 2.1A). When comparing the samples, there is little variation between all of the fossils from the Hayden Quarry (thin sections and polished bone fragments), which all plot together, along with the 250° C matured bone. Although, the 200° C matured bone and the sauropod bone do show slight variation from the others and plot more closely to the sediment matrix sample from the HQ. The HQ matrix sample does show a greater amount of variance from the HQ fossil samples. The two unaltered bones from extant vertebrates and the 100° C matured bone have similar molecular signatures to one another, but differ from the rest of the samples.

To further examine the variation in the samples, we removed the inorganic molecules to compare the amino acid fingerprint (Figure 2.1B). When only considering the amino acid signature, the placement of the specimens did not change considerably, however a few changes are worth noting. The separation (or variance) between the HQ fossils increased, the 250° C and 200° C matured bones separated from the other groupings entirely, the variance between the sauropod and other fossils decreased and the elephant and alligator bones shift slightly towards

the fossils. The variance on the y-axis is greatly decreased in the fossils once the inorganic peaks are removed, but the variance in the matured bone samples (100°, 200°, 250° C) increases. Additionally, the removal of the inorganic peaks decreases the percentage of variance for PC1 (the x-axis) from 46.9% to 36.5%. Additionally, TOF-SIMS molecular maps (Figure 2.2) of the HQ polished bone fragment show that the presence of specific molecules varies between certain bone features. Calcium (Ca) and iron (Fe) are ubiquitous across the bone surface, but show a decreased abundance in certain areas (round microstructures in the bone) that have a higher abundance of strontium (Sr). There is one area of the bone that shows a low abundance of Ca, Fe and Sr and a high abundance of the amino acids glycine (Gly) and alanine (Ala). Otherwise, these amino acids are in extremely low abundance, if present at all, across the bone surface.

To evaluate the presence of additional biomolecules, lipids were detected in fossil bone and the surrounding matrix (Figure 2.3). Lipids were restricted to fatty acids, including unsaturated fatty acids and the lipid profiles were very similar between the fossils and the matrix. Additionally, the associated matrix had more than eight times the extractable lipids than the fossil bone. Then, we evaluated the presence of additional organic molecules present in the HQ bone fragment and surrounding matrix, the theropod and sauropod bones, the unaltered elephant bone and a mammoth bone preserved in permafrost from a previous study (Chapter 1) using an FTIC-R mass spectrometer. In the PCA analysis (Figure 2.4), the placement of the elephant and mammoth bones were most heavily influenced by the lipid and protein compounds, the theropod and sauropod bones were most heavily influenced by the tannin, lignin and amino sugar compounds and both the HQ bone and HQ matrix showed little variation from one another and placement was most heavily influenced by unsaturated and condensed hydrocarbon compounds.

Lastly, we examined the composition (Figure 2.5) and racemization (Figure 2.6) of the amino acids in the HQ bone, HQ matrix, theropod, sauropod and a reference bone from an extant vertebrate. The HQ matrix sample is composed of high levels of serine (Ser) and l-tyrosine (Tyr), but negligible amounts of any other amino acids. The fossils and the elephant bone show similar compositions, but the fossils have higher percentages of Ser. The theropod and HQ fossils have a high percentage of glycine (Gly), whereas the sauropod has a low percentage of Gly and slightly higher percentages of valine (Val), phenylalanine (Phe), leucine (Leu) and isoleucine (Ile). Despite extremely low abundances of amino acids in most of the samples, amino acid racemization (AAR) was done using a new bleaching method and shows high levels of racemization in arginine (Arg) in all fossil samples, including the HQ matrix sample. Phe racemization has occurred in the HQ matrix, but not in the HQ bone. The amount of racemization of the amino acids in the HQ matrix is otherwise low. The HQ bone does show some racemization of glutamine (Glx), and Ser. The theropod bone has the most amino acids that show racemization, including aspartic acid (Asx), Glx, Arg, Phe, Ile and Tyr.

Discussion

To examine the organic preservation of fossils preserved in fluvial environments, we used mass spectrometry to detect animal biomolecules (lipids and amino acids), environmental compounds (e.g., lignin), and evaluated the age of the amino acids using amino acid racemization. Unlike conventional biomolecule studies that demineralize fossil bone to extract organics (e.g., Schweitzer et al. 2007), we studied the intact fossil bone to preserve taphonomic data and organic material from exogenous sources (i.e., terrestrial plant material that led to high abundances of lignin). Amino acids and amino acid fragments were detected in dinosaurian

fossils dating back to the Late Triassic (~212 Ma) and the presence of amino acids, specifically glycine, has often been invoked as evidence of ancient collagen (Schweitzer et al. 2007, Bertazzo et al. 2015, Surmik et al. 2016). However, despite detecting an amino acid signature unique to the fossil bones and distinct from the surrounding matrix, all of the evidence collected here suggests that these amino acids are not original.

Because biomolecules vary in preservation potential (Eglinton & Logan 1991), in addition to examining the amino acids present, we also examined the presence of lipids in the HQ samples to further test the fidelity of molecular preservation at this site. Fatty acids are more labile than biological lipids such as sterols or hopanoids (Sun et al., 1997) and fossils and sedimentary rocks of this age would typically contain the end products or lipid diagenesis - hydrocarbon skeletons such as steranes or *n*-alkanes – as major extractable compounds (e.g. Gold et al., 2016). Furthermore, unsaturated acids are considerably more labile than saturated fatty acids and are typically the first class of lipids to be oxidized and lost upon burial in modern sediments (Sun et al., 1997). Thus, the presence of unsaturated fatty acids in the absence of more stable lipids and diagenetic hydrocarbons indicates that the lipids detected are not syngenetic and are much more likely to be from modern (or very young) sources. Also, the fact that the extractable lipids were so much higher in the matrix sample indicates that the lipids detected in the fossil are not distinct and based on the concentration gradient, are possibly exogenous lipids from the matrix. The presence of exceptionally labile lipids (monounsaturated fatty acids) as major lipids in the fossils analyzed, the similar lipid profiles between fossils and matrices and the much higher concentration of lipids in the matrices suggest that the lipids in the bone came from the matrix and that they are from modern/recent biological sources. Therefore, the lipids detected in these samples are likely not original animal lipids and cast additional doubt on the

preservation of original proteins. Additionally, the racemization of the amino acids and the high levels of serine (an extremely decay-prone amino acid), leads us to conclude that the amino acids detected in the Mesozoic bones are not old enough to be original, ancient (~212 million-year-old) biomolecules.

By analyzing intact fossil bone, we were able to examine the inorganic components of the bone and additional sources of organics, including environmental contaminants (Figure 2.4). High levels of lignin were found in the sauropod and theropod fossils, indicative of contamination from vascular plants. Lignin is a biopolymer that preserves on very long timescales (~315 Ma) (Eglinton & Logan 1991), however it is not possible to determine with these methods if the lignin is ancient or recent, although a more recent source of the lignin may be from plant roots seeking out sources of phosphorous from buried bone. Additionally, iron is present in high intensity in the HQ bone fragment (Figure 2.2) and is a major driver in distinguishing between the fossils in the PCA (Figure 2.1). Iron cross-linking has been hypothesized to bind to organics as a mechanism for preservation (Schweitzer et al. 2012, Surmik et al. 2016), however without reliable information on the age of the organics detected in these analyses, there is little evidence that iron is acting to preserve original biomolecules.

The molecular composition of all of the fossils is similar despite being from different sources (e.g., bone, tooth, coprolite), time periods and burial environments, when considering both the organic and inorganic components of the bones which may be evidence for a taphonomic source of organics that are being introduced to fossils that are found in similar depositional environments. Therefore, fluvial environments are not conducive to the preservation of proteins very early on in preservation, demonstrated by the loss of amino acids in the

maturation experiments from the evaporation of water. In these types of environments, good preservation does not necessarily reflect good molecular preservation.

Conclusions

Despite very good macro and micro-level preservation at the Triassic Hayden Quarry, there is no evidence for original biomolecules preserved in the fossils. Lipid and amino acid evidence demonstrates that organic components in the bone vary from that of the surrounding matrix, however the amino acids present and the extent of racemization suggests that these amino acids are not old enough to be original proteins from the dinosaur bones. Therefore, fluvial environments negatively influence the preservation of water-soluble biomolecules like proteins, and caution should be employed when using amino acids as evidence for protein preservation in deep time. Examining intact bones without homogenizing the samples through demineralization allows for the identification of additional structures that may have influenced preservation that are still present in the fossils. Analyzing the taphonomy of a site is important to detect the sources of contaminants and to explain why organic molecules are either not preserved or not endogenous.

References

Allison, P.A., 1988. Konservat-Lagerstätten: cause and classification. *Paleobiology*, *14*(4), pp.331-344.

Allison, P.A. and Briggs, D.E., 1993. Exceptional fossil record: distribution of soft-tissue preservation through the Phanerozoic. *Geology*, *21*(6), pp.527-530.

Asara, J.M., Schweitzer, M.H., Freimark, L.M., Phillips, M. and Cantley, L.C., 2007. Protein sequences from mastodon and *Tyrannosaurus rex* revealed by mass spectrometry. *Science*, *316*(5822), pp.280-285.

Bertazzo, S. et al. 2015. Fibres and cellular structures preserved in 75-million–year-old dinosaur specimens. *Nature Communications*, *6*, p.7352.

Boatman, E.M. et al. 2014. Synchrotron chemical and structural analysis of *Tyrannosaurus rex* blood vessels: the contribution of collagen hypercrosslinking to tissue longevity. *Microscopy and Microanalysis*, *20*(S3), pp.1430-1431.

Briggs, D.E., Evershed, R.P. and Lockheart, M.J., 2000. The biomolecular paleontology of continental fossils. *Paleobiology*, *26*(sp4), pp.169-193.

Briggs, D.E. and Summons, R.E., 2014. Ancient biomolecules: their origins, fossilization, and role in revealing the history of life. *BioEssays*, *36*(5), pp.482-490.

Buckley, M., Larkin, N. and Collins, M., 2011. Mammoth and mastodon collagen sequences; survival and utility. *Geochimica et Cosmochimica Acta*, *75*(7), pp.2007-2016.

Buckley, M. et al. 2008. Comment on "Protein sequences from mastodon and *Tyrannosaurus rex* revealed by mass spectrometry." *Science*, 319, 33c.

Cappellini, E. et al. 2011. Proteomic analysis of a Pleistocene mammoth femur reveals more than one hundred ancient bone proteins. *Journal of Proteome Research*, *11*(2), pp.917-926.

Cleland, T.P. et al. 2015. Mass spectrometry and antibody-based characterization of blood vessels from *Brachylophosaurus canadensis*. *Journal of Proteome Research*, *14*(12), pp.5252-5262.

Colleary, C. et al. 2015. Chemical, experimental, and morphological evidence for diagenetically altered melanin in exceptionally preserved fossils. *Proceedings of the National Academy of Sciences*, *112*(41), pp.12592-12597.

Collins, M.J., Gernaey, A.M., Nielsen-Marsh, C.M., Vermeer, C. and Westbroek, P., 2000. Slow rates of degradation of osteocalcin: Green light for fossil bone protein?. *Geology*, *28*(12), pp.1139-1142.

Collins et al. 2002. The survival of organic matter in bone: a review. *Archaeometry*, *44*(3), pp.383-394.

Demarchi, B. et al. 2016. Protein sequences bound to mineral surfaces persist into deep time. *Elife*, *5*, p.e17092.

Gold, D.A., O'Reilly, S.S., Luo, G., Briggs, D.E. and Summons, R.E., 2016. Prospects for sterane preservation in sponge fossils from museum collections and the utility of sponge biomarkers for molecular clocks. *Bulletin of the Peabody Museum of Natural History*, *57*(2), pp.181-189.

Irmis, R.B. et al. 2007. A Late Triassic dinosauromorph assemblage from New Mexico and the rise of dinosaurs. *Science*, *317*(5836), pp.358-361.

Dodson, P., Behrensmeyer, A.K., Bakker, R.T. and McIntosh, J.S., 1980. Taphonomy and paleoecology of the dinosaur beds of the Jurassic Morrison Formation. *Paleobiology*, *6*(2), pp.208-232.

Hill, R.L., 1965. Hydrolysis of proteins. In *Advances in Protein Chemistry* (Vol. 20, pp. 37-107). Academic Press.

Irmis, R.B., Mundil, R., Martz, J.W. and Parker, W.G., 2011. High-resolution U–Pb ages from the Upper Triassic Chinle Formation (New Mexico, USA) support a diachronous rise of dinosaurs. *Earth and Planetary Science Letters*, *309*(3-4), pp.258-267.

Keenan, S.W. 2016. From bone to fossil: A review of the diagenesis of bioapatite. *American Mineralogist*, *101*(9), pp.1943-1951.

Lee, Y.C. et al. 2017. Evidence of preserved collagen in an Early Jurassic sauropodomorph dinosaur revealed by synchrotron FTIR microspectroscopy. *Nature Communications*, *8*, p.14220.

Leikina, E., Mertts, M.V., Kuznetsova, N. and Leikin, S., 2002. Type I collagen is thermally unstable at body temperature. *Proceedings of the National Academy of Sciences*, *99*(3), pp.1314-1318.

Nesbitt, S.J. et al. 2009. A complete skeleton of a Late Triassic saurischian and the early evolution of dinosaurs. *Science*, *326*(5959), pp.1530-1533.

Orlando, L. et al. 2013. Recalibrating Equus evolution using the genome sequence of an early Middle Pleistocene horse. *Nature*, *499*(7456), pp.74-78.

Penkman, K.E.H., Kaufman, D.S., Maddy, D. and Collins, M.J., 2008. Closed-system behaviour of the intra-crystalline fraction of amino acids in mollusc shells. *Quaternary Geochronology*, *3*(1-2), pp.2-25.

San Antonio, J.D. et al. 2011. Dinosaur peptides suggest mechanisms of protein survival. *PLOS ONE*, *6*(6), p.e20381.

Schroeter, E.R. et al. 2017. Expansion for the *Brachylophosaurus canadensis* collagen I sequence and additional evidence of the preservation of Cretaceous protein. *Journal of Proteome Research*, *16*(2), pp.920-932.

Schweitzer, M.H. et al. 2014. A role for iron and oxygen chemistry in preserving soft tissues, cells and molecules from deep time. *Proceedings of the Royal Society of London B: Biological Sciences*, *281*(1775), p.20132741.

Schweitzer, M.H., Zheng, W., Cleland, T.P. and Bern, M., 2013. Molecular analyses of dinosaur osteocytes support the presence of endogenous molecules. *Bone*, *52*(1), pp.414-423.

Schweitzer, M.H. 2011. Soft tissue preservation in terrestrial Mesozoic vertebrates. *Annual Review of Earth and Planetary Sciences*, *39*, pp.187-216.

Schweitzer, M.H. et al. 2009. Biomolecular characterization and protein sequences of the Campanian hadrosaur *B. canadensis*. *Science*, *324*(5927), pp.626-631.

Schweitzer, M.H. et al. 2007. Analyses of soft tissue from *Tyrannosaurus rex* suggest the presence of protein. *Science*, *316*(5822), pp.277-280.

Schweitzer, M.H., Wittmeyer, J.L., Horner, J.R. and Toporski, J.K., 2005. Soft-tissue vessels and cellular preservation in *Tyrannosaurus rex*. *Science*,*307*(5717), pp.1952-1955.

Schweitzer, M.H., 2004. Molecular paleontology: some current advances and problems. *Annales de Paléontologie*. Vol. 90. No. 2.

Schweitzer, M., Hill, C.L., Asara, J.M., Lane, W.S. and Pincus, S.H., 2002. Identification of immunoreactive material in mammoth fossils. *Journal of Molecular Evolution*, *55*(6), pp.696-705.

Schweitzer, M.H. and Horner, J.R., 1999, September. Intravascular microstructures in trabecular bone tissues of *Tyrannosaurus rex*. In *Annales de paléontologie* (Vol. 85, No. 3, pp. 179-192). Elsevier Masson.

Schweitzer, M.H. et al.1997. Heme compounds in dinosaur trabecular bone. *Proceedings of the National Academy of Sciences*, *94*(12), pp.6291-6296.

Sun, M.Y., Wakeham, S.G. and Lee, C., 1997. Rates and mechanisms of fatty acid degradation in oxic and anoxic coastal marine sediments of Long Island Sound, New York, USA. *Geochimica et Cosmochimica Acta*, *61*(2), pp.341-355.

Surmik, D. et al. 2016. Spectroscopic studies on organic matter from Triassic reptile bones, Upper Silesia, Poland. *PLOS ONE, 11*(3), p.e0151143.

Szpak, P., 2011. Fish bone chemistry and ultrastructure: implications for taphonomy and stable isotope analysis. *Journal of Archaeological Science*, *38*(12), pp.3358-3372.

Werning SA. 2013. Evolution of bone histological characters in amniotes, and the implications for the evolution of growth and metabolism. PhD dissertation. University of California, Berkeley. 445 p.

White, P.D., Fastovsky, D.E. and Sheehan, P.M., 1998. Taphonomy and suggested structure of the dinosaurian assemblage of the Hell Creek Formation (Maastrichtian), eastern Montana and western North Dakota. *Palaios*, *13*(1), pp.41-51.

Whiteside, J.H. et al. 2015. Extreme ecosystem instability suppressed tropical dinosaur dominance for 30 million years. *Proceedings of the National Academy of Sciences*, p.201505252.

FIGURES


A
PC 2 13.9%
HQ matrix
200° C
Sauropod
250° C
Theropod
HQ bone
HQ femur
HQ tooth
HQ tooth
HQ femur
HQ coprolite
HQ coprolite
Alligator
Elephant
100° C
PC 1 46.9%
B
PC 2 19.8%
250° C
200° C
HQ matrix
Sauropod
HQ bone
HQ femur
Theropod
HQ femur
HQ tooth
HQ tooth
HQ coprolite
HQ coprolite
Alligator
Elephant
100° C
PC 1 36.5%

Figure 2.1 Principal component analyses. (A) PCA of chemical signature of 87 organic and inorganic peaks. The modern bones (alligator and elephant) and the 100° C are more similar chemically to one another than the other samples. The HQ fossils show little variation between one another, but there is a greater amount of variation with the associated matrix. Therefore, there are amino acids present in the fossils that are not present in the associated matrix. (B) PCA of chemical signature of amino acids (63 peaks) and no inorganic peaks. When only the amino acids are considered and the inorganic peaks are removed, the overall variation is similar, however there is a greater spread in the HQ fossils and the experimentally matured bones are no longer chemically similar.

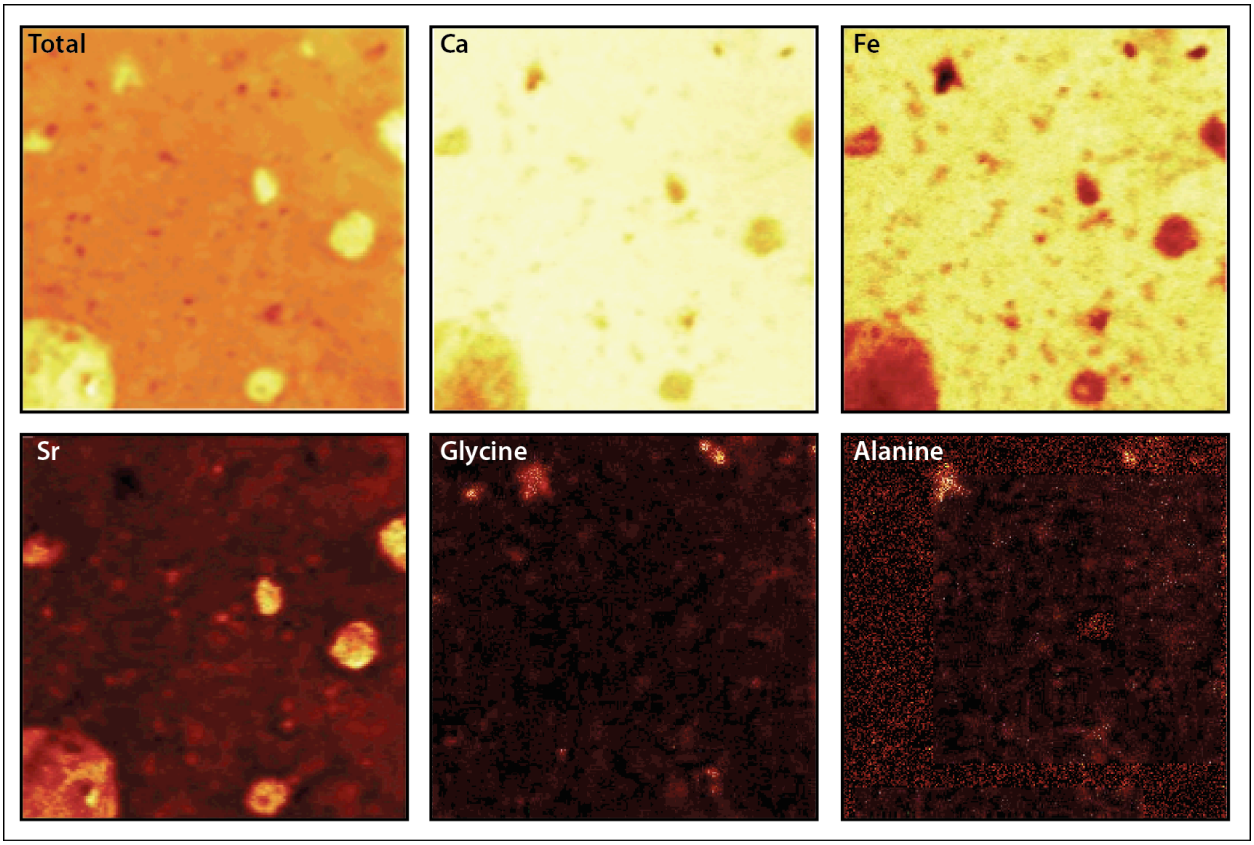

Figure 2.2 TOF-SIMS images of HQ bone. Each image is the same 500 x 500 μm area of the bone. The lighter areas represent a greater concentration of a given element or molecule, while the darker areas represent a lower concentration. Specific features of the bone, like these spheres, have a higher concentration of strontium (Sr) and lower concentrations of iron (Fe) while some elements, like calcium (Ca) are ubiquitous across the sample surface. Amino acids like glycine and alanine are both present in a single area of the bone.

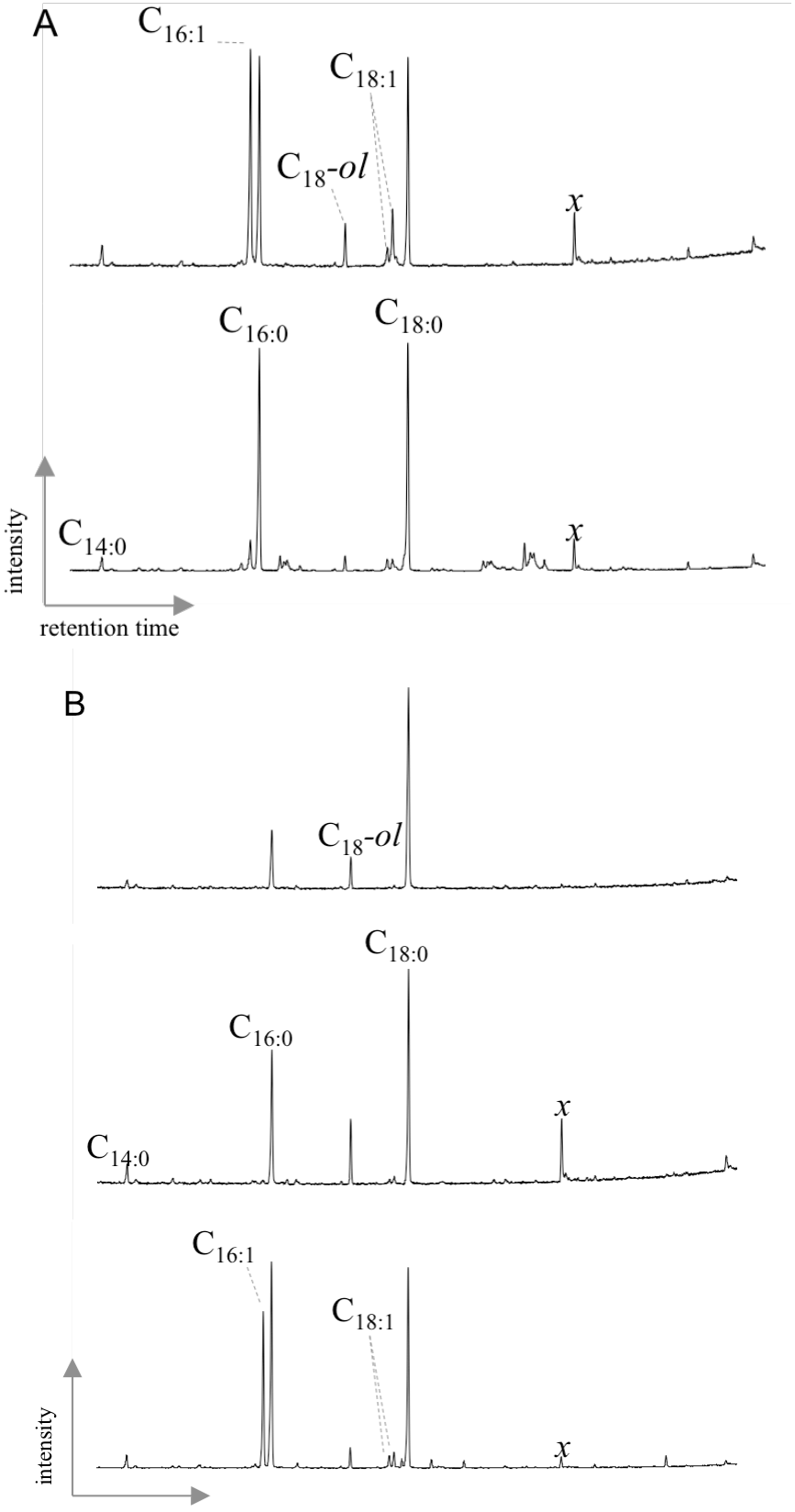
A
C16:1
C18:1
C18-ol
x
C16:0
C18:0
C14:0
x
intensity
retention time
B
C18-ol
C18:0
C16:0
x
C14:0
C16:1
C18:1
x
intensity

Figure 2.3 Partial total ion chromatograms of silyated total lipid extracts from Ghost Ranch (A) Hayden Quarry 4: top is the fossil bone, the bottom is the associated matrix. (B) Hayden Quarry 2: top is fossil bone, middle is bone surface and bottom is associated matrix. Tetradecanoic acid (C14:0), hexadecanoic acid (C16:0, C16:1), octadecanoic acid (C18:0, C18:1, octadecan-1-ol (C18:0-ol) and contaminants (x).

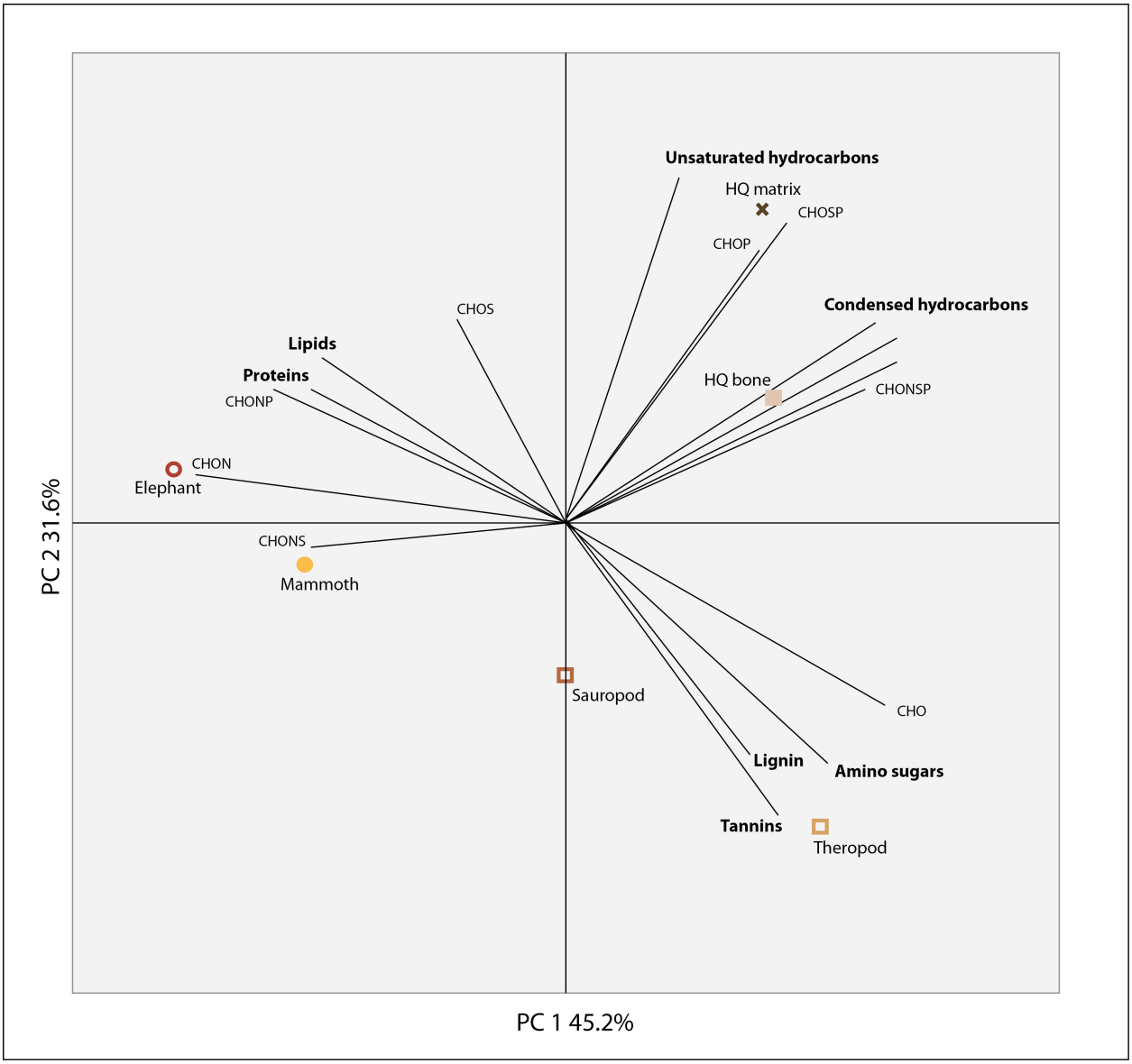

Figure 2.4 Organic extractions and environmental compounds. Examination of fossil bones by grinding them up and not demineralizing them reveals additional compounds in greater abundance than proteins and lipids. Proteins and lipids are in the greatest abundance in the elephant and mammoth bones, whereas the sauropod and theropod bones have higher abundances of lignin, tannins and amino sugars and the HQ bones have a higher abundance of unsaturated and condensed hydrocarbons. Amino acids were found in the dinosaur bones and matrix, but may be masked by the environmental compounds that are more abundant.

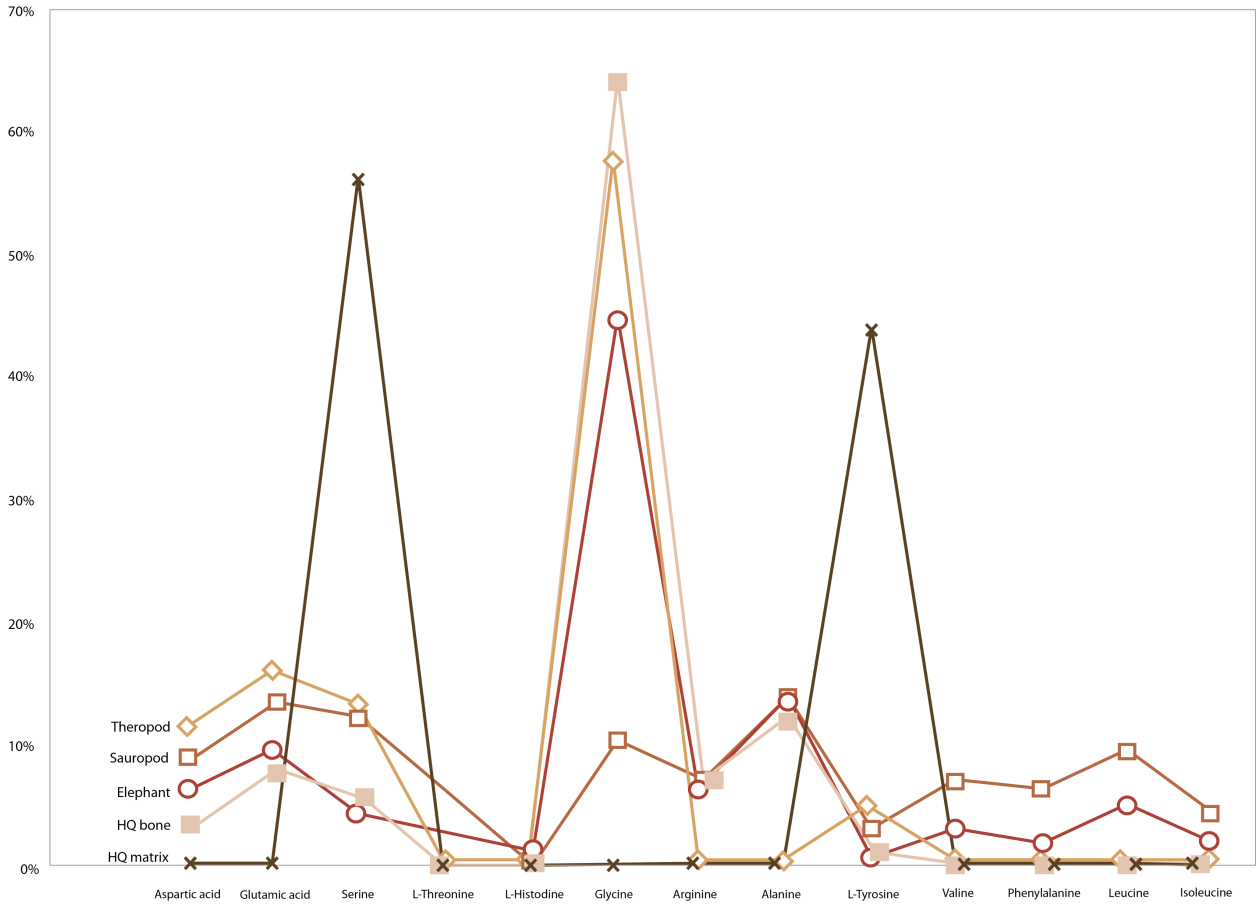

Figure 2.5 Amino acid compositions. The HQ matrix had high percentages of serine and l-tyrosine. Despite a similar overall composition as the elephant reference bone (particularly the percentage of glycine), high percentages of the decay-prone amino acid serine suggests that the amino acids in the HQ and theropod bones are not original.

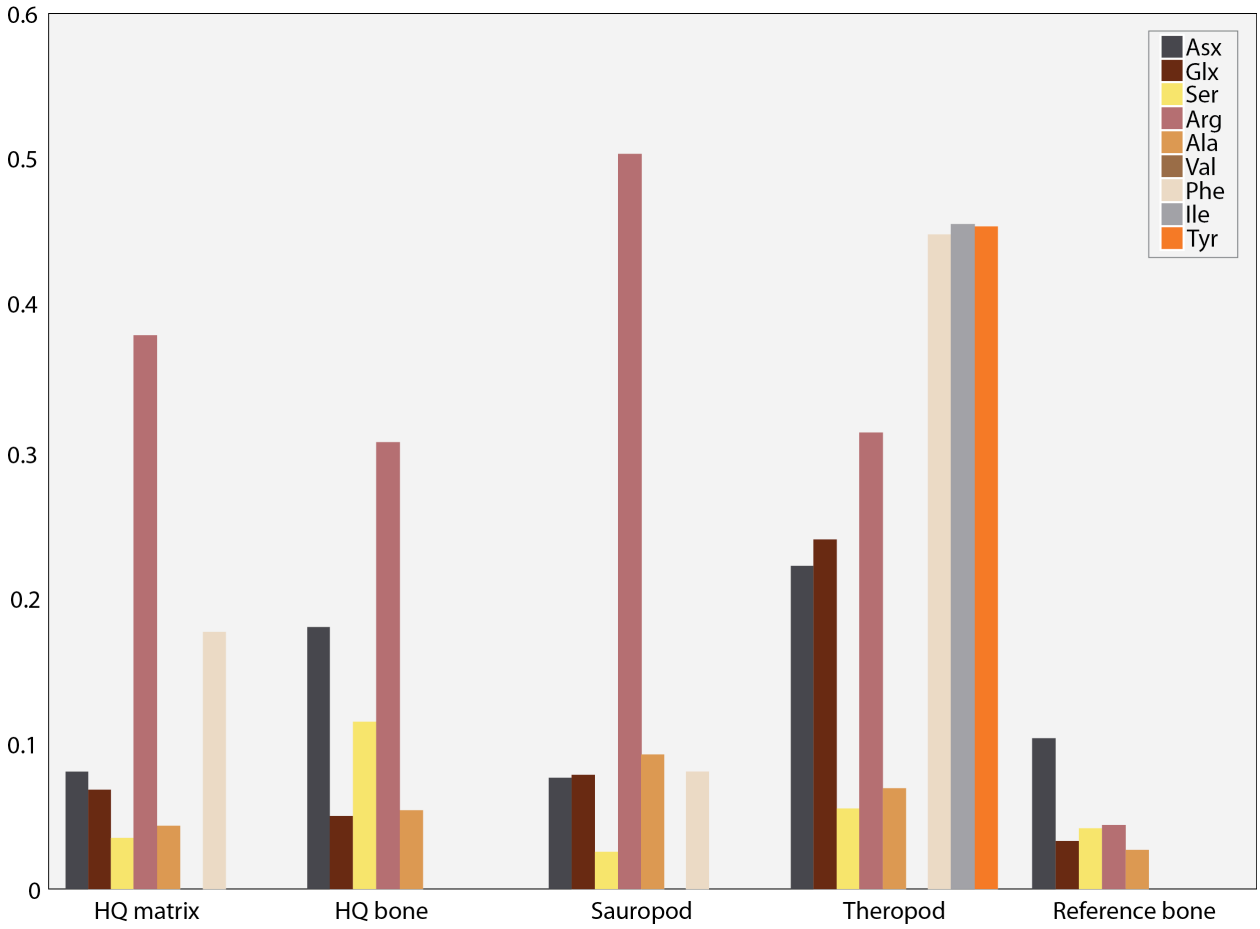

Figure 2.6 Amino acid racemization. All samples show evidence of racemization. The HQ matrix, HQ bone, sauropod and theropod bones all show the presence of arginine that has a high level of racemization. However, the rest of the amino acids have low levels of racemization, except for the theropod, which shows high levels of racemization in aspartic acid, glutamine, phenylalanine, isoleucine and tyrosine as well.

Table 2.1 Amino acid assignments

Amino Acid	**Mass**	**Chemical formula**
Glycine	75	$C_2H_5NO_2$
Alanine	89	$C_3H_7NO_2$
Serine	105	$C_3H_7NO_3$

Proline	115	$C_5H_9NO_2$
Valine	117	$C_5H_{11}NO_2$
Threonine	119	$C_4H_9NO_3$
Leucine	131	$C_6H_{13}NO_2$
Asparagine	132	$C_4H_8N_2O_3$
Lysine	146	$C_6H_{14}N_2O_2$
Glutamic acid	147	$C_5H_9NO_4$
Methionine	149	$C_5H_{11}SNO_2$
Phenylalanine	165	$C_9H_{11}NO_2$
Tyrosine	181	$C_9H_{11}NO_3$

Amino acid fragments		
Mass	**Assignment**	**Source**
27	C_2H_3	Assigned
28	C_2H_4	Assigned
29	C_2H_5	Assigned
30	CH_4N	Orlando et al. 2013
31	CH_3O	Assigned
39	C_2HN	Chapter 1
40	C_2H_2N	Chapter 1
41	C_3H_5	Chapter 1
42	C_2H_4N	Assigned
43	C_3H_7	Orlando et al. 2013
44	C_2H_6N	Orlando et al. 2013
55	C_3H_5N	Chapter 1
56	C_3H_6N	Orlando et al. 2013
57	C_4H_9	Chapter 1
59	CN_3H_5 or C_3H_7O	Orlando et al. 2013
60	C_2H_6NO or C_3H_8O	Orlando et al. 2013
61	C_2H_5S	Orlando et al. 2013
63	CH_5NO_2	Assigned
67	C_4H_5N	Chapter 1
68	C_4H_6N	Orlando et al. 2013
69	C_4H_5O or $C_2H_3N_3$	Orlando et al. 2013
70	C_5H_{10}	Assigned
71	$C_3H_3O_2$	Orlando et al. 2013
72	$C_4H_{10}N$	Orlando et al. 2013
74	C_3H_8NO	Orlando et al. 2013
76	C_2H_6NS or C_5H_2N	Orlando et al. 2013
81	C_4H_5N2 or C_5H_7N	Orlando et al. 2013
82	$C_4H_6N_2$ or $C_3N_4N_4O$	Orlando et al. 2013
83	C_5H_9N	Orlando et al. 2013
84	$C_5H_{10}N$	Assigned
85	$C_5H_{11}N$	Chapter 1
86	$C_5H_{12}N$	Assigned

87	$C_3H_7N_2O$ or $C_3H_9N_3$	Orlando et al. 2013
88	$C_3H_6NO_2$ or C_6H_2N	Orlando et al. 2013
91	C_7H_7	Orlando et al. 2013
92	$C_2H_8N_2O_2$	Assigned
93	$C_3H_{11}NO_2$	Chapter 1
95	C_5H_5NO	Chapter 1
96	$CaCO_2$	Chapter 1
97	$C_4H_3NO_2$	Chapter 1
98	$C_4H_4NO_2$	Orlando et al. 2013
100	$C_4H_{10}N_3$	Orlando et al. 2013
102	$C_4H_8NO_2$	Orlando et al. 2013
103	$C_4H_9NO_2$	Chapter 1
104	$C_4H_{10}NS$ or C_8H_8	Orlando et al. 2013
107	C_7H_7O	Orlando et al. 2013
108	$C_3H_{12}N_2O_2$	Assigned
109	$C_7H_{11}N$	Chapter 1
110	$C_5H_8N_3$	Orlando et al. 2013
111	$C_5H_9N_3$	Chapter 1
112	$C_5H_{10}N_3$	Chapter 1
113	$C_6H_{11}NO$	Chapter 1
116	$C_4H_8N_2O_2$	Assigned
118	$C_4H_{10}N_2O_2$	Assigned
120	$C_8H_{10}N$	Orlando et al. 2013
121	$C_8H_{11}N$	Assigned
122	C_7H_8NO	Chapter 1
124	$C_3H_{14}N_3O_2$	Assigned
127	$C_5H_{11}N_4$	Orlando et al. 2013
128	$C_6H_{10}NO_2$	Assigned
129	$C_{10}H_9$	Assigned
130	C_9H_8N	Orlando et al. 2013
138	$C_6H_6NO_2$	Chapter 1
141	$C_6H_9N_2O_2$	Chapter 1
150	$C_9H_{10}O_2$	Assigned
152	$C_6H_8NO_2$	Chapter 1
159	$C_{10}H_{11}N_2$	Orlando et al. 2013
168	$C_8H_{10}NO_3$	Chapter 1
169	$C_8H_{11}NO_3$	Chapter 1
171	$C_6H_{11}N_4O_2$	Chapter 1
174	Ca_2PO_4	Assigned
175	$C_9H_5NO_3$	Chapter 1
177	$C_9H_7NO_3$	Chapter 1

CHAPTER THREE

SURFACE MASS SPECTROMETRY IN FOSSIL ANALYSES: THE BENEFITS AND DRAWBACKS OF USING TIME-OF-FLIGHT SECONDARY ION MASS SPECTROMETRY (TOF-SIMS) TO ANALYZE ANCIENT BIOMOLECULES

Caitlin Colleary[1*], Andrei Dolocan[2], Jakob Vinther[3], Sterling J. Nesbitt[1]

[1] Department of Geosciences, Virginia Tech, Blacksburg, VA 24061
[2]Texas Materials Institute, University of Texas at Austin, Austin, TX 78712
[3]School of Earth Sciences, University of Bristol, Wills Memorial Building, Queens Road, Clifton BS8 1RJ, United Kingdom

*Corresponding author: colleary@vt.edu

Formatted for *Rapid Communications in Mass Spectrometry*

Abstract

High-resolution mass spectrometry is increasingly being incorporated into studies of extinct organisms (i.e., fossils) as researchers ask questions about what biomolecules might be preserved in ancient animals and how far back in time they can be detected. With the advent of new liquid metal ion guns (LMIG) that work well on biological samples (i.e., bismuth), the use of time-of-flight secondary ion mass spectrometry (TOF-SIMS) has increased in the last two decades in studies analyzing biomolecules such as beta-keratin, melanin and collagen in the fossil record. TOF-SIMS is a surface sampling technique that does not require homogenization of the sample and can therefore detect molecular components in certain features of a fossil (e.g., vascular canals in bone) and molecular differences between the fossil and associated rock matrix at the micron scale. However, no standardization for sample preparation, instrument parameters or data processing has been established among paleontologists. Additionally, misunderstandings about data interpretation and what questions can be addressed using TOF-SIMS have occurred. TOF-SIMS analyses, when used in combination with additional chemical and imaging methods – including protein, lipid and isotope mass spectrometry and scanning electron microscopy – has the potential to demonstrate 1) what biomolecules may persist on long timescales, 2) how these biomolecules are fossilized and 3) how biological structures or mechanisms may contribute to preservation.

Introduction

Fossils have been traditionally viewed as the inorganic remains of past life – often preserving physical features that can used to compare taxa to understand how ancient animals evolved or are related to one another – but the biological compounds that were present in the animal in life were thought to have long since degraded away to be replaced with inorganic minerals (Schweitzer et al. 2007). However, as technology has improved, so has the scale at which we are able to study fossils and with the advent of high-resolution mass spectrometry, the evaluation of fossils at the micron-scale has led to the discovery that biomolecules can persist in the fossil record for potentially hundreds of millions of years (Melendez et al. 2013). Mass spectrometers are now often used in studies on the biology of ancient life to address questions ranging from animal affinities and relationships (Orlando et al. 2014), the evolution of traits (Campbell et al. 2010) and color-based behaviors (Smithwick et al. 2017).

Along with this new ability to detect biomolecules in the fossil record have come studies that have sought to understand how far back in time particular biomolecules will be preserved (Briggs & Summons 2014). Major macromolecules (e.g., nucleic acids, proteins and lipids) as well as pigments, have been evaluated for preservation potential on the scale of millions of years. Nucleic acids are the most decay-prone macromolecule, with a 560-780,000 year old horse representing the oldest full genome sequenced to date (Orlando et al. 2013). Lipids, on the other hand, have very long preservation potential and sterols have been reported in the fossil record in crustaceans as far back as the Devonian (~380 Ma) (Melendez et al. 2013). The preservation potential for proteins and pigments, which arguably preserve on longer time scales than nucleic acids and potentially on similar time scales as lipids, are still unclear. Additionally, how much information about the biology of ancient animals can be discerned from fragmentary

biomolecules, particularly proteins, is still being considered. Here, we will evaluate the use of a mass spectrometer that is often used in studying both proteins and the pigment, melanin, in the fossil record, assess the benefits and drawbacks of using this instrument and present a review on the studies that have sought to use this technology to detect and interpret the presence of these two biomolecules.

Time-of-flight secondary ion mass spectrometry (TOF-SIMS) is a high-resolution mass spectrometer that analyzes the surface of a sample, providing data on the spatial distribution of molecules over an area (e.g., 500 x 500 μm^2) from elements (e.g., hydrogen, 1 atomic mass unit) to complex compounds (e.g., calcium carbonate ($CaCO_3$), 100 atomic mass units) (detailed descriptions of how this instrument works have been published elsewhere, e.g., Thiel & Sjövall 2014.). The first application of TOF-SIMS to study organics in the fossil record analyzed beta-keratin preservation in a feathered dinosaur by pulverizing a fragment of the claw and comparing it to a modern emu claw (Schweitzer et al. 1999), however the presence of keratin in feathered dinosaurs has since been refuted using TOF-SIMS, as well (Saitta et al. 2018).

Over the last few decades, the use of TOF-SIMS has become increasingly common in fossil studies that seek to identify and interpret original biomolecules in ancient animals and is often used as a supplementary analysis in conjunction with other analytical tools (Schweitzer et al. 2007, Orlando et al. 2014, Bertazzo et al. 2015, Surmik et al. 2016). Studies on a range of biomolecules (i.e., porphyrins, pigments and proteins) have incorporated TOF-SIMS to detect ions associated with original molecules and their degradation products with the goal of making interpretations about the biology of extinct animals (Bertazzo et al. 2015).

Studies on exceptionally preserved fossils that contain remnants of soft tissues (i.e., eyes and skin) and integument (i.e., feathers and hair) have incorporated this technology to identify

chemically degraded organic molecules. Researchers detected iron and heme-derived porphyrin molecules in a 46 million-year-old mosquito from the Middle Eocene Kishenehn Formation, which was used as evidence for preservation of degraded blood within the abdomen of the mosquito (Greenwalt et al. 2013). The specimen was prepared by removing a layer of silicate that covered the mosquito, rinsing it with ethanol and mounting it for TOF-SIMS analysis (Greenwalt et al. 2013).

TOF-SIMS analyses were at the center of one of the most recent controversies in paleontology. Oblong and spherical microbodies preserved in feathers and other integument were first identified as bacteria in the fossil record (Wuttke 1983) but were later redescribed as melanosomes, the organelles that contain the pigment melanin (Vinther et al. 2009). The micron-sized structures were identified as melanosomes based on shared morphology and this new interpretation was controversial (Moyer et al. 2014), leading to studies that examined the chemistry of the fossils containing these microbodies to determine if remains of melanin were present. The first study to do this used TOF-SIMS (Lindgren et al. 2012), and found that chemically degraded melanin was present in association with the microbodies present in a fossilized fish eye (Figure 3.1) and since then, a handful of studies on different taxa and types of fossils from a range of time (as far back as the Carboniferous, ~308 Ma (Gabbott et al. 2016) have verified the presence of melanin using TOF-SIMS (Glass et al. 2012, Lindgren et al. 2015, Colleary et al. 2015, Gren et al. 2016). The presence of degraded melanin-containing melanosomes in the fossil record has been used to make interpretations about the colors and color patterning in ancient animals and the biological implications of color from the fossil record (Lindgren et al. 2014, Brown et al. 2017, Smithwick et al. 2017).

TOF-SIMS analyses have been used to determine that fossilized melanosomes contain degraded melanin and has therefore cleared up debates regarding the identification of these structures. TOF-SIMS analyses of melanin have also addressed questions about the evolution of the vertebrate eye (Gabbot et al. 2016) and phylogenetic relationships, including the determination that *Tullimonstrom* is a vertebrate (Clements et al. 2016). Since there is a direct link between melanin and color, researchers have been able to make biological interpretations from these data that can evaluate the role that color-based behaviors (i.e., display, crypsis) and pigmentation have played in the evolution of feathers in dinosaurs (Vinther 2015).

Researchers have also used TOF-SIMS in fossil bone studies, with the goal of identifying collagen (the main organic component of bone) and its degradation products (i.e., peptides and amino acids) (Schweitzer et al. 2007, Orlando et al. 2013, Bertazzo et al. 2015, Surmik et al. 2016). However, these analyses were done on fossils that are not conventionally considered exceptionally preserved (e.g., preserve soft tissue) and the biological implications of discovering the remains of ancient proteins are considerably more nebulous than the implications of discovering other biomolecules (e.g, melanin). Additionally, there is no standardization for sample preparation, instrument parameters, data analysis or reporting methods that it makes it possible to replicate these studies (See Table). Therefore, the ability to detect and make interpretations about proteins preserved in fossil bone and developing a standardized protocol for the use of TOF-SIMS are the main focuses in the following sections.

Using TOF-SIMS to analyze the biomolecules present in fossil bone

Case Study 1: Determining the amino acid chemical fingerprint for bone preservation using TOF-SIMS - Orlando et al. 2014

TOF-SIMS analyses were combined with a series of analytical tools to study a horse phalanx (~560-780,000 years old) that was preserved in permafrost and the full genome of the animal was sequenced. The bone was prepared by making a thin section that was embedded in Epothin resin, cut with a diamond saw, polished and rinsed with milliQ water (Orlando et al. 2014, supplement). TOF-SIMS analyses detected glycine (Gly), proline (Pro) and alanine (Ala) in the extracellular matrix of the bone, whereas different amino acids (i.e., leucine (Leu), tyrosine (Tyr) and tryptophan (Trp)) were detected in the vascular canals (Orlando et al. 2014). Combined with proteomic analyses, the Orlando et al. (2014) determined that this was evidence for the preservation of the degradation products of original collagen. This study developed a method for identifying and assigning amino acid fragments in fossil bone using TOF-SIMS, by detecting the remains of 19 amino acids represented by 40 fragments. Glycine was identified using the fragment CH_4N (30 atomic mas units (amu)), alanine was identified using the fragment C_2H_6N (442 amu) and proline was identified using the fragments C_4H_6N (68 amu), C_4H_8N (70 amu). These fragments can represent a number of different amino acids, but when combined with the proteomic data, the researchers found good evidence for the presence of proteins.

Case Study 2: Biomolecules in bone preserve longer than expected - Bertazzo et al. 2015

Bertazzo et al. (2015) analyzed eight Cretaceous dinosaur bone fragments that were surface collected to determine if bones need to be exceptionally preserved to find the remains of collagen. The researchers defined the bone fragments as "ordinary, unexceptionally preserved fossils." The samples were prepared by breaking off a piece from each of the eight specimens analyzed. They were then coated with platinum and milled and etched using a gallium focused ion beam (FIB) (Bertazzo et al. 2015). In addition to detecting microscopic structures in the

bones that they identified as collagen fibrils and original cellular structures, researchers used TOF-SIMS to detect 11 amino acid fragments that were assigned to six amino acids, including glycine, alanine and proline. In particular, they assigned five fragments (CH_4N, C_2H_4NO, C_3H_6NO, $C_3H_5N_2O$, $C_3H_7N_2O$) to glycine, one to alanine (C_2H_6N) and two to proline (C_4H_6N, C_4H_8N) and attributed these assignments to Schweitzer et al. 2009. They argued that by finding these amino acids in conjunction with what they interpreted as collagen fibrils, this was evidence that collagen was preserved in the fossil record much more often than previously thought (Bertazzo et al. 2015), but they did not address other potential assignments for the fragments they attributed to amino acids, additional potential sources for the amino acids, nor did they test the age of the amino acids.

Case Study 3: Marine reptiles preserve proteins as far back at the Triassic - Surmik et al. 2016

The oldest report of the preservation of degraded collagen is from the bones of two marine vertebrates (i.e., *Nothosaurus* sp. and *Protanystropheus* sp.) from the Triassic Period (~230 Ma). Where were they preserved? How were they preserved? Researchers employed a series of instruments including FTIR and XPS to determine the chemistry of the samples and identify iron in association with specific bone structures (e.g., vessels). The samples were prepared by demineralizing the bone using 0.5M EDTA. Using TOF-SIMS, they detected amino acid fragments they assigned to glycine, alanine, proline, hydroxyproline, leucine, lysine and hydroxylysine and said despite the fact that most of these fragments are ubiquitous, given that they were found together meant that they were indicative of original collagen (Surmik et al. 2016). Additionally, researchers used TOF-SIMS images to analyze “putative blood vessels” in

the fossil bone samples, highlighting that iron is in high intensity around these structures and may play a role in cross-linking for preservation (Figure 3.2).

Case Study 4: Organic preservation in the Cretaceous: A Hell Creek Tyrannosaurus rex - Schweitzer et al. 2007

The most well-studied bone in ancient protein studies is a *Tyrannosaurus rex* bone (MOR 1125) from the latest Cretaceous Hell Creek Formation (Schweitzer et al. 2005, Asara et al. 2007, Schweitzer et al. 2007, Schweitzer et al. 2009, San Antonio et al. 2011, Schweitzer et al. 2013, Schweitzer et al. 2016). TOF-SIMS analysis on this specimen was done using a demineralized portion of the bone. The fossil was prepared by demineralizing using 0.5M EDTA and pressed onto indium foil. Researchers detected glycine, alanine, proline, lysine and leucine. To determine if the amino acids detected in the fossil bone were indicative of original collagen, the ratio of unaltered collagen in bone (33% glycine, 10% alanine) was compared to the TOF-SIMS data from the fossil bone, although this is problematic for biological, taphonomic (Cleland & Shroeter 2018) as well as analytical reasons.

Benefits of using TOF-SIMS in fossil studies

The main draw of using TOF-SIMS in fossil studies is the ability to analyze the sample surface and spatial distribution of molecules, without homogenizing the sample (Figure 3.2). This type of analysis makes it possible to compare between the fossil and the surrounding matrix and examine possible mechanisms for preservation within the fossil itself. The data itself is also extremely high resolution, with a spectra ranging from one atomic mass unit (hydrogen) and continuing on into the thousands (although with decreasing resolution and increasing complexity as you move

up into more complex compounds). The TOF-SIMS data is also available as molecular maps, which as mentioned above offer unprecedented levels of information at the molecular level of a fossil that are still intact. Additional steps can also be used to cut down on surface contaminants (i.e., sputtering) before analyzing the sample. Additionally, the information is stored in the analysis area, so additional analyses can be done after the initial measurements and regions of interest can be explored more in depth.

Drawbacks of using TOF-SIMS in fossil studies

One of the main drawbacks of using TOF-SIMS in fossil studies is that it cannot be used to distinguish between original biomolecules or ancient/modern contamination. Sample preparation, especially for fossil samples, also relies on the ability to get the sample as flat as possible to get usable data and there are limits on the size of samples that can fit into the analysis chamber. Additionally, the large amount of data, which in itself can be considered a benefit, is extremely complex to evaluate and therefore requires additional steps (e.g., multivariate statistics, Graham et al. 2006). Comparisons between samples also relies on the samples being of similar structures, which is also very complicated in fossil studies.

Methodology and Best Practices

I. Specimen size

TOF-SIMS is a surface sampling technique and entire fossils can be placed into the instrument, if they fall within the size constraints of the sample chamber. The largest sample that can fit in the chamber is 10 cm x 15 cm x 2 cm. Therefore, this is a non-destructive technique for smaller fossils that can be placed in the chamber intact (e.g., the fossil cyclostome from Gabbott et al.

2016) (Figure 3.3). There is, however, a tradeoff in the size of the sample being analyzed and the ability to vacuum the chamber. The larger the sample, the more time is needed to pump down to acceptable levels of vacuum. In principle, every mm^2 in height of the sample adds another 2-3 hours of pumping down. However, this is also highly dependent on the moisture content of the sample, as well. If the sample has been kept dry or stored in a vacuum, it will take much less time to bring the chamber to vacuum than it will if the sample has been stored in a humid environment or contains water itself. Also, if the thickness of the sample reaches several centimeters, the suction of the air/water from its volume makes vacuuming extremely difficult due to the slow diffusion of gases and liquid contaminants in the sample, making the pumping time increase exponentially. If an intact fossil is going to be loaded into the chamber, the fossil must also be extremely flat in the area that is going to be analyzed (e.g., the carbonaceous compression of an eye, Gabbott et al. 2016) to avoid topography issues.

The majority of fossil studies using TOF-SIMS have analyzed larger fossils that have been subsampled to fit inside the analysis chamber. Minimal material is required for analysis and small fragments or flakes can be removed from the fossil, with minimal destruction to the fossil. The minimum size of a sample that can be analyzed is 5 mm x 5 mm x 1 mm (the width of a microscope slide or thin section).

II. Specimen preparation

Since the majority of fossil samples are too large to fit into the analysis chamber, the samples must be prepared for analysis. This stage of preparation is when the fossil sample is particularly susceptible to contamination. When manually sectioning samples care should be taken to use nitrile gloves, change blades/bits and sandpaper for each specimen and if modern samples are

also being sectioned, to process the fossils first (from oldest to youngest) and then process the modern samples to avoid introducing modern organics. That being said, using modern standards and matrix controls is very important when examining the presence of organic compounds in fossil samples and should be done whenever possible to establish a baseline for expectations. TOF-SIMS analyses have been done on fossils that include both the feather and surrounding matrix (Colleary et al. 2015), providing information on the difference in the molecular compositions between the two and testing for the presence of organics unique to the fossils.

Additionally, cleaning the samples is also potentially problematic. If fossil samples do contain organics, they are likely in very low abundances or extremely degraded (depending on the age of the specimen), therefore rinsing with water may remove organics, particularly those that are water soluble (i.e., proteins) and acids can potentially degrade organics and remove additional information that can be gained by examining the fossils in their entirety without demineralizing them (one of the greatest benefits of using TOF-SIMS).

Micron scale variation in topography can greatly impact data output (Thiel & Sjövall 2014), therefore samples must be as flat as possible. Early studies used fossil thin sections (e.g., Orlando et al. 2013), which solve the problems associated with variations in topography. However, fossil thin sections are prepared using epoxies with proprietary ingredients that may introduce organics that can conflate with fossil peaks. Additionally, no studies have been done on the behavior (e.g., ionization) of the compounds in epoxy under vacuum. Therefore, additional preparation techniques have been used.

To avoid the potential contamination from epoxies, studies have incorporated manual sectioning to create "thick sections," larger pieces of bone that are structurally stable and can be polished down to create a very flat surface. A variety of methods can be used to achieve this,

including cutting a piece of the fossil with a saw or dremel, and then polishing the top using a dremel polishing bit or grinding/polishing wheels used in making thin sections. Other studies have used instruments to section and polish surfaces, such as focused ion beam (FIB) sectioning (Bertazzo et al. 2015) and ion milling (Reigler et al. unpublished data) (Figure 3.4). FIB sectioning uses an ion beam (typically gallium, Ga) to select areas of a sample and remove them with micron-scale precision. A benefit to this technique is that contaminating the sample is limited and imaging can be done at the same time (Bertazzo et al. 2015). One caveat to using this technique is, to ensure that when coating a sample for previous analyses like imaging, that gold (Au) is used instead of carbon (C) to avoid introducing additional carbon peaks when analyzing the molecular composition with the TOF-SIMS. Ion milling also uses an ion beam that is scanned or rastered across the top of a mounted sample to make it as flat as the metal it is mounted against (Figure 3.5). This technique also flattens the sample with micron-scale precision and removes any issues associated with topography. However, caution must be taken to insure that samples are dry because high water content in modern bone samples can lead to combustion of the sample. Also, depending on the type of fossil being analyzed, ion milling can take an extremely long time, with the time of etching increasing with the hardness and size of the sample.

III. Instrument Parameters

Standardized parameters for analysis and reporting are necessary to recreate previous studies (See Table 3.1). There are a significant number of parameters to consider when using TOF-SIMS, some of which change based on the type of fossil being studied. Here, we focus on the parameters that can be standardized in fossil analyses, although some of these parameters should

still not be considered static and can be altered based on situational needs, like the charging of a sample. To begin analyses, the vacuum needs to be at the minimum 1 x 10^{-6} mbar in the analysis chamber before beginning data acquisition. Next, the type of liquid metal ion gun (LMIG), the analysis gun used to acquire data, is chosen. New LMIGs have been introduced over the last few decades and studies have found that bismuth (Bi, Bi_3) works particularly well on biological samples (Touboul et al. 2005). Then, the sample can be sputtered using the sputter gun. The dual source column – sputtering (DSC-S) uses cesium (Cs) or oxygen (O_2), which is used to ablate the surface of a sample for depth profiling or gentle cleaning of the surface. Sputtering can be used to remove surface contaminants, but introduces an additional step that adds time to analysis and must be standardized across samples. Cesium should be used on fossil samples that are investigating organic compounds so that no additional oxygen is introduced to the sample. Sputtering rate varies significantly from 0.1 nm/s to a few nm/s, with the ion species (Cs, O_2 or C_{60}) and its energy (250 V to 10000 V). In addition to removing surface contaminants, depth profiling using sputtering can reveal the layers underneath the surface and can be used to examine multiple layers of a sample (e.g., enamel and dentin in teeth).

There are two parameters that can be used for charge compensation: a low energy electron beam or, if the sample is extremely insulating, an argon (Ar) leak valve can be used to create an Ar environment (1 x 10^{-6} mbar) in the analysis chamber. Acquisition time can range from a few seconds to days, depending on the complexity of the analysis, however, maintaining the stability of the ion gun, thermal drift and vacuum reserve refreshing is ideal in analyses that are kept under two hours. The maximum analysis area is 500 µm x 500 µm, however larger cm^2 sized areas can be mapped by automatically patching adjacent 500 µm x 500 µm areas. Analyses can also be done using negative or positive ions, with the selection being based on the

electronegativity of the species of interest. As you move from the left to right size of the periodic table, elements shift from the electropositive elements that preferentially ionize positively to the elements that are electronegative and therefore preferentially ionize negatively. For example, carbonaceous species preferentially ionize negatively, however adding two hydrogen atoms to any carbonaceous species produces positive species.

IV. Data output

The data output from TOF-SIMS is in spectra and images. The spectra show the intensity of the secondary ions detected. The intensity of a secondary ion fragment is proportional to its abundance and ionization probability. However, the proportionality factor is largely unknown in most materials. To estimate the absolute amount of a species in a structure (matrix), a reference sample is required (i.e., a sample with a similar structure or matrix that contains a known amount of the species of interest) and should be calibrated with another technique (e.g., energy dispersive X-ray spectroscopy (EDS)). In absence of a reference sample, TOF-SIMS can only compare the relative amounts of a species between samples, as long as the samples have a similar structure.

TOF-SIMS maps show the spatial localization of various species of interest. The species of interest are acquired in parallel, therefore the secondary ion maps show their simultaneous localization at the surface or different planes in depth during a depth profile. TOF-SIMS also has a unique feature called retrospective data analysis which allows the reconstruction of a spectrum, map or depth profile of any species of interest after the data acquisition has ended. Therefore, you can go return at any time and explore regions of interest in the samples analyzed.

TOF-SIMS files vary from a few hundred MB to tens of GB depending on the complexity of the analysis. Depth profiles and high lateral resolution maps tend to take up the most memory space. The files are usually stored on TB-sized external hard drives that are online accessible.

V. Data analysis

Once the data has been collected, the first step is to calibrate the peaks in the IONTOF software. Mass calibration during data reconstruction is very important, ensuring that the peaks representing each species of interest is properly identified and selected. For an accurate mass calibration, peaks that represent well-known species should be selected (e.g., common contaminants such as C, I, OH, F, Na, Si, S, Cl, K and Ca). When looking at carbonaceous materials, using a carbon series such as C (12 amu), C_2 (24 amu), C_3 (36 amu), C_4 (48 amu), etc. can be used for calibration.

After calibrating the peaks, spectra can be compared between samples. TOF-SIMS data can only be used to compare the relative amount of the same species or function (e.g., a ratio) of the same species of interest between samples that have similar structure or for the same sample between its surface and bulk (i.e., during depth profiling). A reference sample needs to be provided for quantification of the absolute amount, which is why it's important in fossil studies to include a modern analogue and sediment control of the surround matrix. However, in fossil studies, the degradation of the organics makes it very difficult to quantify expected abundances and therefore the relative amounts will be compared between samples. Multivariate statistical techniques (e.g., principal component analysis) are often used to compare a large number of species between samples. By selecting the same manifold of species of interest for various

samples and then applying multivariate statistics, the resulting dataset can resolve if the samples contain the same compound of interest. Usually, the manifold of species of interest is selected based on a reference sample (e.g., a modern bone) that is known to contain the compound of interest in large amounts (e.g., calcium phosphate, $Ca_3(PO_4)_2$).

TOF-SIMS data can be used to relatively quantify single species or functions of same species of interest among various samples with similar structure. In addition, multivariate statistics can be applied on selected manifolds to determine if a compound is present in a set of samples. However, the amount of a species in a sample cannot be compared with another species of interest in another sample, even if the samples have similar structure. Only the amount of the same species can be compared between samples or between the surface and bulk for the same sample. Additionally, the amount of the same species of interest cannot be compared between two samples that have different structure.

Future Work

Fossil samples and the associated rock matrix have extremely complicated molecular compositions. Future studies should focus on the influence of the rock substrate on the chemical analysis of the fossil. Work also needs to be done on fossils, the associated matrix and modern analogues, to determine if their structure and compositions are similar enough in all cases to be compared to one another. Also, contaminants in the rock matrix need to be identified that may interfere with the manifold of species of interest in the fossilized organic compound under investigation. Additionally, future work should also examine the amount of degradation and alteration that has occurred in the fossils at the molecular level to understand how they can be compared to modern samples.

The use of TOF-SIMS in fossil studies is still in its infancy and considerations need to be made regarding the comparison between samples and how to untangle complicated organic samples. However, the use of TOF-SIMS, particularly molecular maps, have the potential to unravel taphonomic processes that lead to the preservation of organic compounds. By following standardized parameters and reporting standards, the interest in using this technology in fossil studies can lead to better practices in the analysis of the molecular components of fossils without losing information by demineralizing and extracting organics.

References

Asara, J.M., Schweitzer, M.H., Freimark, L.M., Phillips, M. and Cantley, L.C., 2007. Protein sequences from mastodon and *Tyrannosaurus rex* revealed by mass spectrometry. *Science*, *316*(5822), pp.280-285.

Bertazzo, S. et al. 2015. Fibres and cellular structures preserved in 75-million–year-old dinosaur specimens. *Nature Communications*, *6*, p.7352.

Briggs, D.E. and Summons, R.E., 2014. Ancient biomolecules: their origins, fossilization, and role in revealing the history of life. *BioEssays*, *36*(5), pp.482-490.

Brown, C.M. et al. 2017. An exceptionally preserved three-dimensional armored dinosaur reveals insights into coloration and Cretaceous predator-prey dynamics. *Current Biology*, *27*(16), pp.2514-2521.

Campbell, K.L. et al. 2010. Substitutions in woolly mammoth hemoglobin confer biochemical properties adaptive for cold tolerance. *Nature Genetics*, *42*(6), p.536.

Cleland, T.P., Schroeter, E.R. and Schweitzer, M.H., 2015. Biologically and diagenetically derived peptide modifications in moa collagens. *Proceedings of the Royal Society of London B*, *282*(1808), p.20150015.

Cleland, T.P. and Vashishth, D., 2015. Bone protein extraction without demineralization using principles from hydroxyapatite chromatography. *Analytical Biochemistry*, *472*, pp.62-66.

Cleland, T.P. and Schroeter, E.R., 2018. A Comparison of Common Mass Spectrometry Approaches for Paleoproteomics. *Journal of Proteome Research*, *17*(3), pp.936-945.

Clements, T. et al. 2016. The eyes of Tullimonstrum reveal a vertebrate affinity. *Nature*, *532*(7600), p.500.

Colleary, C. et al. 2015. Chemical, experimental, and morphological evidence for diagenetically altered melanin in exceptionally preserved fossils. *Proceedings of the National Academy of Sciences*, *112*(41), pp.12592-12597.

Gabbott, S.E. et al. 2016. Pigmented anatomy in Carboniferous cyclostomes and the evolution of the vertebrate eye. *Proceedings of the Royal Society of London B*, *283*(1836), p.20161151.

Glass, K. et al. 2012. Direct chemical evidence for eumelanin pigment from the Jurassic period. *Proceedings of the National Academy of Sciences*, *109*(26), pp.10218-10223.

Graham, D.J., Wagner, M.S. and Castner, D.G., 2006. Information from complexity: Challenges of TOF-SIMS data interpretation. *Applied Surface Science*, *252*(19), pp.6860-6868.

Greenwalt, D.E., Goreva, Y.S., Siljeström, S.M., Rose, T. and Harbach, R.E., 2013. Hemoglobin-derived porphyrins preserved in a Middle Eocene blood-engorged mosquito. *Proceedings of the National Academy of Sciences*, p.201310885.

Gren, J.A. et al. 2017. Molecular and microstructural inventory of an isolated fossil bird feather from the Eocene Fur Formation of Denmark. *Palaeontology*, *60*(1), pp.73-90.

Lee, Y.C. et al. 2017. Evidence of preserved collagen in an Early Jurassic sauropodomorph dinosaur revealed by synchrotron FTIR microspectroscopy. *Nature Communications*, *8*, p.14220.

Lindgren, J. et al. 2012. Molecular preservation of the pigment melanin in fossil melanosomes. *Nature Communications*, *3*, p.824.

Lindgren, J. et al. 2014. Skin pigmentation provides evidence of convergent melanism in extinct marine reptiles. *Nature*, *506*(7489), p.484.

Lindgren, J. et al. 2015. Molecular composition and ultrastructure of Jurassic paravian feathers. *Scientific Reports*, *5*, p.13520.

Lindgren, J. et al. 2017. Biochemistry and adaptive colouration of an exceptionally preserved juvenile fossil sea turtle. *Scientific Reports*, *7*(1), p.13324.

Melendez, I., Grice, K. and Schwark, L., 2013. Exceptional preservation of Palaeozoic steroids in a diagenetic continuum. *Scientific Reports*, *3*, p.2768.

Moyer, A.E. et al. 2014. Melanosomes or microbes: testing an alternative hypothesis for the origin of microbodies in fossil feathers. *Scientific Reports*, *4*, p.4233.

Orlando, L. et al. 2013. Recalibrating *Equus* evolution using the genome sequence of an early Middle Pleistocene horse. *Nature*, *499*(7456), p.74.

Plet, C. et al. 2017. Palaeobiology of red and white blood cell-like structures, collagen and cholesterol in an ichthyosaur bone. *Scientific Reports*, *7*(1), p.13776.

Saitta, E.T. et al. 2018. Preservation of feather fibers from the Late Cretaceous dinosaur *Shuvuuia deserti* raises concern about immunohistochemical analyses on fossils. *Organic Geochemistry*, *125*, pp.142-151.

San Antonio, J.D. et al. 2011. Dinosaur peptides suggest mechanisms of protein survival. *PLOS ONE*, *6*(6), p.e20381.

Schroeter, E.R. et al. 2017. Expansion for the *Brachylophosaurus canadensis* collagen I sequence and additional evidence of the preservation of Cretaceous protein. *Journal of Proteome Research*, *16*(2), pp.920-932.

Schweitzer, M.H. et al. 1999. Beta‐keratin specific immunological reactivity in feather-like structures of the Cretaceous Alvarezsaurid, *Shuvuuia deserti*. *Journal of Experimental Zoology*, *285*(2), pp.146-157.

Schweitzer, M.H., Wittmeyer, J.L. and Horner, J.R., 2005. Gender-specific reproductive tissue in ratites and *Tyrannosaurus rex*. *Science*, *308*(5727), pp.1456-1460.

Schweitzer, M.H. et al. 2007. Analyses of soft tissue from *Tyrannosaurus rex* suggest the presence of protein. *Science*, *316*(5822), pp.277-280.

Schweitzer, M.H., Avci, R., Collier, T. and Goodwin, M.B., 2008. Microscopic, chemical and molecular methods for examining fossil preservation. *Comptes Rendus Palevol*, *7*(2-3), pp.159-184.

Schweitzer, M.H. et al. 2009. Biomolecular characterization and protein sequences of the Campanian hadrosaur *B. canadensis*. *Science*, *324*(5927), pp.626-631.

Schweitzer, M.H. et al. 2014. A role for iron and oxygen chemistry in preserving soft tissues, cells and molecules from deep time. *Proceedings of the Royal Society of London B: Biological Sciences*, *281*(1775), p.20132741.

Schweitzer, M.H., Zheng, W., Zanno, L., Werning, S. and Sugiyama, T., 2016. Chemistry supports the identification of gender-specific reproductive tissue in *Tyrannosaurus rex*. *Scientific Reports*, *6*, p.23099.

Smithwick, F.M., Nicholls, R., Cuthill, I.C. and Vinther, J., 2017. Countershading and stripes in the theropod dinosaur *Sinosauropteryx* reveal heterogeneous habitats in the Early Cretaceous Jehol Biota. *Current Biology*, *27*(21), pp.3337-3343.

Surmik, D. et al. 2016. Spectroscopic studies on organic matter from Triassic reptile bones, Upper Silesia, Poland. *PLOS ONE*, *11*(3), p.e0151143.

Thiel, V. and Sjövall, P., 2014. Time-of-flight secondary ion mass spectrometry (TOF-SIMS): Principles and practice in the biogeosciences. *Principles and Practice of Analytical Techniques in Geosciences*, *4*, p.122.

Touboul, D., Kollmer, F., Niehuis, E., Brunelle, A. and Laprévote, O., 2005. Improvement of biological time-of-flight-secondary ion mass spectrometry imaging with a bismuth cluster ion source. *Journal of the American Society for Mass Spectrometry*, *16*(10), pp.1608-1618.

Vinther, J., 2015. A guide to the field of palaeo colour: Melanin and other pigments can fossilise: Reconstructing colour patterns from ancient organisms can give new insights to ecology and behaviour. *BioEssays*, *37*(6), pp.643-656.

Vinther, J., Briggs, D.E., Clarke, J., Mayr, G. and Prum, R.O., 2010. Structural coloration in a fossil feather. *Biology Letters*, *6*(1), pp.128-131.

Wuttke, M., 1983, ‘‘Weichteil-Erhaltung’’ durch lithifizierte Mikroorganismen bei mittel-eoz¨anen Vertebraten aus den O¨lschiefern der ‘‘Grube Messel’’ bei Darmstadt: Senck-enbergiana Lethaea, v. 64, p. 509–527.

Zhang, F. et al. 2010. Fossilized melanosomes and the colour of Cretaceous dinosaurs and birds. *Nature*, *463*(7284), p.1075.

FIGURES

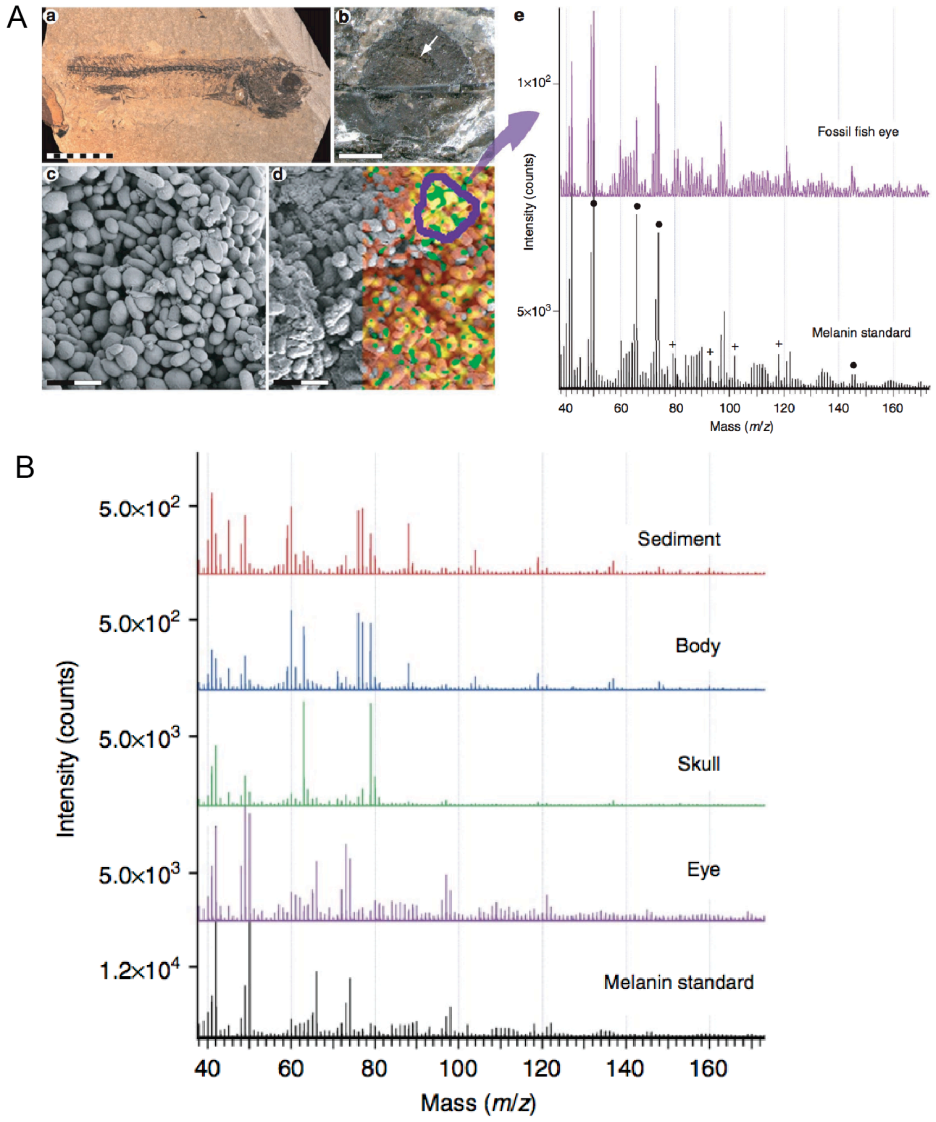

Figure 3.1 Figures from Lindgren et al. 2012. (A) Shows the microbodies in the fossilized eye of a fish and the area that was analyzed using TOF-SIMS. The spectra from the fossil eye was compared to a modern melanin standard and common peaks are noted. (B) Shows comparison of TOF-SIMS mass spectra between a modern melanin standard, different areas of the fossil and the sediment surround the eye. Researchers developed a chemical fingerprint of 45 peaks to compare melanin to modern and fossil samples

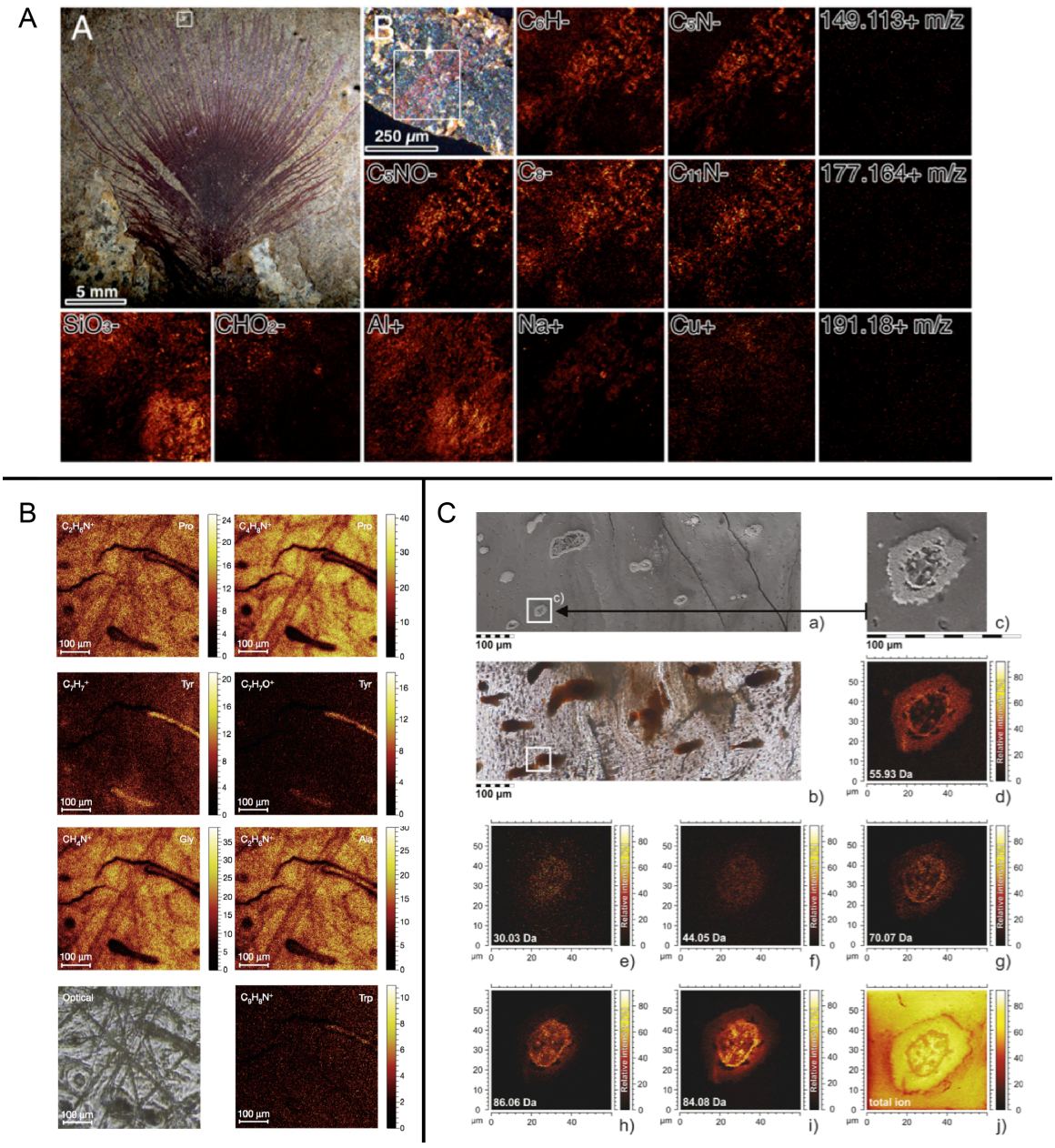

Figure 3.2 TOF-SIMS images from fossil studies. (A) From Colleary et al. 2015. Images of a fossil feather show the presence of melanin-related molecules in the feather that are absent in the surrounding matrix. (B) From Orlando t al. 2014. Images of a fossil show the presence of amino acids in the extracellular matrix of the bone and the vascular canals. (C) From Surmik et al. 2016. Images of a structure of fossil bone and the molecules associated with it.

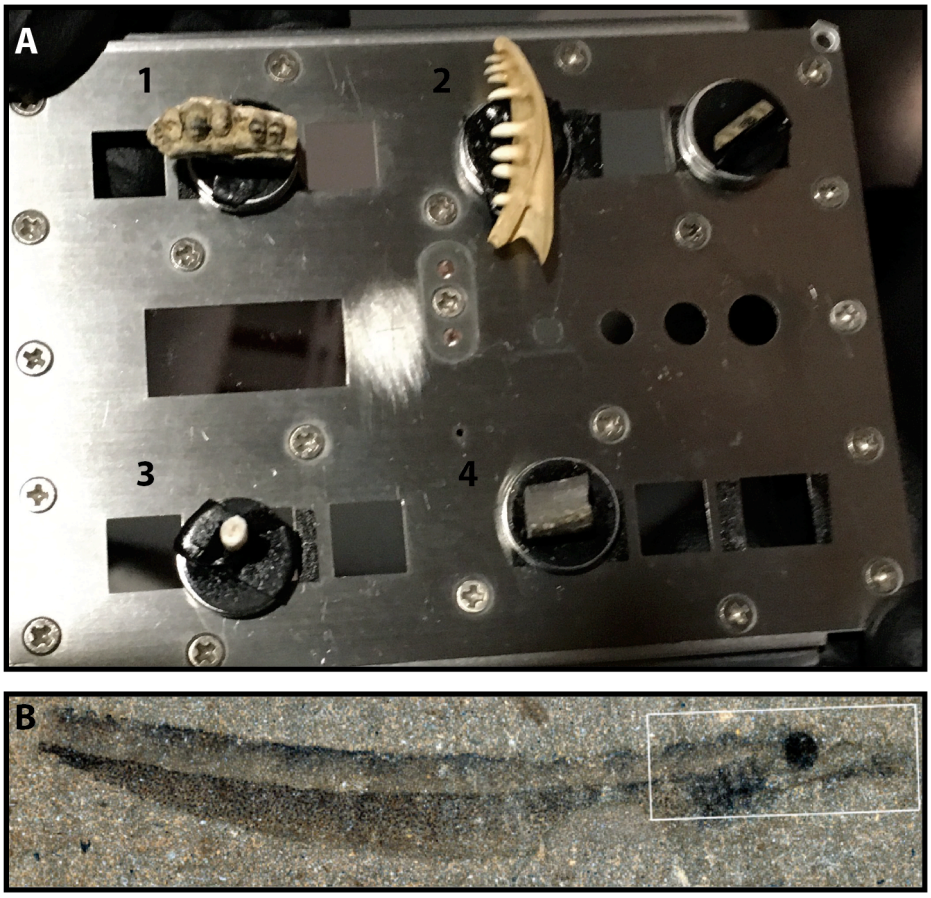

Figure 3.3 The sizes of fossil samples. (A) The stage that is loaded into the chamber can hold samples of various sizes (1 = ~13 mm, 2 = ~25 mm, 3 = ~3 mm, 4 = ~8 mm). (B) Entire fossils can be analyzed, like this cyclostome from Gabbott et al. 2016 (~10 cm).

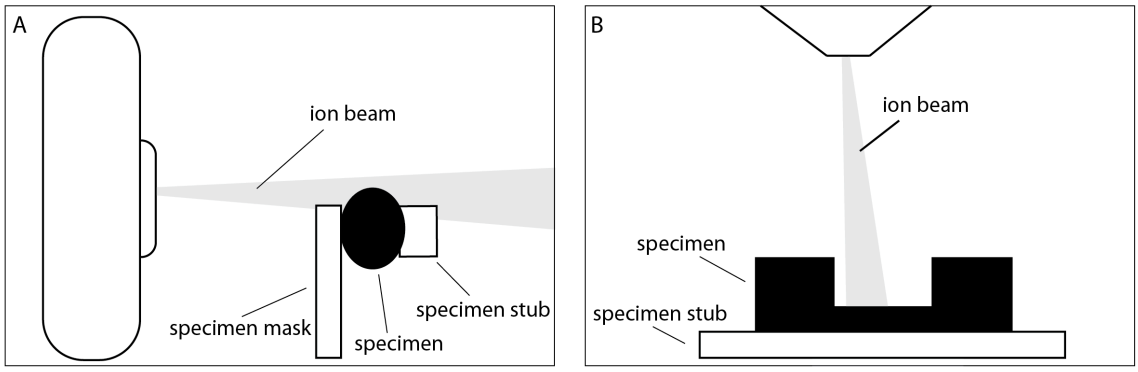

Figure 3.4 Instrument sectioning sample preparation methods for TOF-SIMS. (A) The Hitachi Ion Mill uses an argon ion beam to flatten the surface of the sample. The sample is mounted to a specimen mask that the ion beam cannot permeate, and the beam is oscillated back and forth over the specimen, removing the portion above the specimen mask. (B) Focused ion beam (FIB) etching uses liquid metal ions (i.e., gallium) at high beam currents to flatten the surface of a sample. FIB operates under similar principles as scanning electron microscopes and can also image at low beam currents.

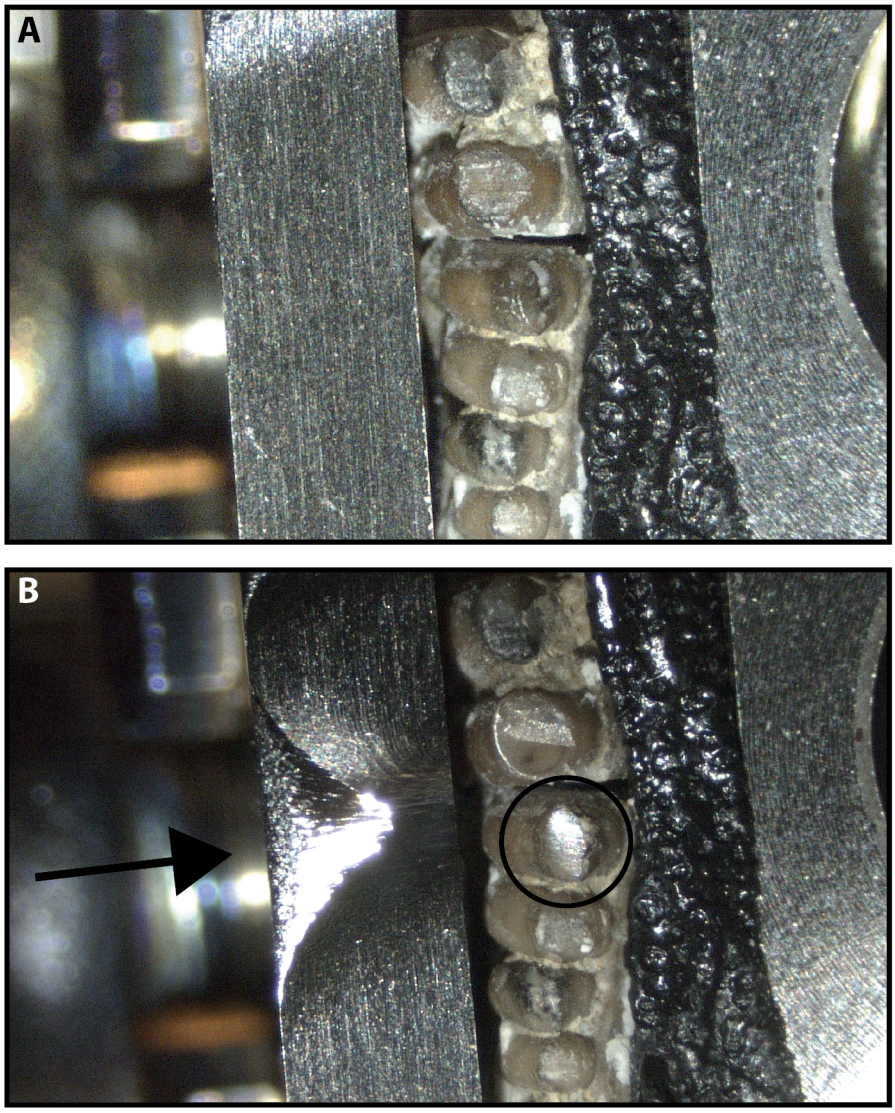

Figure 3.5 (A) jaw mounted in the ion mill. (B) As the ion beam scans across the surface, the tooth that is being flatten fluoresces (circled) and the ion beam warps the specimen mask (arrow).

Study	Fossil type	Instrument	Primary ion	Electron beam	Positive/ Negative ions	Mass range	Mass resolution	Analysis area	Sputter ion	Calibration peaks
Schweitzer et al. 2007	Bone	Phi-Evans TRIFT I	___	<20 eV	Positive	___	~4000	___	___	___
Orlando et al. 2014	Bone	TOF.SIMS 5 (UT Austin)	30 keV Bi_3+	21 eV	Both	0 to 880 amu	2000	500 x 500 µm²	O_2 and Cs	22
Bertazzo et al. 2015	Bone	TOF.SIMS5 – Qtac100 LEIS	Bi_3+	___	Positive	___	___	128 x 128 pixels	___	5
Lindgren et al. 2015	Bone and Melanin	TOF-SIMS V	25 keV Bi_3+	low energy	Both	0 to 146 amu	~5000	256 x 256 pixels	___	___
Surmik et al. 2016	Bone	TOF-SIMS 5 (University of Silesia)	30 keV Bi+, Bi_3++	___	Both	1-800 Da	5000-9000	50 x 50 µm² to 500 x 500 µm²	Cs	5 (positive) 6 (negative)
Schweitzer et al. 1999 A + B	Beta-keratin	PHI-Evans TRIFT I	15 keV Ga+	___	Positive	___	3000-6000	80 x 80 µm²	___	1
Plet et al. 2017	Bone	Tescan Lyra with TOFWERK TOF-SIMS detector	20 kV Ga+	___	Negative	___	___	20 x 20 µm²	___	___
Greenwalt et al. 2013	Porphyrins	TOF-SIMS IV	25 keV Bi_3+	___	Positive	___	___	~300 x 300 µm²	___	___
Lindgren et al. 2012	Melanin	TOF-SIMS IV	25 keV Bi_3+	low energy	Negative	2000 Da	~5000	50 x 50 µm² 500 x 500 µm²	___	___
Lindgren et al. 2014	Melanin	TOF-SIMS IV	25 keV Bi_3+	low energy	Negative	___	~5000	256 x 256 pixels	___	___
Colleary et al. 2015	Melanin	ION TOF TOF-SIMS.5	30 kV Bi_3+	21 eV	Negative	0 to 146 amu	~1-3000	100 x 100 µm² 500 x 500 µm²	None	9
Lindgren et al. 2017	Melanin	TOFSIMS IV	25 keV Bi_3+	low energy	Both	___	~5000	___	___	___

CHAPTER 1 SUPPLEMENTARY DATA

Figure S1.1 TOF-SIMS spectra of the Chapter 1 samples (elephant bone, mammoth bones, maturation experiments and sediment martrix). 67 peaks were selected from the range of 30 – 181 atomic mass units. Peaks were selected based on a previous study (Orlando et al. 2013) and additional peaks that were obvious or absent in the samples.

Elephant bone

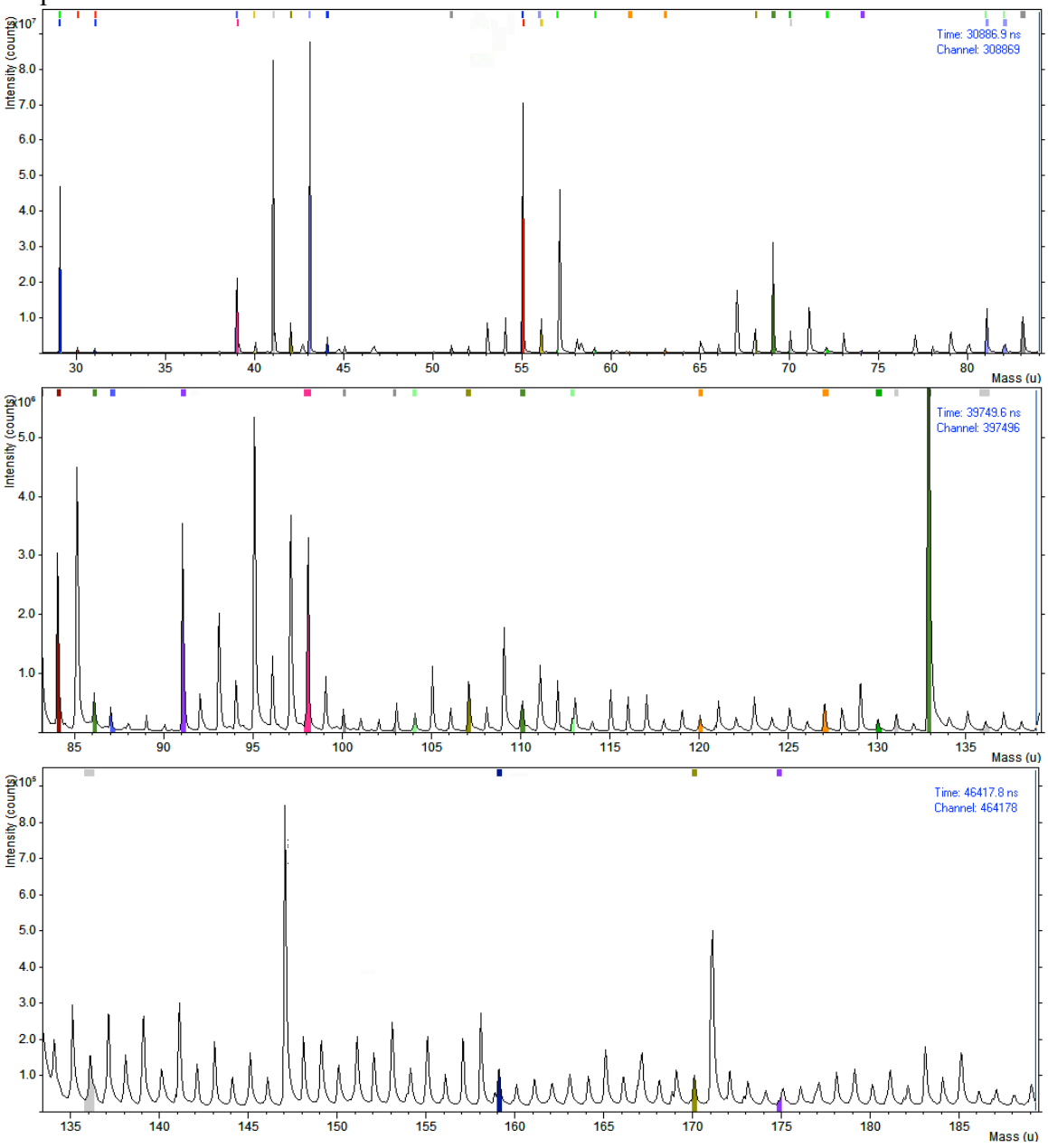

Mammoth bone (Permafrost)

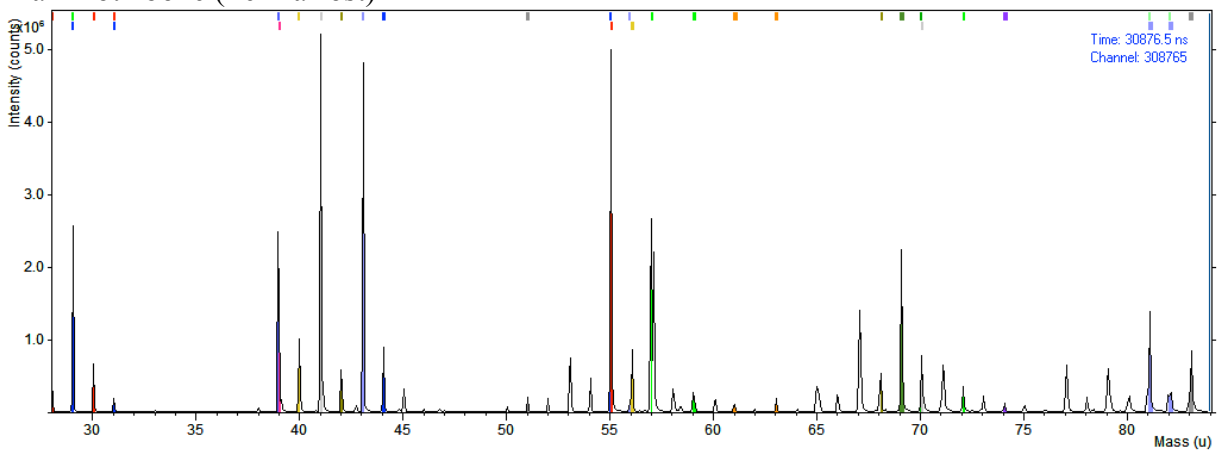

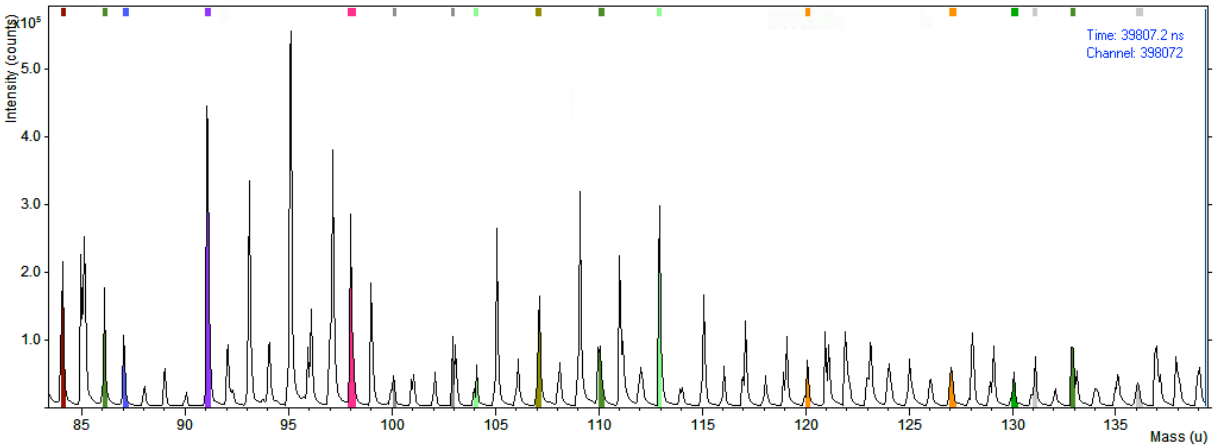

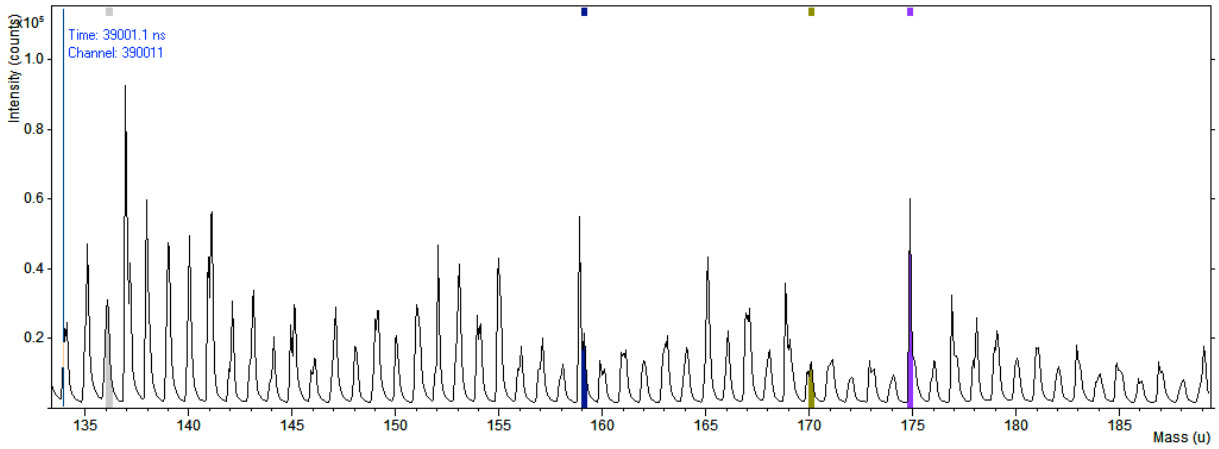

Mammoth bone (Asphalt)

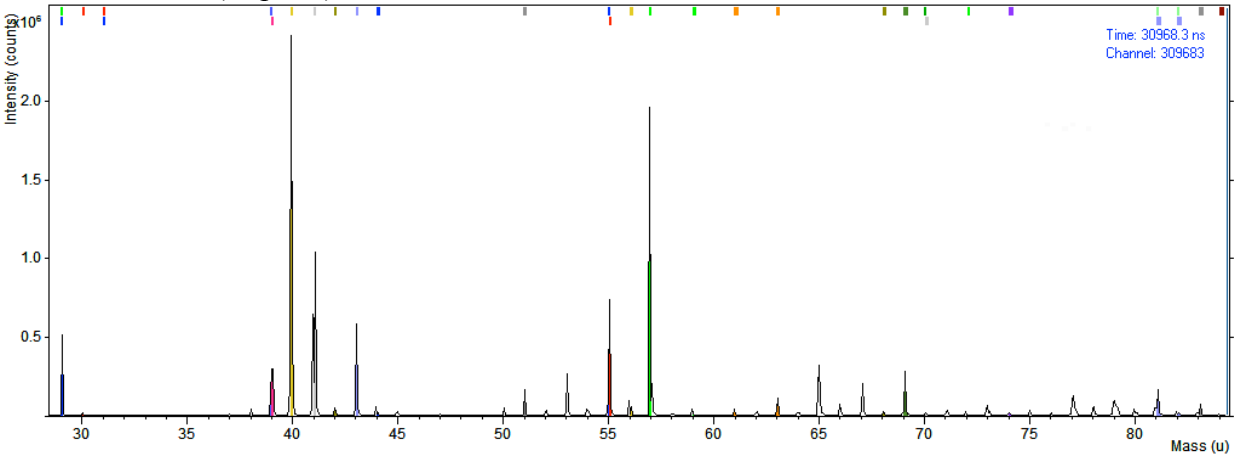

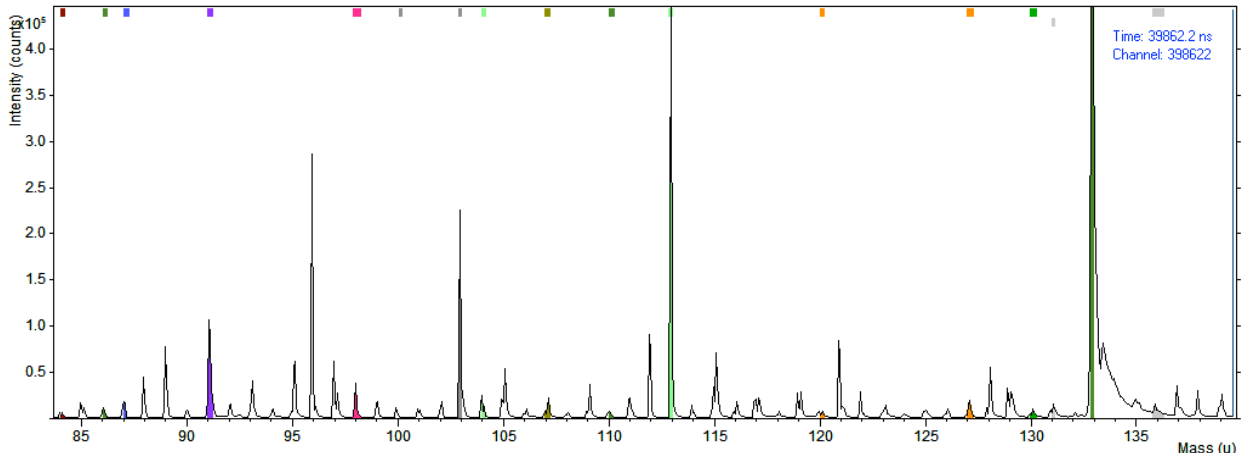

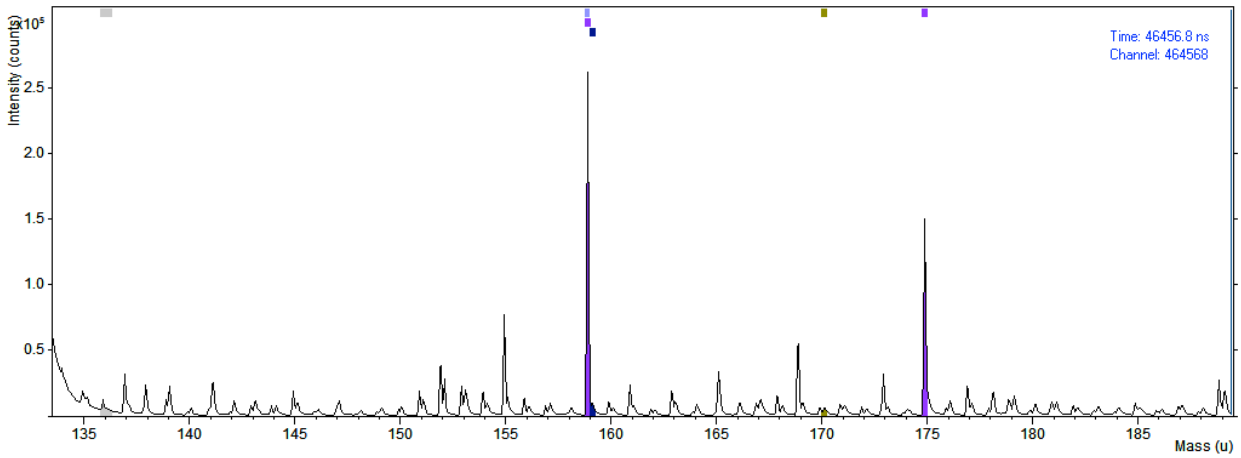

Mammoth bone (Channel deposit)

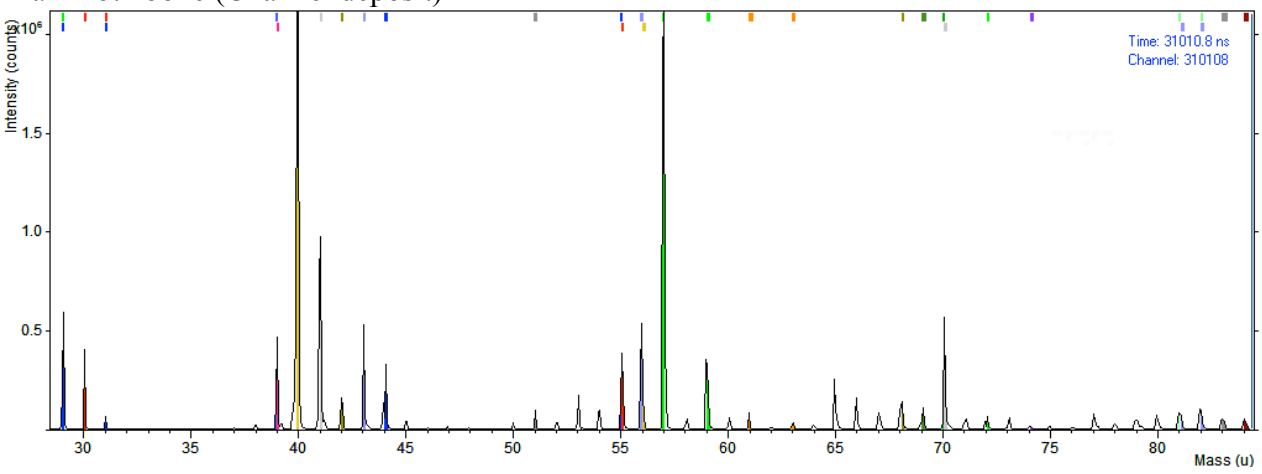

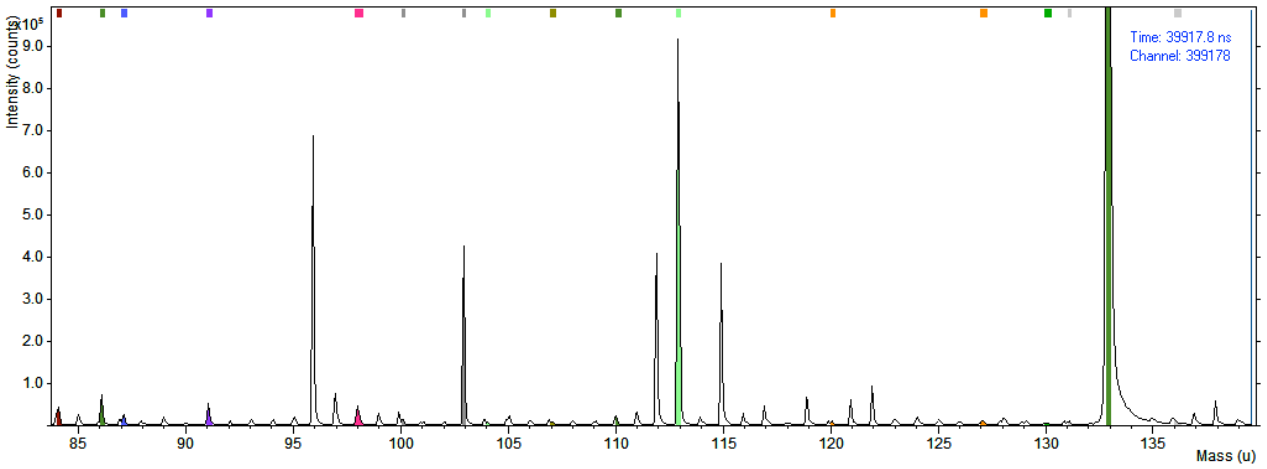

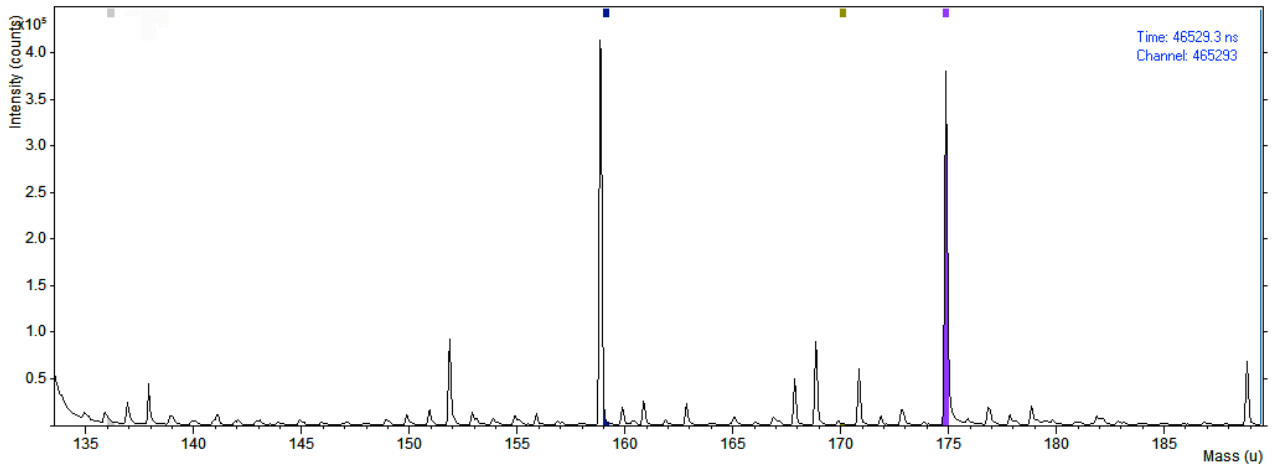

Mammoth (Hot spring-fed sink hole)

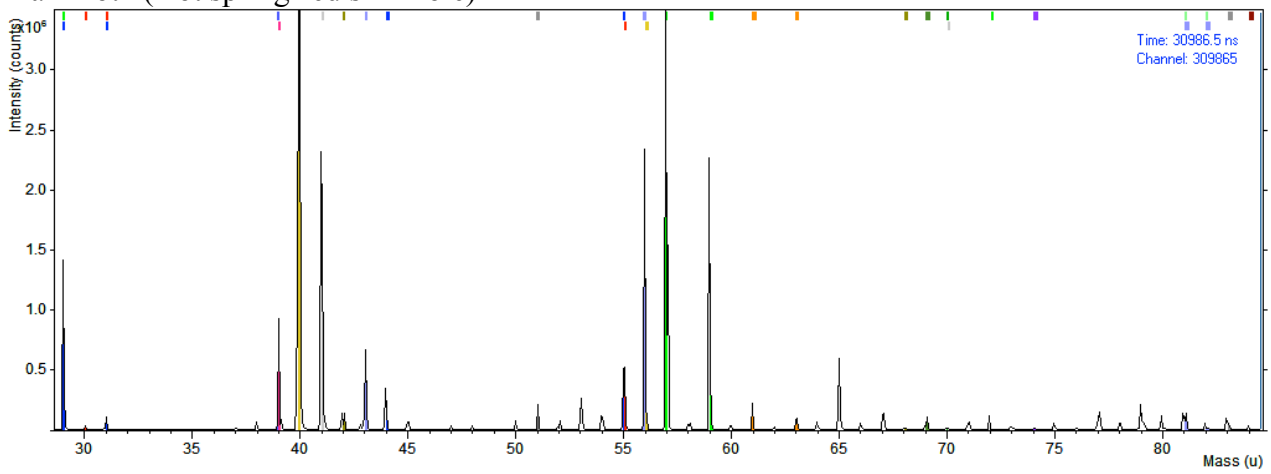

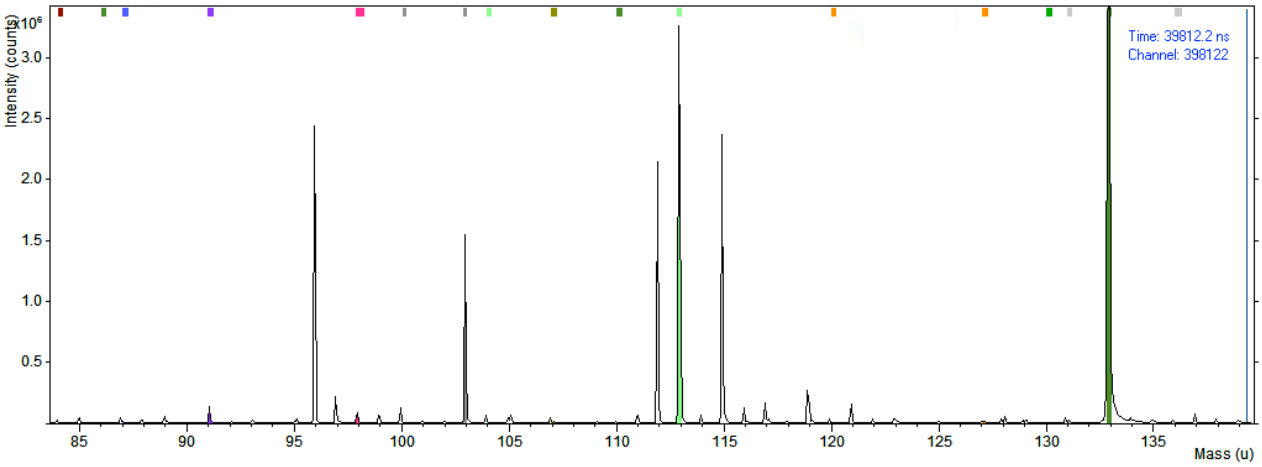

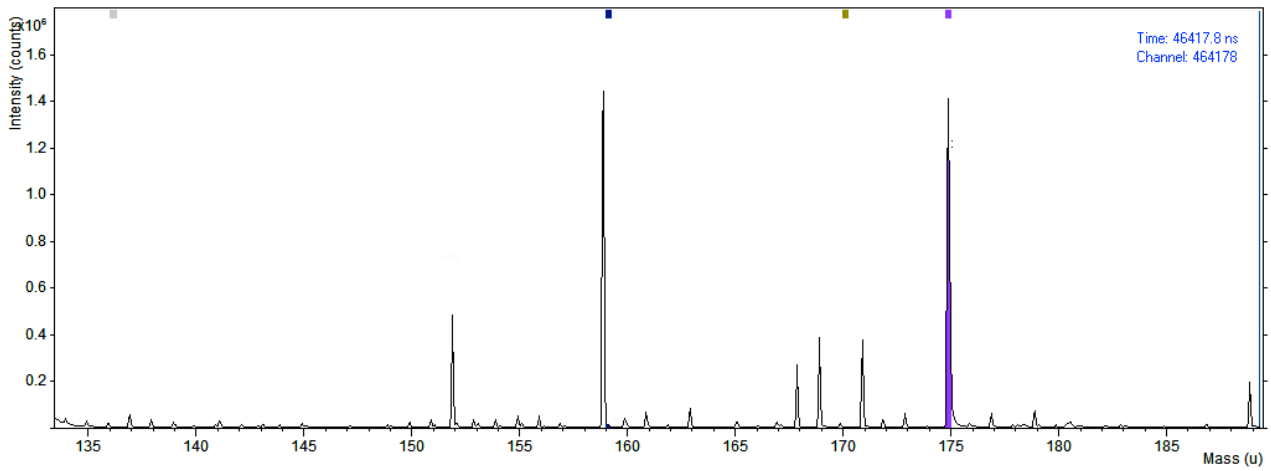

Maturation experiment (100° C)

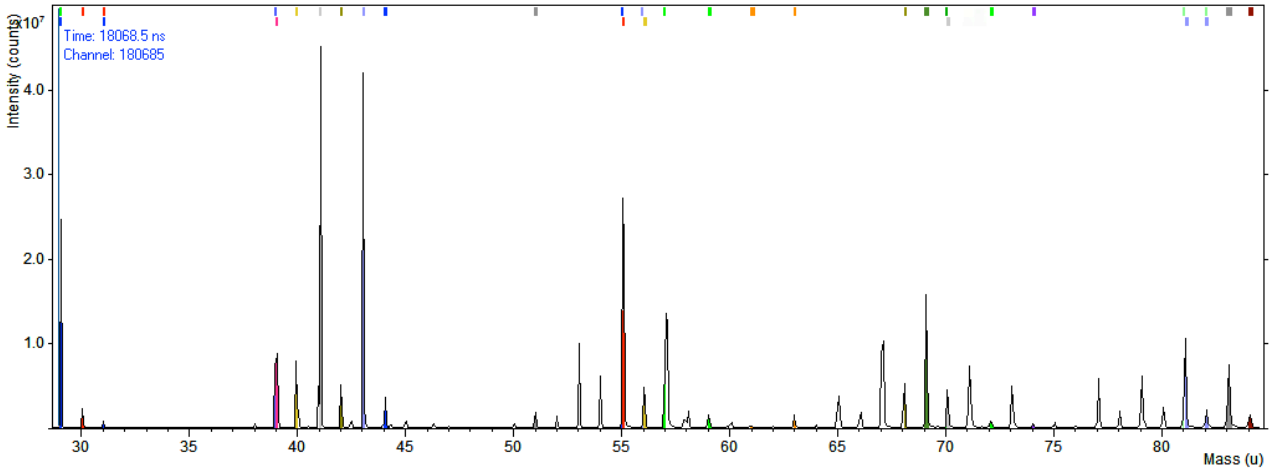

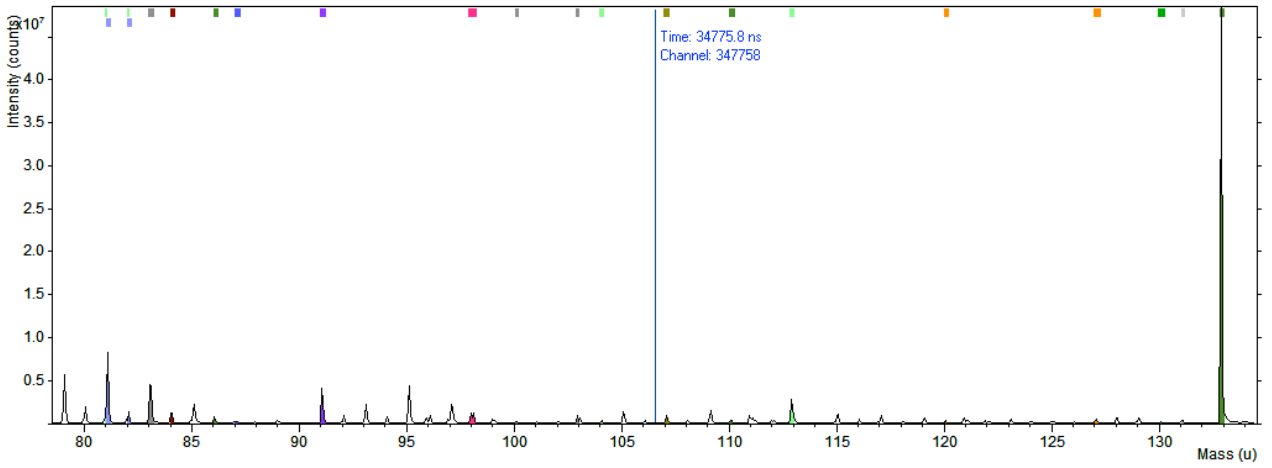

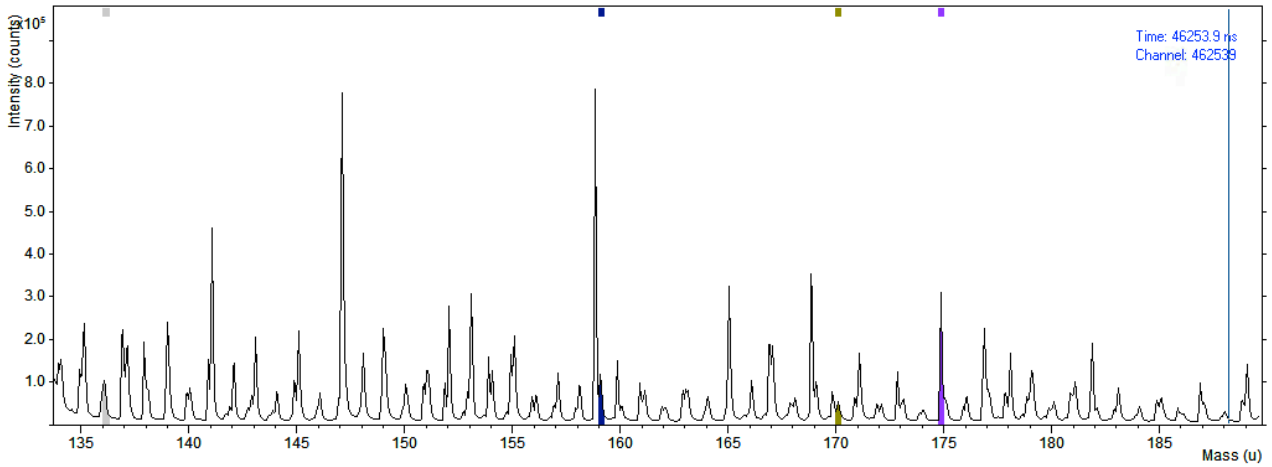

Maturation experiment (200° C)

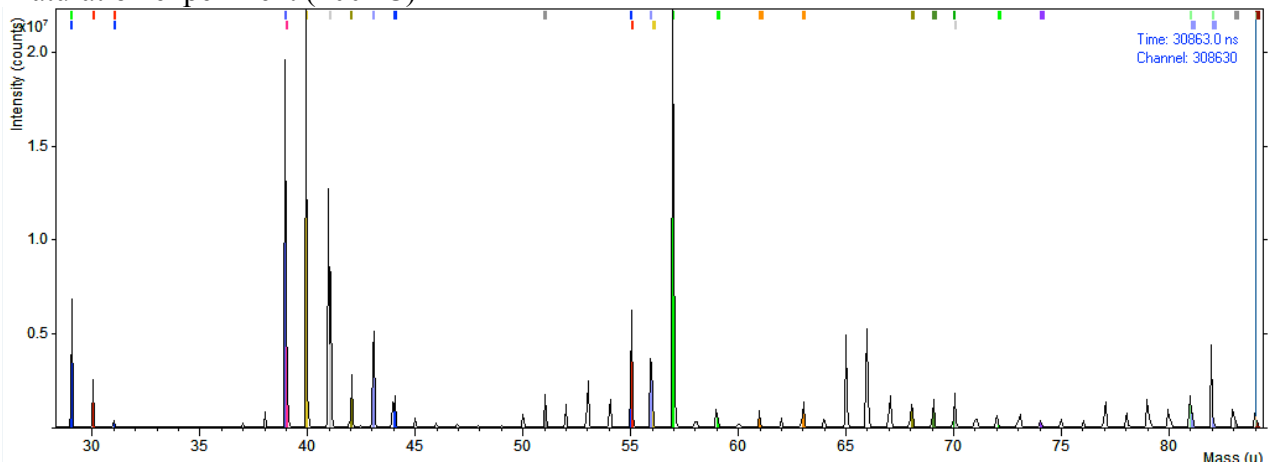

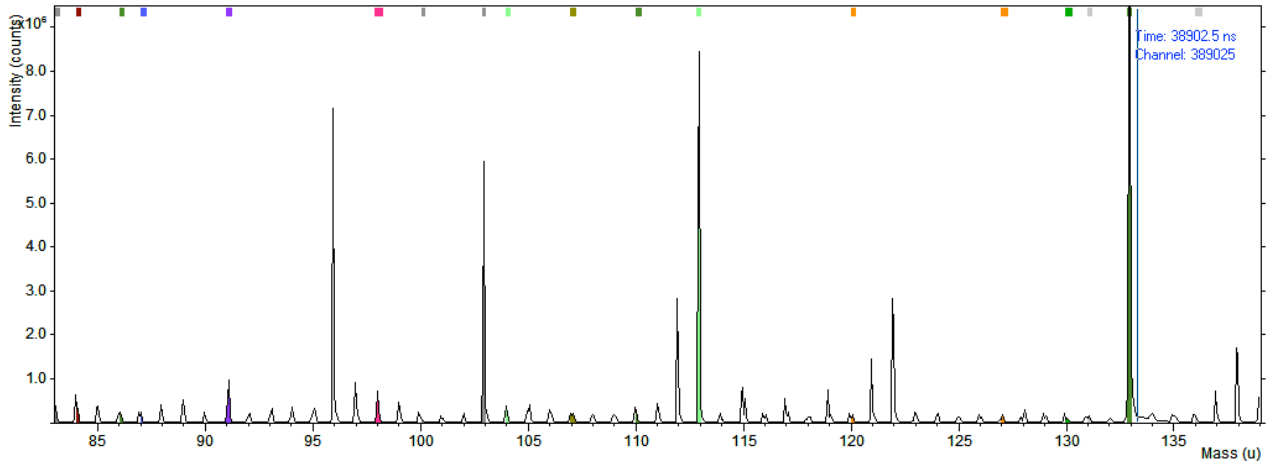

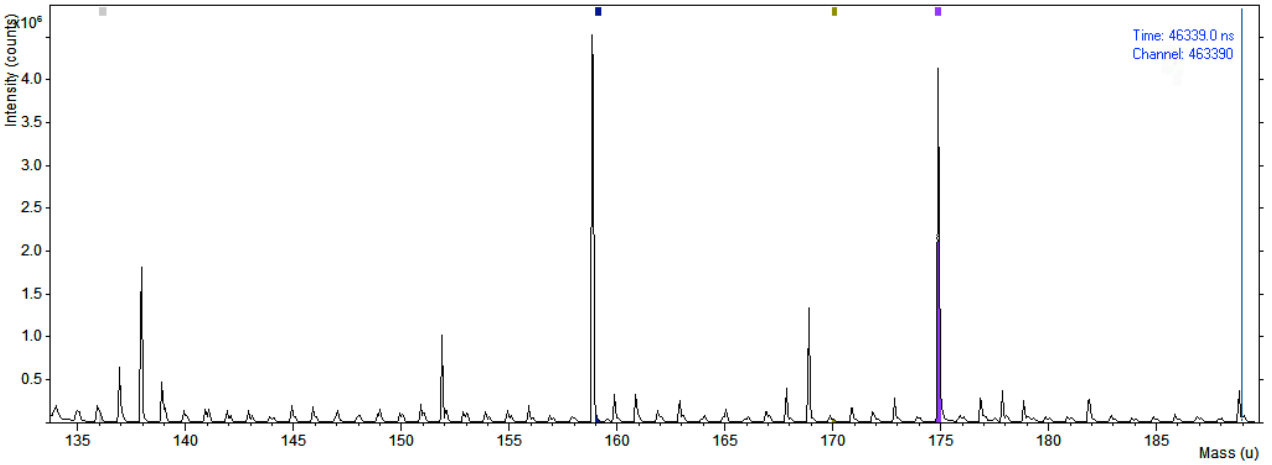

Maturation experiment (250° C)

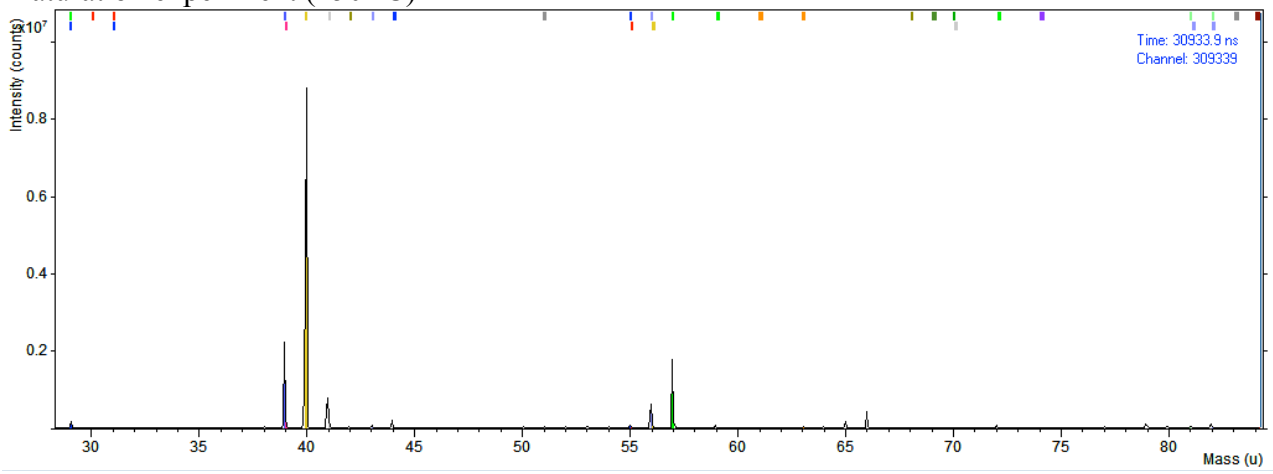

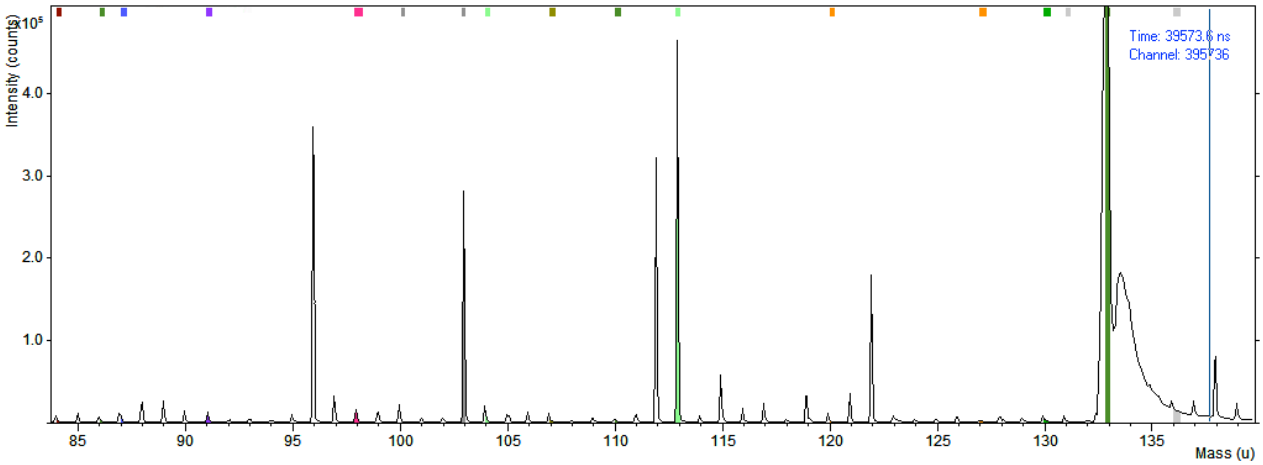

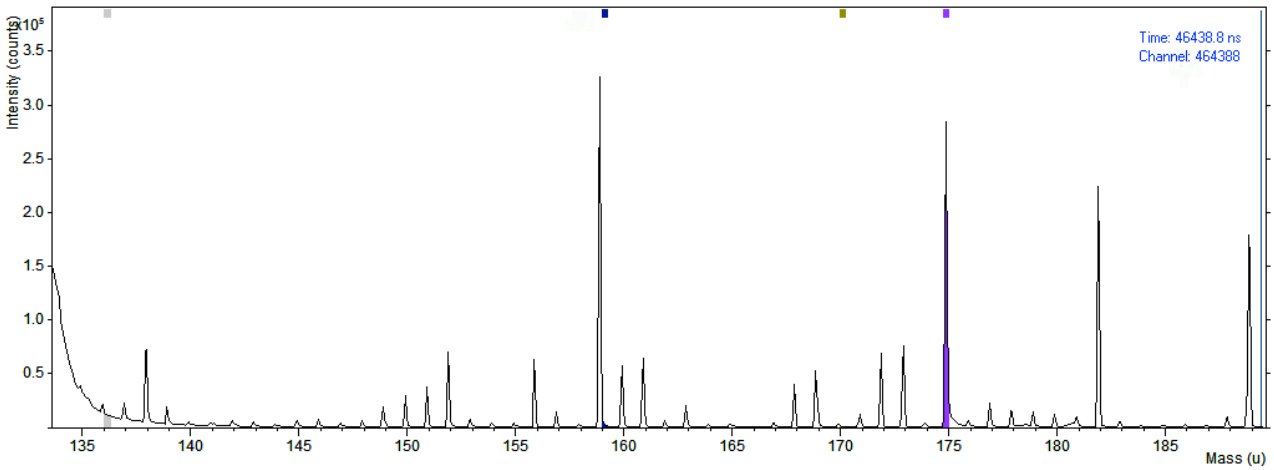

Sediment matrix (Hot spring-fed sink hole)

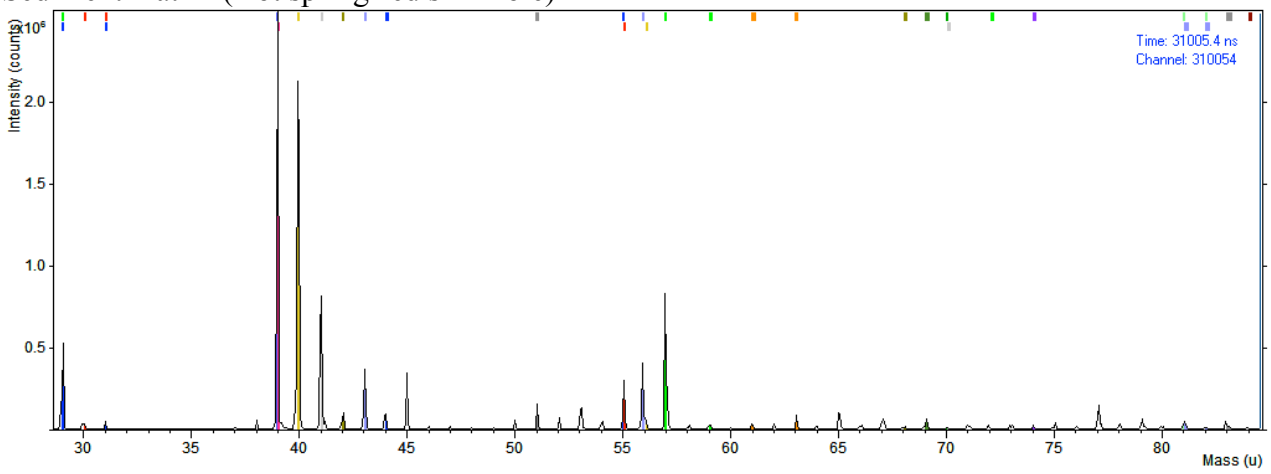

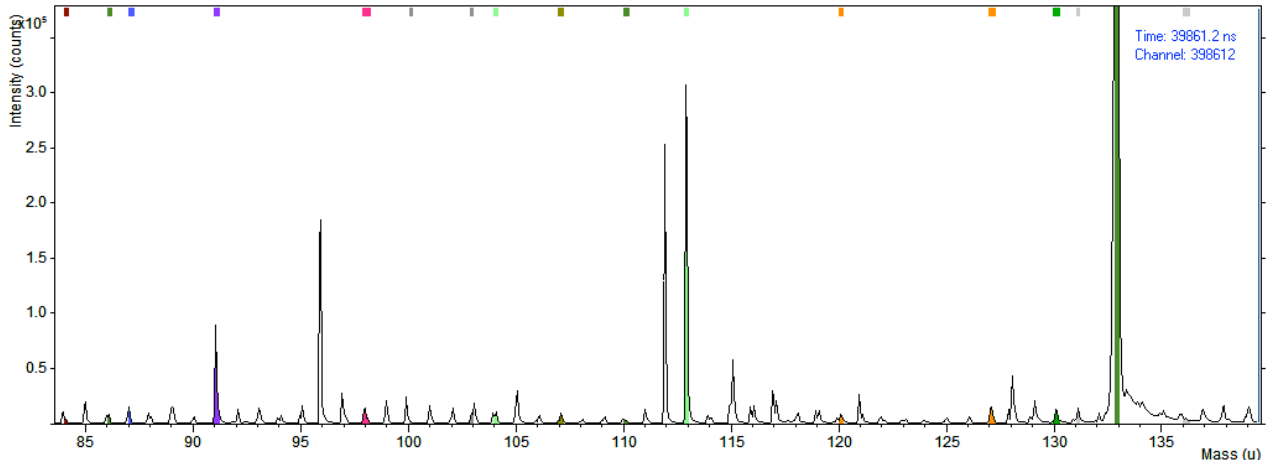

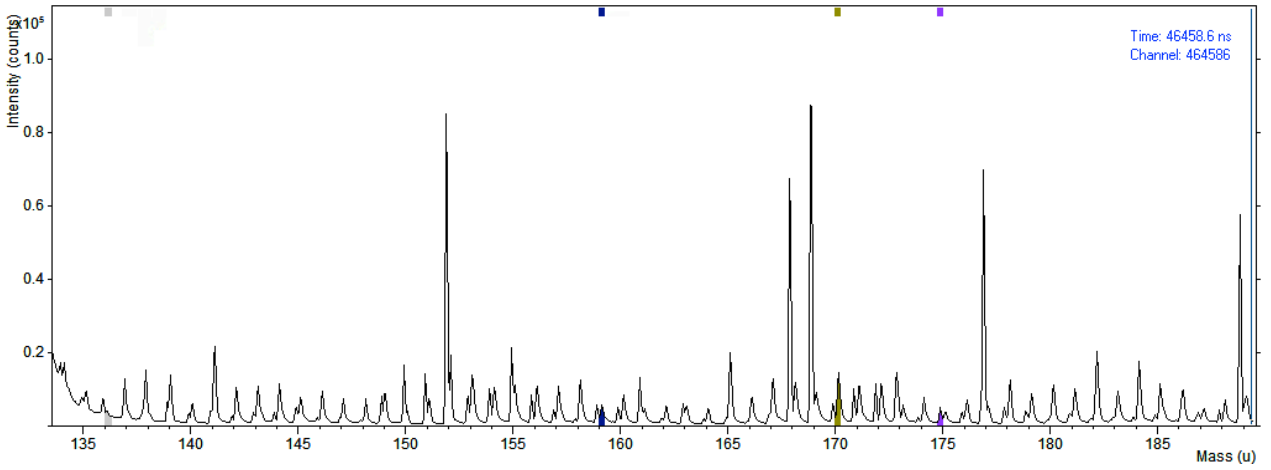

Sediment matrix (Channel deposit)

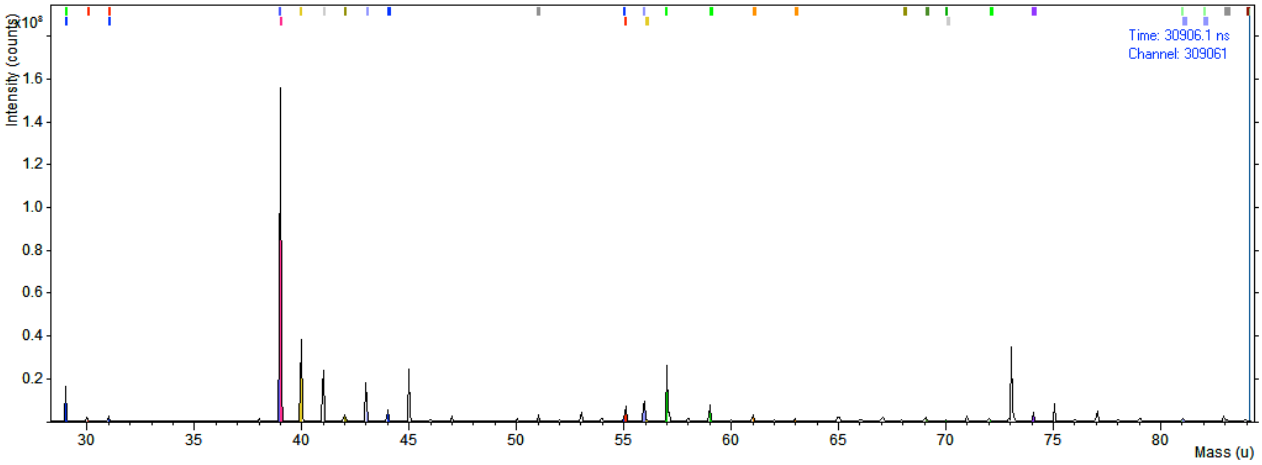

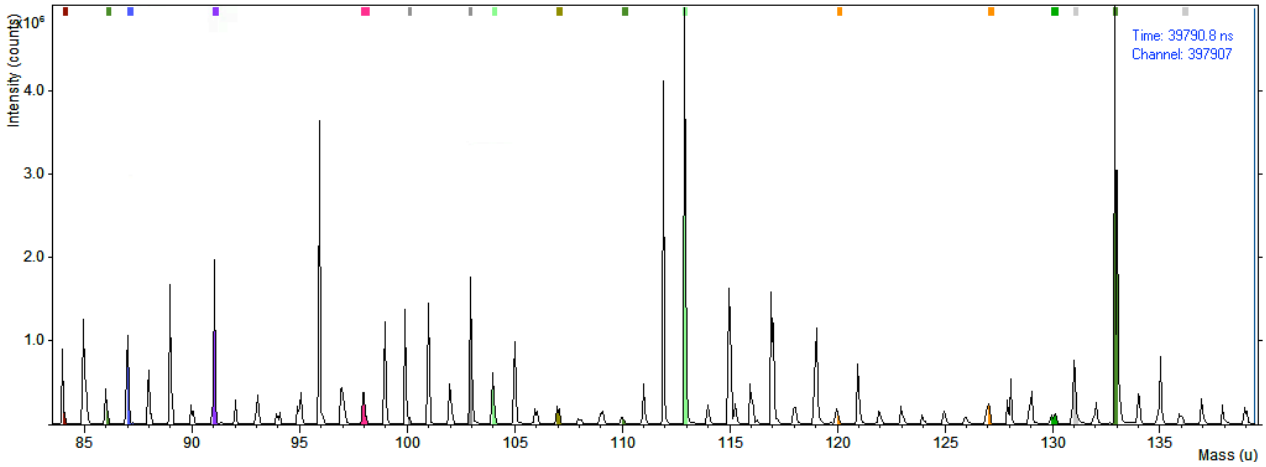

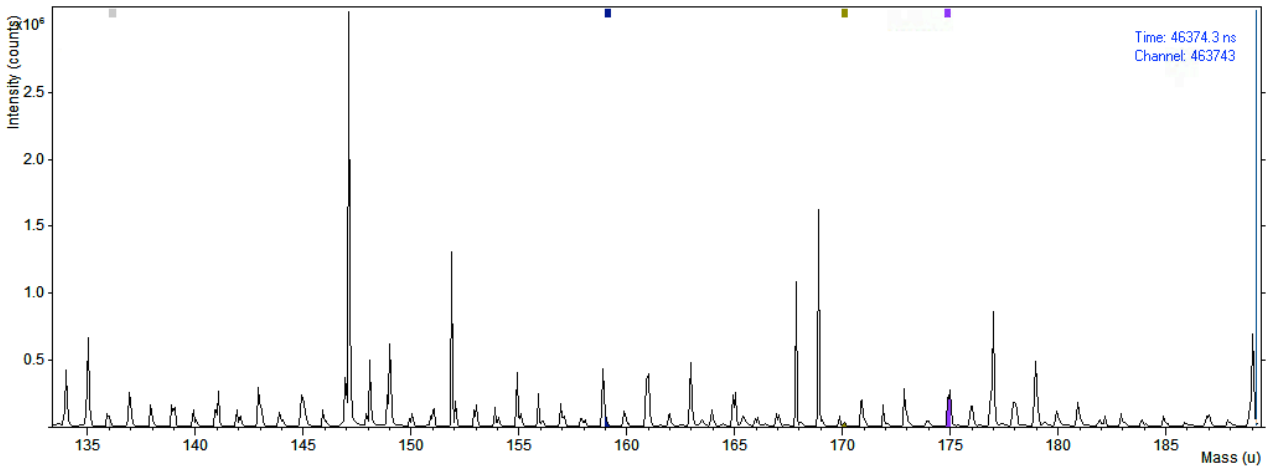

Figure S1.2 The loadings for the principal component analysis (PCA), Figure 1.1. The arrows represent the influence of the 67 amino acid and amino acid fragments on the placement of the samples on the PCA. The numbers are the atomic mass units of each fragment.

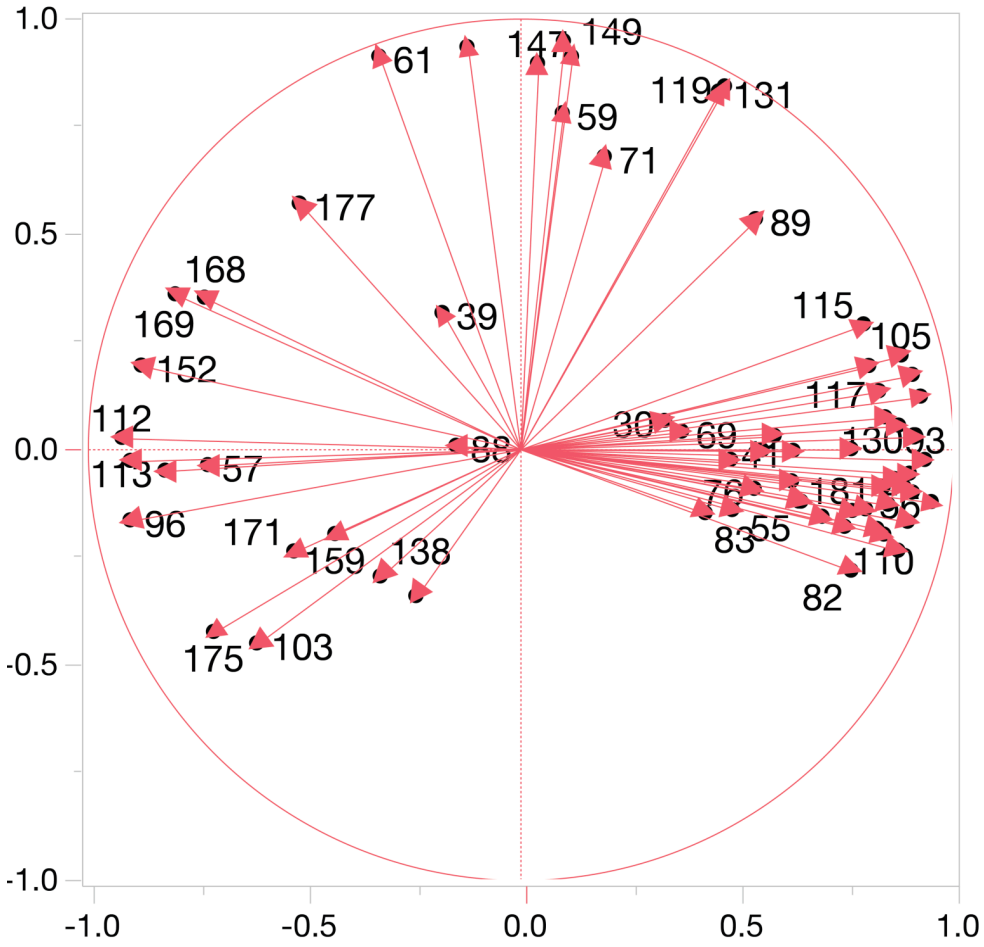

Table S1.1 Raw data of the measured intensities of the TOF-SIMS spectra.

Filename	Sample	30
20151221_E_loc1_pos_1_3	Elephant	33822
20180112_Bi3_Rib_loc1_pos_1_1	Alligator	30410
MammothSite_1_1	M	5679
RandomMammoth_1_0	RM	512719
TarPitsMammoth_1_0	TP	18556
MammothSiteSED_1_0	MS	52115
100C_Loc1_1_0	100C	2930346
200C_Loc1_1_0	200C	2628306
250C_Loc1_1_0	250C	21067
Y_Loc1_1_0	Y	726054
RMS_Loc1_1_0	RMS	1823615

39	40 Ca	41	43	44	55	56 Fe
409727	15678	1771485	2118181	110966	1834869	267699
615656	388424	1918985	2027679	73886	1746413	241511
943483	25519343	3492530	328755	21874	558682	13477
508529	8312941	1342706	441534	422126	437765	228820
549645	3100289	826923	631499	25555	814727	61559
4254012	3952491	900470	194033	8559	340666	43613
13597934	9907899	6803576	41726190	3842295	41931881	7215799
7239723	67059961	12071354	5246709	1700830	5171713	1469107
292768	12110540	1283741	64563	6526	96074	14668
1559648	1175540	5402643	5094416	933597	5329994	917669
13379472	54525416	23484047	7801514	1335585	1056420	1585644

57	59	60	67	68	69	71
1538891	54523	21681	673946	184919	961229	652975
1021736	107410	25419	603469	172333	813655	312560
10327927	242054	5293	136871	12603	60437	77539
4256342	217008	91471	122395	224930	159694	35576
2025673	10171	1114	235967	39600	10672	20788
1172259	42554	7707	98266	18211	16759	42636
10205496	1873887	1081624	18347415	5671327	21585761	366659
40029037	510282	254220	1870182	1638866	361340	374217
1950173	8317	2006	33082	13936	13684	15439
2725170	347679	346169	1906656	632491	213551	202328
26127803	7872510	607831	891588	526602	448911	1003963

72	74	75	76	81	82	83
71108	6375	27569	5957	452922	110959	452302
50645	139856	91491	8761	385201	79965	320769
2706	18948	35506	11432	187474	59026	116985
95495	24508	19939	11621	81694	56156	58126
4325	8498	48882	20238	196652	20083	15607
8188	27384	15771	2561	34275	17914	73034
1195591	1012181	880252	278337	11576851	2472258	755974
224456	150257	599020	343579	923724	411855	298871
2067	5796	19589	17503	14177	173888	3534
372264	179114	117285	47517	1571176	387677	109971
291566	3213692	37853	144592	237683	70132	602575

85	87	88	89	91	93	95
24714	21948	6156	12101	115846	84989	296420
141255	20047	4847	8644	136552	106469	262924
84064	19679	45042	28747	23591	13870	15783
49015	57339	7653	14176	99740	29554	45929
21557	34954	11922	38100	200816	69544	122548
42399	25649	17444	17540	5563	29739	29432
3833926	458117	82142	525966	6971853	3715462	8111231
705730	77902	196634	371389	1549485	555495	621317
23864	29864	29864	38876	20668	4868	15242
307946	252376	62808	107615	829345	576256	1161905
533437	419375	119867	529915	2300190	419703	393062

96 Ca2O	97	98	100	103	104	105
4339	221456	11436	17792	16511	14902	47364
46716	148844	93002	9176	24243	22862	66260
3822043	265229	112437	17416	2029225	25648	110568
1215456	167477	137929	32738	798714	12532	40436
378994	111692	63252	2967	26476	19051	84269
369452	45298	34104	8748	22234	16647	15532
1627728	4296117	2231413	400614	1258609	573343	2324455
7912533	480436	1042661	71250	7279380	273551	218373
679487	60155	15987	2938	441495	4986	15232
76115	547410	448180	97290	164148	87633	374140
4308513	736579	259488	103053	646445	178957	854604

107	109	110	111	112	115	117
52286	99430	28919	10433	3858	32646	31833
50359	74817	19338	36837	24065	29109	69929
60372	16386	9863	132578	2843859	152302	63838
19088	21556	41107	82801	824097	65662	29971
27781	58229	13425	27465	169486	138205	47928
3965	13486	7034	28423	366809	34745	48900
1767807	2762106	733449	1592389	758868	2221325	1586596
348279	218783	229586	935950	4185479	815380	396370
5152	14162	3467	23246	454582	13649	7839
307970	598408	163427	419941	164907	318751	241941
145303	116042	30654	668973	4394046	960633	375973

119	120	122	127	130	131	141
21925	11295	2240	10220	10943	18685	16557
70415	12680	11974	17008	11909	56043	14200
29626	5764	55166	37040	7777	42314	23788
16809	23742	180732	39213	12866	24075	38737
48971	13423	43544	50092	20825	37290	70870
19252	8266	11468	28157	3451	10590	8735
1322551	495545	739557	903500	360506	883769	903931
262014	289216	4913292	333649	175934	261034	289126
6059	2871	283431	6662	4482	2530	13080
186882	136207	195231	146112	106823	175773	98178
1571008	77162	290190	258863	136205	1329318	394759

147	149	152	165	175	181	SUM
63505	16632	10126	12717	4648	9131	13141786
380070	51499	8141	11601	6150	9679	13233898
13043	17442	730767	71999	2803616	18780	55928286
9030	9436	213323	33881	989286	10764	23056959
36406	18793	71418	96164	296170	32375	11192025
4255	30565	172744	5777	11778	7783	12829442
2059309	398646	549497	729446	600627	314174	263354107
261747	289933	1380288	288808	6749393	140819	194698825
2947	6997	135826	6603	590820	2196	19133265
75629	48001	133692	125031	121103	48834	39204617
4465614	1140093	1553764	396470	510466	77285	177765023

CHAPTER 2 SUPPLEMENTARY DATA

Figure S2.1 TOF-SIMS spectra of the Chapter 2 samples (dinosaurian bone, matured bone, elephant and alligator bone and the sediment matrix). 87 peaks were selected from the range of 30 – 181 atomic mass units. Peaks were selected based on a previous study (Orlando et al. 2013), peaks selected in Chapter 1 for the mammoth analysis and additional peaks that were present or absent in the samples.

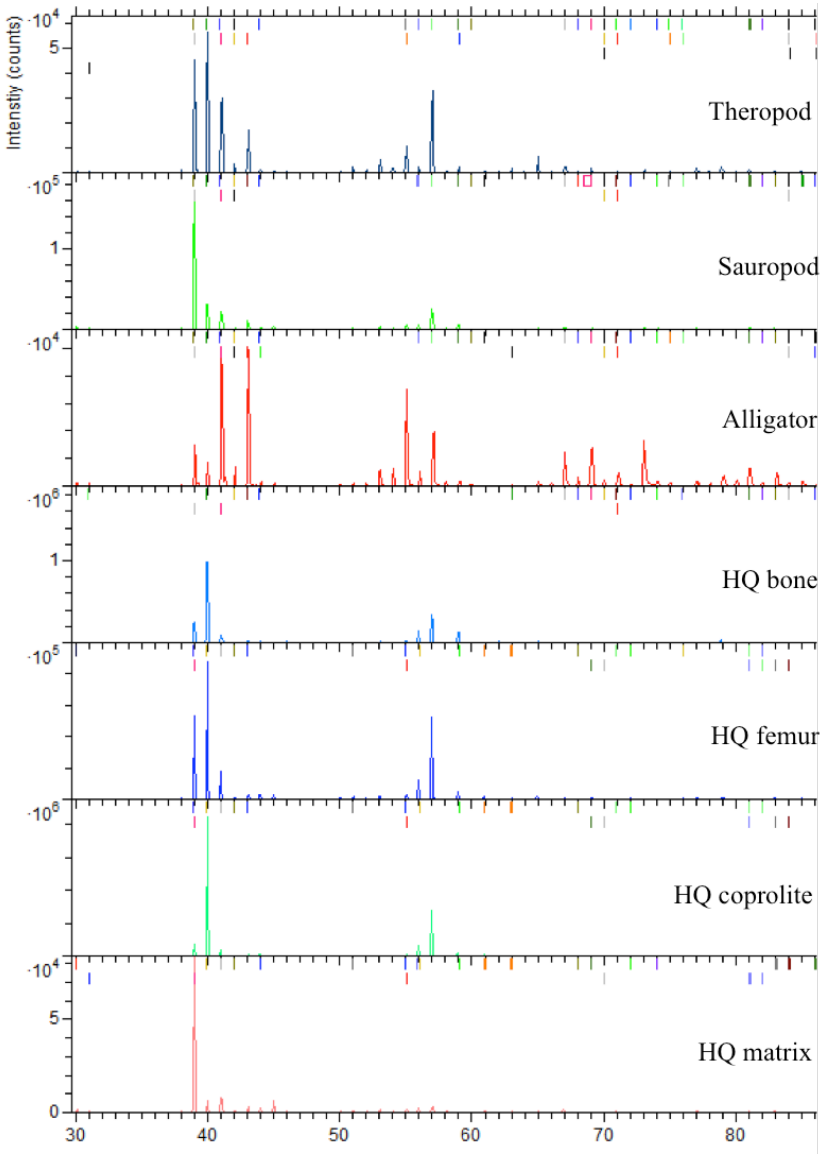

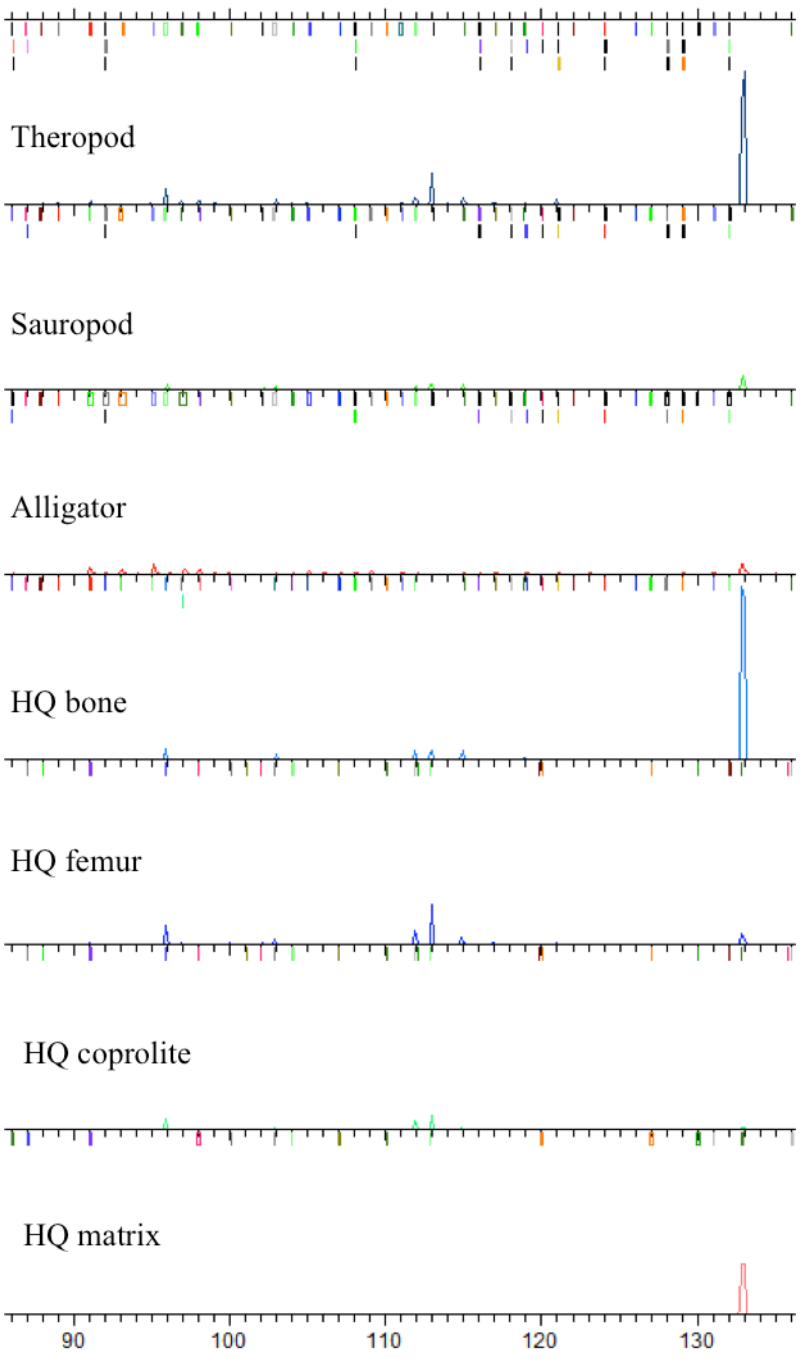
Theropod
Sauropod
Alligator
HQ bone
HQ femur
HQ coprolite
HQ matrix
90
100
110
120
130

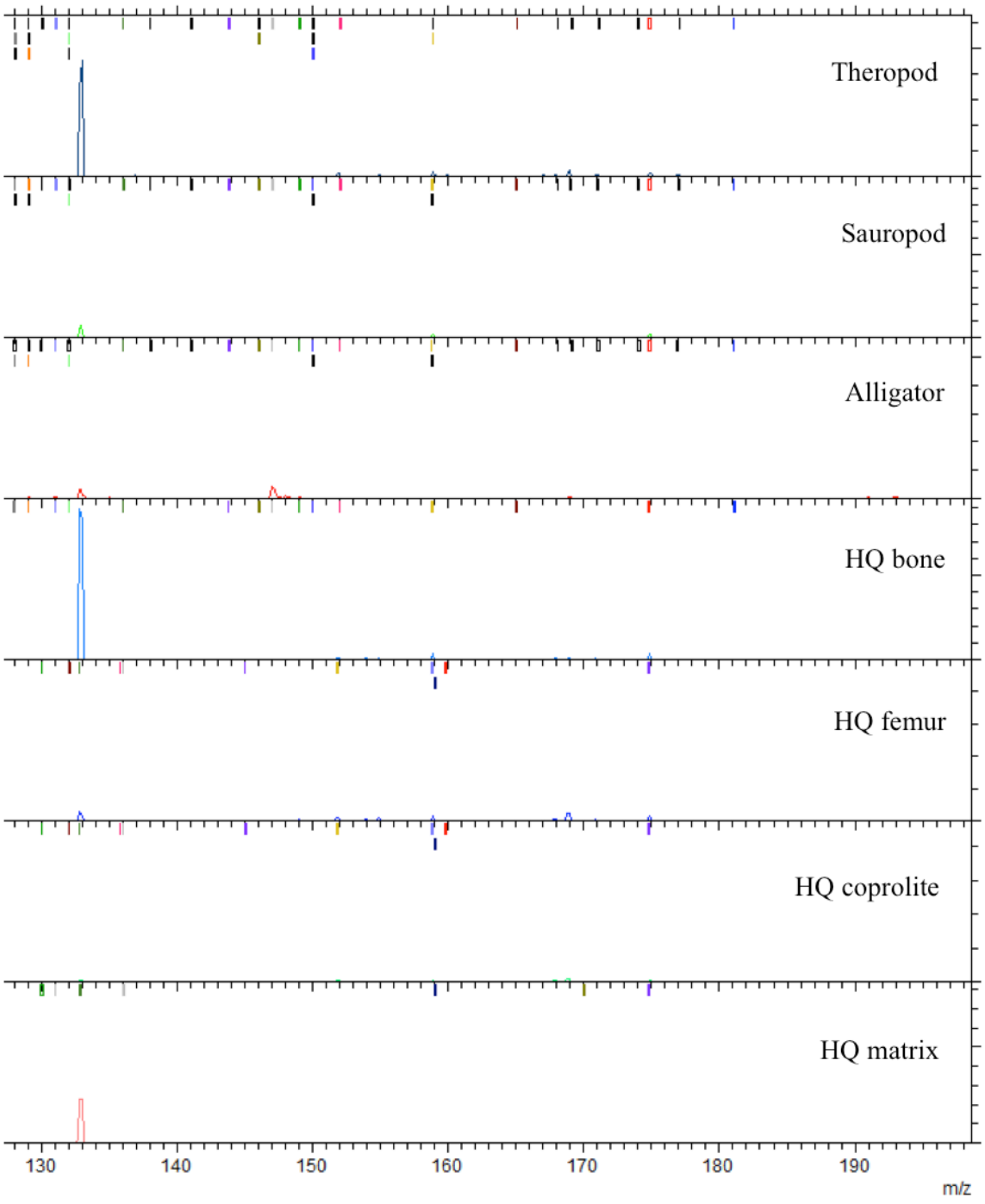
Theropod
Sauropod
Alligator
HQ bone
HQ femur
HQ coprolite
HQ matrix
130
140
150
160
170
180
190
m/z

Figure S2.2 Loadings for PCA-A (Figure 2.1) show the 87 amino acid and amino acid fragments that influenced the placement of the samples on the PCA. The numbers are the atomic mass units of each peak.

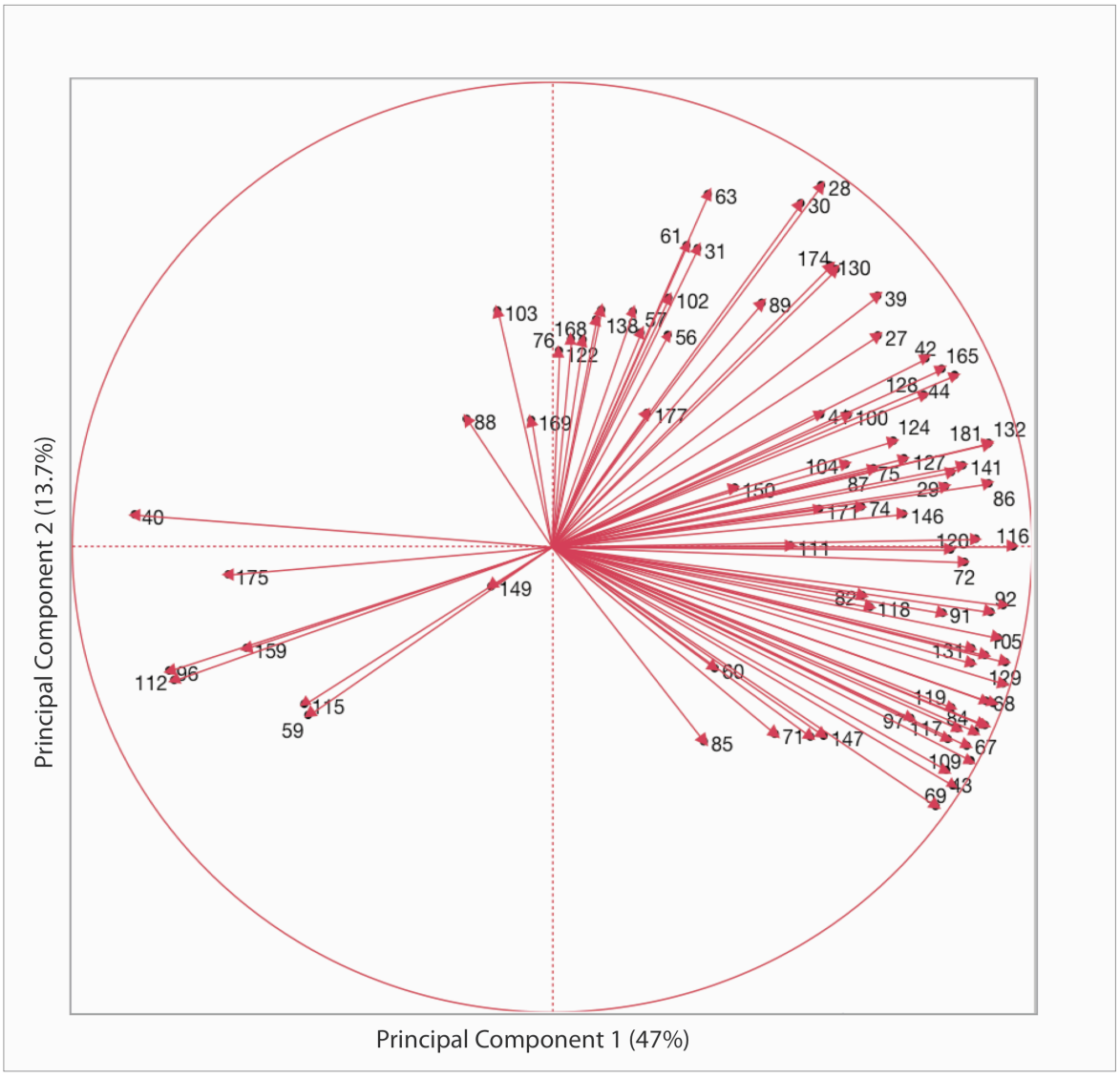

Figure S2.3 Amino acid abundances. CC2 – CC4 are the fossil samples and show extremely low abundances of amino acids when compared to the reference bone sample. A new treatment of the fossils was established to extract levels of amino acids that made it possible to do amino acid racemization (Figure 2.6) and compare the abundances of amino acids (Figure 2.5).

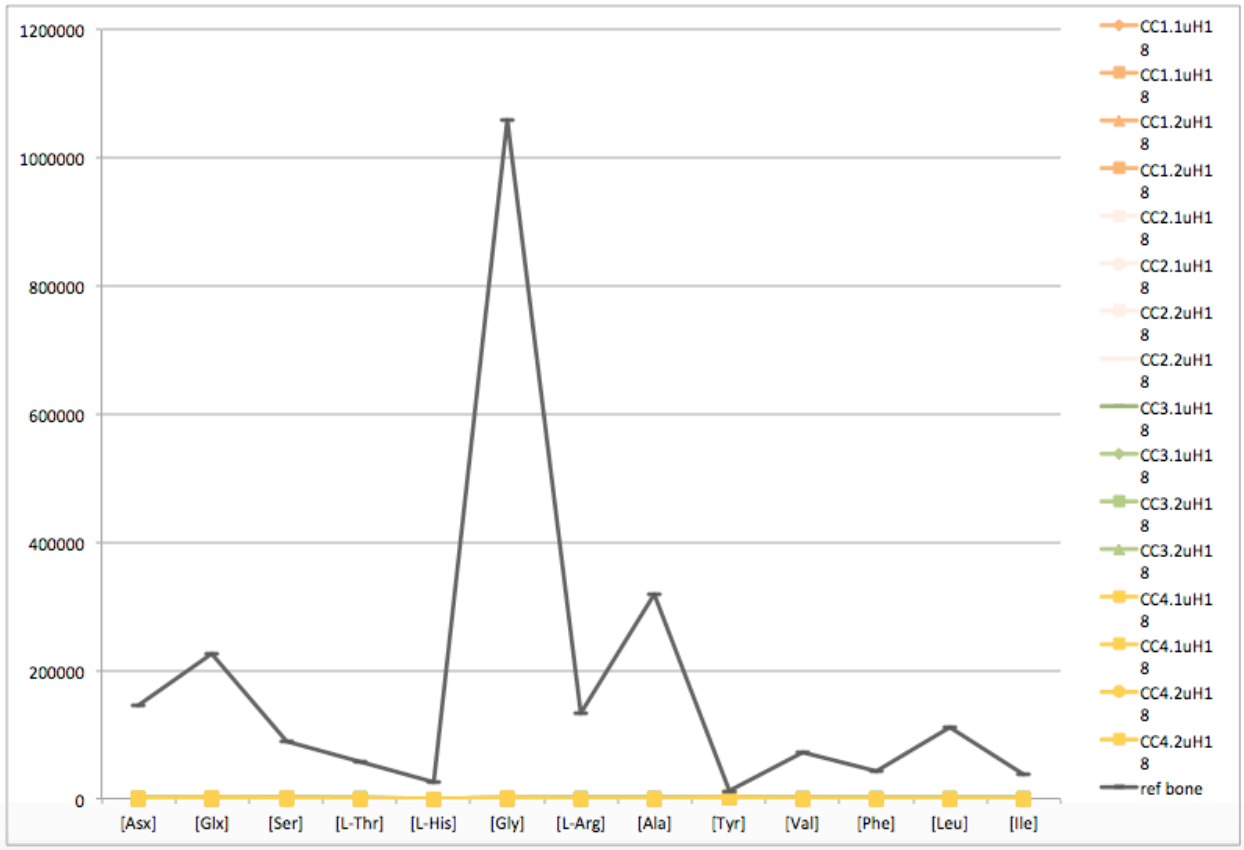

Table S2.1 Raw data of the measured intensities of the TOF-SIMS spectra.

Filename	Sample	30	39	41	43	44	55	59	60
20180110_Bi3_D6_loc2_pos_1_1	Sauropod	167287	905956	1304934	499381	157321	467398	98202	11172
20180110_Bi3_D5_loc5_pos_1_2	T. rex	31008	745743	1633285	902835	34717	655764	35615	9149
20170714_GR_bone_pos_1_3	Grbone	394820	1961551	3393133	935310	234329	1026490	246960	210955
20151221_E_loc1_pos_1_3	Elephant	33822	409727	1771485	2118181	110966	1834869	54523	21681
20130628_Femur_Target1_afterO2_pos_2_1	GRfemur1	95918	758635	1597330	690369	99346	825252	1223293	2283
20130628_Femur_Target2_afterO2_pos_1_1	GRfemur2	32116	406482	415613	173317	37563	181975	4988711	10383
20130711_Tooth_Target1_afterO2_pos_1_1	GRtooth1	87254	1560969	2149092	1090252	88355	1273280	2795542	17508
20130711_Tooth_Target2_afterO2_pos_1_1	GRtooth2	61794	761064	1058286	475117	55154	492634	3263647	1385
20130711_Coprolite_Target1_afterO2_pos_1_1	GRcoprolite1	59067	934961	2033587	1629684	97142	1221794	4024794	504153
20130711_Corporilte_Target2_afterO2_pos_1_1	GRcoprolite2	197466	3864608	8129938	8317442	423449	6273261	3460962	25316
20180112_Bi3_Rib_loc1_pos_1_1	Alligator	30410	615656	1918985	2027679	73886	1746413	107410	25419
20170714_GRS_II_pos_1_1	Grsed	140399	431517	679108	139643	72611	277932	30223	6790
20160408_100C_Loc1_1_0	100C	2930346	13597934	6803576	41726190	3842295	41931881	1873887	1081624
20160408_200C_Loc1_1_0	200C	2628306	7239723	12071354	5246709	1700830	5171713	510282	254220
20160408_250C_Loc1_1_0	250C	21067	292768	1283741	64563	6526	96074	8317	2006

61	67	68	69	71	72	74
31069	140862	34719	131738	72179	58341	98502
6901	162943	28584	106036	36641	3542	13001
46151	331746	83111	186996	87034	38383	32909
8869	673946	184919	961229	652975	71108	6375
68969	308113	49074	225615	43905	49031	15821
49795	60742	12120	44678	11261	11581	1490
86438	524908	134352	1267755	77812	25184	5097
50540	166222	30376	161822	30161	24455	6436
33654	406431	76211	369277	143108	16234	3050
42706	2218817	407595	2232234	819826	55038	3042
12140	603469	172333	813655	312560	50645	139856
70865	61345	20665	38676	14435	17800	23074
259051	18347415	5671327	21585761	366659	1195591	1012181
153276	1870182	1638866	361340	374217	224456	150257
11743	33082	13936	13684	15439	2067	5796

75	76	81	82	83	85	87
24373	19636	150086	29550	50257	22646	29724
30962	10022	66675	9145	23425	9903	13161
75385	41225	236511	62980	105594	20325	11558
27569	5957	452922	110959	452302	24714	21948
104803	155715	170464	22598	53548	289766	43596
42798	87472	34327	5658	16445	468294	19577
116032	227407	382678	44457	103922	827022	52713
71360	139593	96597	13360	38753	573400	24083
36973	34562	205742	30949	106513	88918	20915
90224	58906	1217340	164590	639707	42825	67866
91491	8761	385201	79965	320769	141255	20047
26624	17887	64854	16966	24474	5574	7136
880252	278337	11576851	2472258	755974	3833926	458117
599020	343579	923724	411855	298871	705730	77902
19589	17503	14177	173888	3534	23864	29864

89	91	93	95	98	100	102
15719	91784	38164	43390	20015	30381	120057
12122	108758	22452	23735	7588	2384	2499
38464	269525	59001	73282	43493	23519	18401
12101	115846	84989	296420	11436	17792	6864
72076	442057	95432	84687	29586	26274	268158
23668	117699	27206	19084	19030	38179	49540
70868	519937	188197	150440	42156	56568	96240
39370	220182	57238	48495	4515	25366	119439
39725	327320	83282	113187	16142	7806	23934
103411	1301046	492247	721461	81744	7791	15510
8644	136552	106469	262924	93002	9176	2380
8185	48226	11903	11258	16007	10053	33999
525966	6971853	3715462	8111231	2231413	400614	465943
371389	1549485	555495	621317	1042661	71250	268265
38876	20668	4868	15242	15987	2938	5900

103	104	105	107	109	110	111
255746	19312	38300	25614	29365	11430	15010
132694	8306	30501	8257	5556	3078	77282
4702538	40789	94452	41579	25079	16004	20458
16511	14902	47364	52286	99430	28919	10433
65693	70600	57885	38139	16534	4520	27719
30238	51126	84475	11310	17378	1201	18486
85376	144358	107524	77665	99616	8285	80835
40916	54745	44474	19059	20040	2961	73894
60852	20392	14768	38368	24884	5830	84672
219799	87594	120605	240145	142783	31819	509700
24243	22862	66260	50359	74817	19338	36837
22444	11654	15085	7416	7765	4234	3593
1258609	573343	2324455	1767807	2762106	733449	1592389
7279380	273551	218373	348279	218783	229586	935950
441495	4986	15232	5152	14162	3467	23246

112	115	117	119	120	121	122
378001	47647	21484	24059	9331	15372	9480
186999	45743	19400	6544	4915	9679	3170
7279079	197623	53983	40674	19726	50295	13126
3858	32646	31833	21925	11295	25053	2240
2586112	1271359	72786	32431	8742	16540	22300
9871155	4904886	91312	17414	6036	7581	77110
5832744	2736815	107434	73411	15813	36824	27365
10159883	3184983	110199	23288	8761	11934	13478
14685441	3688493	88620	36161	9803	17707	5261
8156065	3050672	273271	184247	43099	98895	20674
24065	29109	69929	70415	12680	28786	11974
30401	24114	7808	4832	2700	3690	2952
758868	2221325	1586596	1322551	495545	833992	739557
4185479	815380	396370	262014	289216	207387	4913292
454582	13649	7839	6059	2871	3791	283431

127	130	131	132	138	141	146
24509	21217	18459	8163	3608	19138	5083
12110	4693	7357	2833	3629	21266	2030
39634	36482	25546	17223	13003	39118	10273
10220	10943	18685	7378	8239	16557	5250
51261	10992	32700	6594	5607	47764	13313
17151	4103	5237	2205	2947	8307	15454
45351	14057	36636	9219	8098	50275	30022
21118	5033	14955	4941	5919	20891	18177
27929	11657	22882	6329	4701	29270	7021
127301	48640	130777	25574	13044	154061	10455
17008	11909	56043	14153	7724	14200	8789
7113	20804	6781	4406	10603	8775	1958
903500	360506	883769	251901	357537	903931	164149
333649	175934	261034	171472	3184339	289126	139215
6662	4482	2530	3366	174669	13080	3415

147	149	152	159	165	168	169
15086	48266	12816	317797	18522	4872	10046
17257	4894	16176	201730	17781	3487	15072
25806	33126	41802	6052286	39971	11161	16750
63505	16632	10126	2019	12717	4784	6954
14294	364966	47188	1250519	48919	5514	12198
16372	472728	23792	5330653	9183	4514	8998
28182	1165847	41594	4216374	45295	7643	15517
19040	299166	34741	2840425	19805	7338	23475
25230	39409	30401	3219606	25473	8076	19899
51257	49501	102776	2948730	118166	15407	32115
380070	51499	8141	2409	11601	2402	7601
3262	16569	6929	15061	11327	2170	2585
2059309	398646	549497	291026	729446	181626	230114
261747	289933	1380288	174706	288808	642454	125256
2947	6997	135826	9675	6603	76109	106086

171	174	175	177	181	SUM
9205	3616	367216	7128	7386	6687127
6709	2538	167045	10235	10047	5817608
16737	8475	6506419	27273	13073	35858704
28501	2556	4648	3636	9131	11197670
5835	6379	1203865	23296	7815	15362093
6331	3836	6084738	41985	6800	34661846
11592	9817	4230104	91773	14887	33568783
6955	6675	3012118	23977	5851	28270059
8480	5967	3305149	35180	12593	38315619
27896	17845	2648931	36423	55822	61270457
17479	2805	6150	11138	9679	11499626
2710	1981	9548	1829	5133	2616461
159139	78290	600627	478664	314174	233770358
354420	128508	6749393	585514	140819	83685929
24125	1958	590820	47710	2196	4756925